

QUANTITATIVE ELECTROMYOGRAPHIC AND GONIOMETRIC
ANALYSES OF NORMAL AND PATHOLOGICAL HUMAN GAITS

TO RUTH, ABBY AND CHAD

QUANTITATIVE ELECTROMYOGRAPHIC AND GONIOMETRIC
ANALYSES OF NORMAL AND PATHOLOGICAL HUMAN GAITS

BY

CECIL HERSHLER, B.Sc., B.Sc. (Hons.), M.Sc.

A Thesis

Submitted to the Faculty of Graduate Studies
in Partial Fulfilment of the Requirements

for the Degree

Doctor of Philosophy

McMaster University

November, 1977

DOCTOR OF PHILOSOPHY (1977)
(Electrical Engineering)

McMASTER UNIVERSITY
Hamilton, Ontario

TITLE: Quantitative Electromyographic and Goniometric
Analyses of Normal and Pathological Human Gaits

AUTHOR: Cecil Hershler, B.Sc. (U.C.T.)


B.Sc (HonB.) (U.C.T.)

M.Sc. (U.C.T.)

SUPERVISOR: Professor M. Milner

NUMBER OF PAGES: xvii, 273

ABSTRACT



This thesis is directed generally towards a deeper understanding of normal and pathological biped locomotion. Attention has been focussed mainly on electromyographic (EMG) and kinematic aspects of gait. Emphasizing consistency and repeatability of acquired data, the characteristics of surface EMG signals from m. vastus lateralis and m. rectus femoris during several steps of level walking under controlled repeatable gait conditions at three different speeds for several normal subjects have been studied. The variance ratio, a statistical descriptor for repeatability, has been devised. The findings indicate that the variance ratio offers a simple means for selecting an optimal processor for rectifying and averaging the signals. It is of value also in determining an optimal location for surface electrodes on a muscle.

Included in the thesis is original research relating to kinematic information presented in the form of knee-angle/hip-angle diagrams. Cyclic loops which had been utilized in the past mainly for their visual representation have been quantified using a shape recognition technique.

Quantitative analyses of angle-angle diagrams associated with 5 normal subjects, an above-knee (A/K) amputee and a cerebral-palsied (C.P.) patient, who had an implanted cerebellar stimulator, were carried out. The quantification and physical interpretations of the parameters[™] extracted from the angle-angle diagrams provided a valuable adjunct to visual assessment of the gaits and elicited significant information regarding overall coordination and control during each gait. Using these methods an in-depth assessment of the efficacy of the cerebellar stimulator implanted in the C.P. patient was accomplished.

The thesis also describes an initial attempt, using the methods of time series analysis, at modelling the transfer function between several inputs given by the EMG signals of selected muscle groups and an output which is either the hip or knee angle trajectory. The model was able to suggest which individual muscles were synergistic, whether the inputs chosen were good predictors of the output and the relative contribution of each input in predicting the output.

ACKNOWLEDGEMENTS

I would like to express my gratitude to Dr. M. Milner for his encouragement, support and supervision during the entire period of this thesis.

I would like to thank Dr. J.F. MacGregor, Dr. A.J. McComas and Dr. N.K. Sinha for discussions concerning some of the aspects of this work.

Further thanks are also due to the entire Biomedical Engineering Department, Chedoke Rehabilitation Centre and in particular to Dr. H. de Bruin, S. Naumann, W. Brugger, L. Cellini and M.S. Abdel-Azim for the many stimulating discussions.

Special thanks are due to the members of the Word Processing Centre in the Engineering Building who typed this manuscript and to the secretaries of the Biomedical Engineering Department for their unfailing cooperation and support.

Appreciation is gratefully expressed to McMaster University for its financial support and to the Wilson Trust Fund, Chedoke Hospitals, which made available the PDP11/10 computer.

Finally, I am grateful to my wife, Ruth, and children, Abby and Chad, for their constant patience and encouragement during the course of this work.

Glossary

EMG	electromyographic
A/K	above-knee (amputee)
C.P.	cerebral palsied
A	area (of closed angle-angle diagram)
P	perimeter (of closed angle-angle diagram)
P_A	perimeter/square root (area)
HS	heel-strike
HT	foot-flat (heel and toe)
HO	heel-off
TO(SW)	toe-off (onset of swing)
ST	onset of stance
IEMG	"integrated" EMG signal (continuous)
FWRI	integral of full wave signal (discrete epochs)
VR	variance ratio
W	window length
W_{min}	"Optimal" window length
rf	m. rectus femoris
vl	m. vastus lateralis
R	right sided
L	left sided
B	bilateral (Chapter 5)
CS	cerebellar stimulation
H	H-reflexes

SSEP	somatosensory evoked potentials
VEP	visual evoked potentials
BSEP	brain stem evoked potentials
EEG	electroencephalogram
NMS	neuromusculo-skeletal
C_i $i=1,4$	input coefficients (knee model)
C_i $i=1,3$	input coefficients (hip model)
C_8, C_7	level parameters
b	delay (msec)
B	Backward shift operator defined by $Ba_t = a_{t-1}$ (Chapter 6)
X1 (RF)	m. rectus femoris EMG
X2 (BF)	m. biceps femoris EMG
X3 (S)	m. semitendinosus EMG
X4 (G)	m. gastrocnemius EMG
y_{knee}	knee angle
y_{hip}	hip angle
N_t	Noise model
χ^2	Chi-square statistic

TABLE OF CONTENTS

	PAGE
CHAPTER 1: INTRODUCTION	1
CHAPTER 2: A BACKGROUND REVIEW OF HUMAN LOCOMOTION	9
2.1 Historical Survey of Investigations Into the Kinematics of Gait	9
2.1.1 -Pre-20th Century:	11
2.1.2 Current Research in Gait (20th Century)	13
2.2 Review of Electromyographic (EMG) Investigations During Gait	26
2.2.1 Introduction	26
2.2.2 Review of the Literature	28
2.3 Anatomical Aspects of the Muscles of the Lower Limb	37
2.3.1 Introduction	37
2.3.2 Anatomical Aspects of Human Locomotion	37
2.3.3 The Muscular System	44
2.4 The Phasing of the EMG Activity and the Function of the Muscles of the Leg During Normal Locomotion on a Level Surface	51
2.4.1 Muscles crossing the front of the hip joint: Iliopsoas	52
2.4.2 The three gluteal muscles (and m. tensor fascia lata)	53
2.4.3 The muscles of the front of the thigh; m. quadriceps femoris (m. rectus femoris, 3 vasti, m. sartorius)	55
2.4.4 The muscles of the medial side of the thigh; m. gracilis, m. adductor longus, brevis and magnus	58
2.4.5 The muscles of the back of the thigh; hamstrings (m. biceps femoris, m. semimem- branosus, m. semitendinosus)	59

TABLE OF CONTENTS (cont'd)		PAGE
2.4.6	The extensor muscles of the leg (m. tibialis anterior, m. extensor digitorum longus, m. extensor hallucis longus)	61
2.4.7	The m. peroneus longus and m. peroneus brevis	64
2.4.8	The superficial plantar-flexors (m. gastrocnemius, m. soleus)	65
2.4.9	Deep plantar-flexors (m. flexor hallucis longus, m. flexor digitorum longus and m. tibialis posterior)	66
2.5	Conclusions	69
CHAPTER 3:	CURRENT EXPERIMENTAL TECHNIQUES AND EQUIPMENT USED IN LOCOMOTION STUDIES	70
3.1	Introduction	70
3.2	Measurement of the Kinematic Variables in Gait	71
3.2.1	The Period and Phases of the Walk Cycle	71
3.2.2	Measurement of Spatial and Angular Information	78
3.2.3	The Stroboscopic Flash-Photography System	78
3.2.4	The Electrogoniometer System	83
3.2.5	The Optoelectronic System	90
3.3	Measurement of the Electromyographic (EMG) Signal	94
3.3.1	Monitoring of the EMG signal	94
3.3.2	Amplification and Processing of the Raw EMG Signal	98
3.3.3	Storage of the EMG Signals	103
3.3.4	Analysis of EMG signals	103
CHAPTER 4:	AN OPTIMALITY CRITERION FOR PROCESSING ELECTROMYOGRAPHIC (EMG) SIGNALS RELATING TO HUMAN LOCOMOTION	104
4.1	Introduction	104
4.1.1	Major Concerns	104
4.1.2	Reliability	106
4.2	Background	108

TABLE OF CONTENTS (cont'd)		PAGE
4.3	Optimality Criterion	115
4.4	Experimental Procedure	118
4.5	Computer Processing	120
4.6	Results and Discussion	122
	4.6.1 Processed Signals	122
	4.6.2 Repeatability Curves	124
	4.6.3 Selection of Processor	126
	4.6.4 Electrode Position	128
	4.6.5 Walking Speed	128
	4.6.6 Optimal Electrode Sites and Walking Speeds	130
	4.6.7 Window Length and Walking Speed	132
4.7	Conclusions	132
	4.7.1 Potential Uses	132
CHAPTER 5:	QUANTITATIVE ANALYSES OF ANGLE-ANGLE DIAGRAMS IN THE ASSESSMENT OF LOCOMOTOR FUNCTION	135
5.1	The Quantification of Angle-Angle Diagrams	135
	5.1.1 Introduction	135
	5.1.2 Background	137
	5.1.3 On Angle-Angle Diagrams	139
	5.1.4 Limitations of Visual Inspection	141
	5.1.5 Key Factors	142
	5.1.6 New Directions	144
	5.1.7 Physical Interpretation of Variables	144
	5.1.8 Experimental Procedure	151
	5.1.9 Results and Discussion	159
	5.1.10 Conclusions	182
	5.1.11 Potential Uses	183
5.2	Preliminary investigation of influence of cerebellar stimulation on gait by analyzing angle-angle diagrams	184
	5.2.1 Introduction	184
	5.2.2 Results and Interpretation	187
	5.2.3 Experiment I	189
	5.2.4 Experiment II	199
	5.2.5 Experiment III	206
	5.2.6 Summary and Conclusions	214
CHAPTER 6:	TRANSFER FUNCTION TIME SERIES MODELLING	220

TABLE OF CONTENTS (cont'd)		PAGE
6.1	Introduction	220
6.2	Justification of the Black-Box Modelling Approach	223
6.3	The Use of Transfer-Function Models in Biological Research	225
6.4	Proposed Form of Model	227
6.5	Design of Experiment	228
6.6	Experimental Acquisition of Input-Output Data	231
	6.6.1 Order of System Dynamics	232
	6.6.2 Delay b	234
6.7	Results	236
6.8	Discussion of Results	239
6.9	Conclusions	242
APPENDIX 1:	TWO PROGRAMS USED FOR QUANTITATIVE ANALYSIS OF EMG SIGNALS AND ANGLE-ANGLE DIAGRAMS	244
APPENDIX 2:	THEORETICAL BACKGROUND TO THE MODELLING PROCEDURE	248
A2.1	Transfer Function Models	248
A2.2	Discrete Dynamic Models Represented by Difference Equations	249
A2.3	Transfer Function Models with Added Noise	250
A2.4	Identification, Fitting and Checking of Transfer Function Models	252
A2.5	Identification of Transfer Function Models	254
A2.6	Fitting the Transfer Function Model	256
REFERENCES		262

LIST OF ILLUSTRATIONS

FIGURE		PAGE
2.1	Kinematics of normal ambulation	10
2.2	Outer aspect of right hip bone	38
2.3	Right femur from in front	39
2.4	Right tibia and fibula from in front	40
2.5	Position of patella during flexion and extension of knee	41
2.6	Bones of right foot viewed from above	42
2.7	Dissection of muscles of front of right thigh	45
2.8	Deep dissection of muscles of back of right thigh	48
2.9	Muscles of left leg from lateral side	49
3.1	Resistor network for footswitches	72
3.2	Normal footswitch patterns	72
3.3	Footswitch patterns for a C.P. patient	74
3.4	A stroboscopic "stick" - diagram	75
3.4A	A knee-angle/hip-angle diagram derived using the stroboscopic method	76
3.5	A "stick" - diagram utilizing the optoelectronic method	77
3.5A	A knee-angle/hip-angle diagram derived utilizing the optoelectronic method	78
3.6	Patient dressed in black cat suit	80
3.7	Stroboscopic flash-photography system including patient, background, walkway, camera and stroboscope	81

LIST OF ILLUSTRATIONS (cont'd)		PAGE
3.8	Self-aligning electrogoniometer system	84
3.9	Circuit diagram for electrogoniometer system	86
3.10	Display devices	86
3.11	Electrogoniometer system attached about the knee	88
3.12	The optoelectronic system	91
3.13	Light sources attached to pertinent anatomical landmarks on body of subject	92
3.14	Surface electrodes, alcohol swab and electrode paste	95
3.15	The pre-amplifier	99
3.16	Circuit diagram for the differential amplifier	99
3.17	Circuit diagram for high pass filter and amplifiers	101
3.18	Circuit diagram of the rectifier and averager used in the Locomotion Laboratory	102
4.1	Influence of placement of electrodes on the derived electrical muscle activity	113
4.2	A repetitive time varying signal	116
4.3	Electrode placement on m. rectus femoris (Subject A)	119
4.4	EMG signal processing for Subject C (m. vastus lateralis). Top electrode position	123
4.5	EMG signal processing for Subject C (m. vastus lateralis). Lowest electrode position	124
4.6	Repeatability curves for different electrode positions, Subject F	125
4.7	Numerator and denominator of the variance ratio as a function of window length	127
4.8	Repeatability curves for different speeds of walking, Subject A	129

LIST OF ILLUSTRATIONS (cont'd)		PAGE
4.9	Repeatability curves for different speeds of walking, Subject D	130
5.1A	A typical normal knee-angle/hip-angle diagram, Subject A	145
5.1B	Direction of flexion and extension	146
5.2	Three superimposed angle-angle diagrams	147
5.3	P_A versus L/B	150
5.4	Three superimposed angle-angle diagrams for normal subject A	160
5.5	Plots of area, perimeter and P_A versus average walking speed for normal subject A	162
5.6	Four superimposed angle-angle diagrams for the left (prosthetic) leg of the A/K amputee	168
5.7	Five superimposed angle-angle diagrams for the right leg of the A/K amputee	169
5.8	Plots of area, perimeter and P_A versus average walking speed for the left (prosthetic) leg of the A/K amputee	170
5.9	Plots of area, perimeter and P_A versus average walking speed for the right leg of the A/K amputee	171
5.10	Plots of P_A versus average walking speed for both legs of the A/K amputee with each measured point representing a different setting of the prosthesis	172
5.11	Angle-angle diagrams obtained in Expt. I	189
5.12	P_A versus stimulator-on time for Expt. I	195
5.13	Angle-angle diagrams obtained in Expt. II	200
5.14	P_A versus stimulator-off time for Expt. II	201
5.15	Angle-angle diagrams obtained in Expt. III	207
5.16	P_A versus stimulator-off time for Expt. III	208
6.1	Input-output data for footstep #4	233

LIST OF ILLUSTRATIONS (cont'd)		PAGE
6.2	Model predictions for footstep #4	238
A1.1	Flow-chart for program 10E2.FOR	245
A1.2	Flow-chart for program 10XYX.FOR	247

LIST OF TABLES

TABLES		PAGE
3.1	Characteristics of a typical differential amplifier	100
4.1	Optimal electrode positions and processor ranges for six different subjects	131
5.1	C.P. patient neurological data	154
5.2	Best linear fits for normal gait	163
5.3	Stance/swing ratios for A, P of angle-angle diagrams taken from a normal subject	166
5.4	Best linear fits for amputee gait	174
5.5	Stance/swing ratios for A, P of angle-angle diagrams taken from the prosthetic leg of the A/K amputee	175
5.6	Stance/swing ratios for A, P of angle-angle diagrams taken from the right (intact) leg of the A/K amputee	178
5.7	Stance/swing ratios for A, P of angle-angle diagrams taken from the C.P. patient	181
5.8	Summary of results for normal, A/K and C.P. subjects	181
5.9	Loop parameters derived from data in Experiment I	194
5.10	Footswitch parameters for Experiment I	197
5.11	Loop parameters derived from data in Experiment I	202
5.12	Footswitch parameters for Experiment II	204
5.13	Loop parameters derived from data in Experiment III	209
5.14	Footswitch parameters for Experiment III	212

LIST OF TABLES (cont'd)		PAGE
6.1	Determination of the order of the system dynamics	234
6.2	Statistics for determination of delay b	235
6.3	Final parameter values and confidence limits for footstep #4	237
6.4	Chi-square statistics for footstep #4	239
6.5	Sequencing of inputs in order of decreasing weighting	241

CHAPTER 1
INTRODUCTION

This thesis was essentially conducted within the confines of the Locomotion Laboratory, Department of Biomedical Engineering, Chedoke Rehabilitation Centre, Hamilton. The thesis is multidisciplinary in that an effort has been made to incorporate the viewpoints of a number of different disciplines in this work. Some of these are: Electrical Engineering, Physiology, Anatomy, Statistics and Mathematics. The thesis is directed generally towards a deeper understanding of normal and pathological biped locomotion. Attention has been focussed mainly on kinematic and electromyographic aspects of gait. It involved theoretical considerations in respect of statistical analyses with associated physical interpretations, model building and model testing and practical work concerned with the conducting of experiments on both patients and normal volunteers as well as the collection of pertinent data. The primary goals of clinical personnel involved in locomotor rehabilitation are:

- (1) The better design of prostheses for disabled persons.
- (2) The assessment of locomotor function for both diagnosis and evaluation of therapeutical and surgical techniques associated with various gait

pathologies.

The above goals cannot be attained without the appropriate melding of science and technology with medicine. This thesis contributes to the realization of the above goals by introducing original and objective methods of measuring and assessing locomotor function. In particular, the research presented in this thesis is concerned with the processing and analysis of surface electromyographic (EMG) signals, the analysis and interpretation of joint angle trajectories and an initial attempt to relate the EMG signals to the pertinent joint angular histories at the hip and knee using methods of time series analysis. The specific contributions of the research presented in this thesis are now summarized according to each chapter.

Chapter 2 is a general background review of the research literature associated with those aspects of human locomotion considered in this thesis. It is a review which gives the uninitiated reader a rapid overview of what is a complex and extensive field. The chapter is divided into four distinct sections. Section 2.1 is a review of kinematic investigations into gait. Section 2.2 is a corresponding background review of EMG studies associated with human locomotion. Section 2.3 is a brief description of the anatomy of the lower limb while. Section 2.4

summarizes the phasic activity and functions of the various muscle groups in the lower limb during locomotion. The information reviewed in this chapter is used in Chapters 4 and 6 and has, in addition, been published in the form of an educational monograph (Hershler, 1977a).

Chapter 3 describes the experimental techniques utilized in the Locomotion Laboratory for the measurement of spatial and angular trajectories and the recording of EMG signals. The three measuring systems described are respectively the stroboscopic flash-photography system originally developed by Milner et al (1973), the electrogoniometer system developed by members of the Biomedical Engineering Department after the design of Lamoreux (1971) and the optoelectronic system recently introduced by Brugger and Milner (1977). The advantages and disadvantages of each system are critically reviewed so as to allow the reader a unique comparison of the various measuring systems in the Laboratory. An internal progress report (Hershler, 1976) describes even further the stroboscopic flash-photography system and contains details on how the data are interfaced with the CDC6400 computer at McMaster University. An additional progress report (Hershler, 1977b) summarizes the contents of Chapter 3. The experimental descriptions in Chapter 3 form an integral part of the remainder of the thesis.

Chapter 4 presents a statistical analysis of surface electromyographic signals collected from selected skeletal muscles during normal locomotion on a level surface. A statistical criterion originally proposed by Hershler and Milner (1976) allows the user to determine a practical optimal processor for rectifying and averaging the EMG signal. The statistical criterion is essentially a variance ratio which quantifies the repeatability of a given number of EMG signals. The same method used with multiple arrays of electrodes allows one to find an optimal position for placement of the electrode pair on the muscle surface. In this case the electrode pair that provides the most consistent and repeatable information for a chosen number of footsteps is optimal. Varying statistical consistencies over the surface of the muscle suggest a possible correlation between muscle function and statistical significance of EMG activity. This is a unique and interesting development in the study of EMG signals and the various results of this chapter have been published in an internal progress report and are to be published in IEEE Transactions on Biomedical Engineering (Hershler and Milner, 1977a). The methods introduced in this chapter are used in the modelling procedure outlined in Chapter 6.

Chapter 5 covers original research relating to kinematic information presented in the form of knee-angle/

hip-angle diagrams. Cyclic loops which had been utilized in the past mainly for their visual representation have been quantified using a shape recognition technique. Essentially, parameters such as the area A , perimeter P and the dimensionless quantifier $P_A = P/\sqrt{A}$ have been examined for various kinds of gaits (normal, A/K amputee and cerebral palsy) under different conditions. This quantification coupled with physical interpretations of the parameters extracted from the angle-angle diagrams produced significant results. In particular, the physical interpretations include aspects regarding range, coordination and overall control. Statistical analyses of the various parameters extracted, when coupled with a visual display of the pertinent angle-angle diagrams, rendered a more complete assessment of locomotor performance and function. The chapter is divided into two sections. Section 5.1 is a report on quantitative analyses of angle-angle diagrams associated with 5 normal subjects, an above-knee (A/K) amputee and a cerebral-palsied (C.P.) patient who had an implanted cerebellar stimulator. Also included is a discussion of the limitations of visual inspection of the diagrams as well as a delineation of a number of key parameters which are of value in interpreting and assessing the diagrams and making the data from them amenable to statistical analyses. These results elicited significant observations regarding the overall coordination and control

during each gait and made it possible to provide substantial answers towards the following questions:

- (1) What are the control mechanisms inherent in each of the gaits?
- (2) How does a change in the alignment of the prosthesis effect the gait on both sides of the A/K amputee?
- (3) What are the effects of switching the stimulator off (on) on the gait of the C.P. patient?

The results of section 5.1 have also been written up in a progress report (Hershler and Milner, 1977b). Section 5.2 is an example of the multidisciplinary character of this thesis whereby a neurologist, neurosurgeon, pediatric resident and three bioengineers contributed as a group to the in-depth analysis and interpretation of the C.P. gait study. The joint efforts of this group, which included the author of this thesis has resulted in the publication of this work in the form of a monograph (Milner et al, 1977). It was gratifying to note that the ideas on parameter quantification of angle-angle diagrams suggested by this author in section 5.1 were utilized in this work. Assessment of the efficacy of a cerebellar stimulator implanted in the C.P. patient was accomplished and the quantification of angle-angle diagrams emerged as a powerful

adjunct to the visual assessment of angle-angle diagrams in the diagnosis and interpretation of locomotor pathology.

Chapter 6 describes an initial attempt, using the methods of time series analysis, at modelling the transfer function between several inputs given by the EMG signals of selected muscle groups and an output which is either the hip or knee angle trajectory. Utilization of this model produced several interesting observations.

- (1) The model was able to suggest which individual muscles (of a larger muscle group) were synergistic.
- (2) The adequacy of the model showed whether the inputs chosen were good predictors of the output.
- (3) The modelling results allowed a weighting to be associated with each muscle input which gave the relative contribution of each input in predicting the output.

Relevant information from Chapters 2, 3 and 4 was used in the modelling procedure. The thesis has been written in such a way that each chapter is independent containing pertinent conclusions and suggestions for future work. In order to achieve an overall unity, however, where possible

each chapter refers to other parts of the thesis which cover material related to the research work being discussed.

CHAPTER 2

A BACKGROUND REVIEW OF HUMAN LOCOMOTION

2.1 , Historical Survey of Investigations Into the Kinematics of Gait

The study of movement is divided into:

(1) kinematics, the position of a body in space at a particular time and

(2) kinetics, the forces which produce or alter motion. The present review covers papers investigating the kinematics of gait. Based on Edelstein (1965) we define the gait cycle as one stride of the same leg which encompasses the events from the moment one heel strikes the floor until the same heel contacts again. This cycle consists of two phases, stance and swing. Stance phase is comprised of heel-strike (HS), foot-flat (HT), mid-stance (when the trunk is vertically atop the extremity) followed by heel-off (HO) and toe-off (SW). Swing consists of acceleration, mid-swing and deceleration. Figure 2.1 depicts the various phases of a normal gait cycle.

In the study of certain types of pathological gait, however, it is not as simple to recognize the various phases

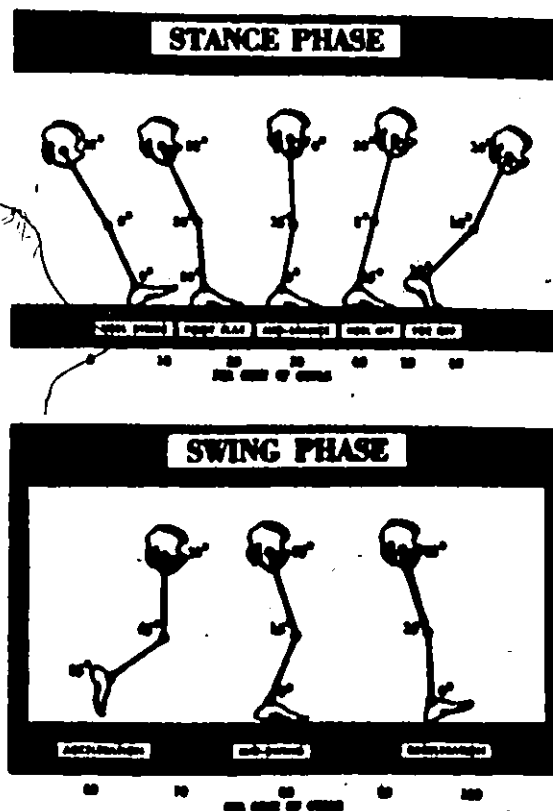


Figure 2.1
Kinematics of Normal Ambulation
(From Edelstein, 1965)

of the gait cycle. This is due to the fact that, at times, onset of stance (ST) can be caused either with the toe (dropfoot) or with the heel (HS) and the toe could be making contact with the ground throughout swing (SW) as occurs during toe-dragging. Hence for pathological gait we again consider two phases for the gait cycle but we label them as follows:

ST: onset of stance and

SW: onset of swing

2.1.1 Pre-20th Century:

Aristotle (384 B.C.-322 B.C.) was probably the earliest person in our history to comment meaningfully on animal gait. The New Encyclopaedia Britannica (1976) records that one of Aristotle's four biological treatises covered the locomotion of animals and in *De Incessu Animalium* (On the Progression of Animals) the problems of local motion were considered by constructing a kind of animate mechanics of limbs according to their numbers and their kinds of joints.

Leonardo da Vinci (1452-1519) the Italian artist and scientist, in addition to being ranked in artistic merit with Michaelangelo and Raphael as one of the three masters of the High Renaissance, was one of the first to make a scientific study of human and animal motion. Among his most famous treatises is the *Treatise on the Flight of Birds* where for the purposes of secrecy notes were written in inverted script from right to left so that they could be read only if held to a mirror. (Merit Students Encyclopaedia, 1976):

Steindler (1953), however, considers Borelli (1608-1679) to have the distinction of being the first truly great trailblazer in the field of gait studies and analysis. He confers this distinction on Borelli not so much for what he

did in the mechanical analysis of locomotion itself but because of his fundamental concept of muscle action. Borelli was also the first to determine the centre of gravity which is of fundamental importance in the calculation of the events of locomotion. In his book, *De Motu Animalium*, Borelli (1682) describes the forward displacement of the centre of gravity beyond the supporting area and the manner in which the forward swinging of the limbs saves the body from losing balance. Borelli thus laid the foundation for the concept of propulsion and restraint in gait.

Following the work of Borelli, very little was accomplished in the study and analysis of gait until the first half of the nineteenth century. Wilhelm and Edward Weber (1836) observed and measured the alternation of swing and support, the inclinations of the trunk in either phase, the relationship between the duration and length of the step. They also initiated investigations into the muscle effort involved in propulsion and restraint.

Marey (1885) was probably the first to contribute to gait analysis using the technique of photography. Successive exposures were made on the same photographic plate by means of a rotating disk in front of the camera. The subject was dressed entirely in black on which brilliant metal buttons and shining bands were attached to represent

joints and bony segments. The subject, illuminated by the sun, was photographed as he walked in front of a black screen. This method is known as geometric photography, since the pictures obtained show points and lines only. It is interesting to note that nearly a century later variations of this method are still in use in gait laboratories.

The photographic method used by Marey was modified by Braune and Fischer (1895). They substituted Geissler luminous tubes for the white strips but took from six to eight hours to get the subject ready for a gait study. To these men, however, belongs the credit for the first rational scientific investigation of the problems in human locomotion. Their work represented a monumental effort of calculative investigation into the velocities, accelerations and forces of the various body segments during locomotion.

2.1.2 Current Research in Gait (20th Century)

Bernstein and his associates (1935) published a comprehensive volume on research into the biodynamics of locomotion. In this study the accuracy obtained by Braune and Fischer was questioned and techniques developed to improve this accuracy. In all, the gait of 65 subjects was investigated with many more photographs taken of the subject during one complete cycle of walking.

Braune and Fischers' data for locations of the centres of gravity of the various segments, their radii of gyration and their relative masses were used in the Bernstein study but in addition, experiments included investigation of normal walking of men both carrying weights and unburdened as well as an analysis of fatigue effects due to these conditions. The analytic method pioneered by Braune and Fischer has not been utilized extensively but has attained some degree of accuracy in the hands of Liberson (1936) and Elftman (1939a). The analytic method consists of the theoretical calculation of the forces producing motion based upon a knowledge of the centres of gravity and the acceleration of the body segments involved. The forces thus calculated are attributed to the muscles acting in the general direction of the calculated force.

During the past forty years, Elftman has been a major contributor to the study of gait. Included among numerous papers on the dynamics of human locomotion are the distribution of pressure in the human foot (1934), the measurement of external forces in walking (1939a), forces and energy changes in the leg during walking (1939a), the forces exerted by the ground (1939d) and the rotation of the body in walking (1939c), the work done by muscles in running (1940), the actions of muscles in the body (1941), torsion of the lower extremity (1945), basic pattern of human

locomotion (1951), body dynamics and dynamic anthropometry (1955a), knee action and locomotion (1955b), Biomechanics of muscle (1966), basic function of the lower limb (1967), and dynamic structure of the foot (1969).

Saunders et al (1953) using a variety of techniques including force plates and cinematography, analysed various factors involved in normal or minimum energy-wasting gait. Using as a model stiff compass type gait in which no movement occurs at hip, knee, ankle and foot joints, Saunders et al (1953) listed six determinants of gait that decrease the excursion of the centre of gravity and thus decrease energy expenditure.

The six determinants listed were as follows:

- (i) Pelvic rotation
- (ii) Pelvic tilt
- (iii) Knee flexion during stance
- (iv,v) Knee and ankle interaction (foot and knee mechanisms)
- (vi) Lateral displacement of the pelvis

Schwartz and Heath (1947) measured the temporal and pressure components of gait in the shod and unshod foot. Although the measurements were undoubtedly affected by the presence of pressure-sensitive disks taped to the plantar surface of the foot, Schwartz and Heath found that for pathological


gaits resulting from various functional disabilities, the duration of the stance phase was significantly greater than normal and the pressure curves were grossly different from normal. Thus they concluded that variations within the limits of normal locomotion could not produce a record characteristic of any significant functional disability.

Smith et al (1960) extended the work of Schwartz and Heath (1947) in analysing the temporal components of motion in human gait with the aid of a device called the electrobasometer. The function of such a device is based on the principle of passing a very small load current (approximately $100 \mu A$) through the subject's body and through a metallic runway on which the subject walks. The contact of the foot with the walkway activates electronic relays which time separately the contact movements of each foot. Results of their systematic studies catalogued the time characteristics of stride and contact movements in walking and running, the effects of the shoe on gait, sex differences in walking and fast walking, the change in locomotion with age, the influence of artificial weights on movements in walking and the correlation between time values of gait movements and body height and weight. The main criticism relating to their extensive study was their neglect to investigate the influence of a variation in walking speed on their measured variables. Normal pace and maximum pace are meaningless

terms unless adequately quantified.

Using a method of interrupted - light photography, Murray et al (1966) recorded 16 displacement patterns of locomotion of the same 30 normal men for both free and fast speed walking. It was found that the subjects accomplished the forward speed of faster walking by increasing both the stride length and the cadence. Increased stride lengths were accomplished mainly by increased transverse rotation of the pelvis, increased hip flexion of the forward extremity at the time of ipsilateral heel-strike and increased ankle extension of the rear extremity at the time of contralateral heel-strike. In the faster speed of walking, the stride width increased and the out-toeing angle decreased.

Grieve and Gear (1966) also observed that steplength and cadence varied linearly with forward walking speed for normal adult subjects. An increase in walking speed for normal subjects was achieved by uniform and characteristic changes in both steplength and cadence. The time of swing and time of support were found to be inversely proportional to walking speed. Time-distance measurements were found to be reproducible when the entire velocity relationships were considered. This particular feature of gait viz. that many of its parameters are velocity dependent could assume even more importance in the study of pathological gait. It has



been observed that patients with diseased joints have a slower than normal walking speed. Hence it becomes crucial that in the study of their gait one distinguishes which variations from normal are due to differences in walking speed and which due to gait abnormalities.

Grieve (1968) published an extremely important paper on the "whole range" approach to the study of gait. He argued that studies based upon the whole range of speeds would go further towards an understanding of the walking mechanism than a further elaboration of the fixed-cadence approach. In addition he proposed a new format for presentation of joint angle histories. He suggested that, since clinical acceptability depends upon the information being presented in a palatable form, the joint angles of the lower limb be plotted against each other. These angle diagrams present walking cycles in cyclic loops with a further attraction that normal and abnormal gaits produce characteristic, easily recognisable, loops. Grieve (1968) himself remarks . . . "They present cycles in cyclic form. By contrast angle-time diagrams appear on-line as graphs of variable length, more graphs are required to present the same amount of information and there are beginning and end-discontinuities which hinder the visualisation of a cyclic process . . ."

Leavitt et al (1971) using an electronic goniometer and foot-switches completed a gait analysis on 20 subjects. There are, however, a number of limitations associated with their work. No consideration was given to the variation in the gait parameters with speed of walking. Also no mention was made of the possibility of calibration error due to movement and possible slippage of the goniometer harness during the gait study. Although their study revealed that characteristics of gait could be quantified with their method, they did not present their findings in the most clinically digestible form.

Smidt et al (1971) describe an accelerographic method which uses harmonic analysis to evaluate gait. The results of the harmonic analysis on 22 normals and 5 patients were converted to a harmonic ratio, which is the sum of the coefficients for the even numbered harmonics divided by the sum of the coefficients for the odd-numbered harmonics, and which provided an index of smoothness for the acceleration curves. From their data obtained from the study, the following classification scheme for harmonic ratios was suggested to indicate smoothness of walking. Normal implies values greater than 2.00; fair implies 1.50 to 2.00; poor implies 1.00 to 1.49 and very poor is less than 1.00.

Lamoreux (1971) using a sophisticated exoskeletal goniometric motion-measuring device measured several kinematic variables on normal subjects and paid particular attention to the effects of changes in walking speed on these variables. These variables include step length, step frequency, pelvic motions in space, hip, knee and ankle joint rotations. His work stands out by his attention to detail and consideration of the many degrees of freedom involved.

Johnston and Smidt (1969) made a three dimensional study of hip motion using an electrogoniometer. With a potentiometer oriented in each of three primary axial planes, 33 normal subjects were studied and average angular motion at the hip joint was 52 degrees in the sagittal plane, 12 degrees in the coronal plane and 13 degrees in the transverse plane.

Kettelkamp et al (1970) made an electrogoniometric study of knee motion in normal gait using the same electrogoniometer system described in detail by Johnston and Smidt (1969). In this manner they were able to measure the knee angles in the three planes. Since potential differences existed between the actual knee motion and motion of the goniometer arms, due to the fact that the apparatus was not located directly at the knee joint, corrections to the

knee-joint motion were calculated analytically assuming the knee-joint to be a ball-and-socket joint. The magnitude of correction for extension and flexion did not exceed 2 degrees. To investigate the effects of inaccurate placement of the goniometer with respect to the true axes, they calculated the values for an error of 12.7 mm in both directions along the sagittal, coronal and transverse axes and found that the effects of the assumed malalignment between the goniometer and the centre of the knee joint were insignificant when compared with the accuracy of measuring rotation with dynograph recordings.

Sutherland and Hagy (1972) using motion picture cameras measured gait motions in 3 planes. The film was processed and then viewed, frame by frame, on a Vanguard Motion Analyzer. This method of measurement avoids many of the disadvantages of the electrogoniometric method which requires a moderate amount of apparatus to be attached to the patient and which might, in fact, alter the patient's normal gait. With this method no apparatus is attached to the patient and measurements can be made of both lower extremities at the same time. The motion picture record is permanent and can be repeatedly checked for accuracy or for additional measurements. The principal disadvantage of this method is the somewhat exacting and time-consuming technique of extracting the data.

Winter et al (1972) developed a television-computer technique to record and process image information required for the kinematic analysis of human gait. Reflective markers were attached to pertinent anatomical landmarks on the subject's body and the trajectories traced out by these markers were tracked by means of the television camera for up to 5 footsteps. An appropriate computer interface allowed temporal and spatial information to be calculated and stored in the computer for further analysis.

Milner et al (1973) followed on the suggestion of Grieve (1968) and used knee-angle/hip-angle diagrams to assess locomotor function. Using a stroboscopic photographic method to acquire the relevant data they showed that a normal subject exhibited characteristic angle-angle diagrams for five different speeds. They also analysed pre-operatively the gait of 5 patients suffering from osteo-arthritis of either the left or right hips. The shapes of their angle-angle diagrams differed from normal and the shape of the diagram for the affected side differed radically from that of the contra-lateral side. It was clear that this method of representing the data was extremely useful because of the large amount of information conveyed in a simple manner and also in view of the distinct angle-angle patterns obtained for the patients tested.

Milner et al (1974) followed up the above pre-operative study on the same patients. From an examination of the pre- and post-operative angle-angle plots it was seen that there had been a dramatic change in the post-operative condition. Also, the shapes of the left and right side patterns were very similar post-operatively.

Bajd et al (1974) developed a simple method for measuring step length based on a trigonometric formula and using only data provided by an electrogoniometer system involving both legs of the subject. A 3% average error was obtained.

Winter et al (1974) used a T.V. computer system to study aspects of noise reduction inherent in the measurement of kinematics of locomotion. They noted that although this noise may not be visibly evident in the spatial or angular trajectories it could cause large inaccuracies when velocities and accelerations are determined by direct differentiation. Spectral analysis of kinematic data obtained from the T.V. computer system indicated that the spatial signal was contained in the first 7 harmonics. Joint angles obtained from the spatial co-ordinates have the same bandwidth. Thus digital filtering with an upper cut-off at the 7th harmonic (i.e. 6 Hz) reduced the high frequency noise content of the data so that linear and

angular velocities could be calculated by direct differentiation.

Smith et al (1976) used the same approach as Milner et al (1973,74) to assess pre- and post-operatively 12 patients undergoing the Attenborough knee joint replacement. The results again demonstrated that angle-angle diagrams enhanced the objective assessment of the knee-joint replacement procedure.

Grundy et al (1975) improved upon the methods of Schwartz and Heath (1947) by measuring the forces under the foot using a high sensitivity force-plate combined with simultaneous filming of the sole of the foot. The recording of the data and the calculations and plotting of results were much simplified by computer aid.

Up to this point, the review has mainly considered papers dealing with kinematic measurements in the sagittal plane. This does not imply that motions in other planes are of minimal concern, but rather that this is a result of the experimenter's difficulty in measuring these transverse motions easily and accurately. Levens et al (1948), however, measured the transverse rotations of the segments of the lower extremity (with respect to the longitudinal axes) during locomotion. Using three synchronized 35

millimeter motion-picture cameras, they measured the average relative transverse rotation of the tibia with respect to the femur to be 8.7 ± 2.7 degrees and the average relative transverse rotation of the femur with respect to the pelvis to be 8.4 ± 2.5 degrees. They found that inward and outward rotations of the segments are related to weight-bearing and restrictions placed upon the normal transverse rotations will, to varying degrees, modify the synchrony and rhythm of walking. Eberhart et al (1968) using a similar measuring system on 12 normal subjects obtained similar ranges for the relative transverse rotations (w.r.t. longitudinal axes) of the segments of the lower extremity. They also measured the rotations of the leg segments in the frontal plane and found that for eight normal subjects during level surface walking that the range never exceeded 5 degrees.

It is clear, therefore, that the greatest angular and linear displacements of the leg segments occur in the plane of progression (sagittal plane). Since a measuring system, which would enable one to measure these extra motions, was unavailable, this thesis concerns itself solely with motions in the sagittal plane.

2.2 Review of Electromyographic (EMG) Investigations During Gait

2.2.1 Introduction:

Anatomical deduction is historically the oldest and most widely employed method of determining the function of a muscle, to ascertain its origin and insertion, and to deduce what motion would occur should the muscle undergo contraction. This procedure had obvious limitations and has led to many erroneous conclusions. Palpation, which reached its highest development in the hands of Scherb (1927) consists in the exploration of the individual muscle with the examining fingers while the subject is walking on a treadmill. The alternate hardening and softening of the muscle in relationship to the position of the extremity permits some evaluation of its function. The accuracy of such a method is open to question; and the results cannot be utilized for quantitative data.

Electromyography, which is the amplification and recording of the action potentials of muscles as a method of studying their activities, is a relatively new tool. Combined with other techniques, the simultaneous recording of action potentials from various individual skeletal muscles provides the best information on the role of skeletal muscles in simple and complex motions. Its main

advantage is its ability to reveal the precise phasic relationships of muscle actions.

The interested reader will note that in the following survey and in section 2.4 of this chapter there may exist differences in the conclusions reached by independent experimenters. These can be due to differences between the interpretation of the data, differences in type and location of electrodes used and certainly differences of interpretation in respect of citing zero or non-zero levels of activity (Paul, 1971).

Chapter 4 devotes attention to the disturbing realization that different experimenters use different methods of processing to examine the electromyographic signals. A statistical criterion has been suggested which allows the user to determine the optimal electrode position, type of electrode and form of signal processing.

The other relevant factor is the different walking speeds at which the tests were conducted. In most cases the walking speeds were not reported exactly and this is of particular importance as demonstrated by Milner et al (1971a). (Grieve (1968) and Lamoreux (1971) both stress this point - not necessarily in relation to EMG.)

2.2.2 Review of the literature

A lengthy and concentrated study of human locomotion was conducted by the University of California's (1953) Biomechanics Laboratory (formerly the Prosthetic Devices Research Project) in Berkeley using electromyographic data.

Close and Todd (1959) studied the phasic EMG activities of the muscles of the lower extremity as well as the effects of tendon transfer. The type of question they were concerned with was: "... if the tibialis anterior, a swing phase muscle is transferred posteriorly to the calcaneus, will it be able to change its phase of action and serve as a stance-phase muscle as does the soleus muscle which it is intended to replace or re-enforce? ..." The study which was begun in 1954 consisted of individual electromyographic tests conducted on 125 muscles on which tendon transfer had been done. About 85 patients were studied. In many cases it was possible to make a pre-operative as well as a post-operative study of the transferred muscle. In the subjects tested it was possible to stimulate the muscle such that the position of the recording electrodes could be ascertained. Dual-wire internal electrodes were used. Close and Todd's (1959) results clearly depict the phasic character of the various leg muscles. It is also clear from their diagrams that walking elicits very slight EMG activity in the thigh and

leg muscles compared with voluntary free movements. Close and Todd concluded that tendon transfers generally retain their pre-operative phasic activity. They also appear to regain their pre-operative duration of contraction and electrical intensity. A non-phasic transfer usually fails to assume the desired action of the muscle for which it has been substituted. Thus a phasic transfer is generally superior to a non-phasic transfer.

Radcliffe (1962) gives a graphic account of the interaction between the knee and ankle joints and of the phasic actions of the major muscle groups in the leg during a typical walking cycle. The curves shown in his paper represent the average of actual measurements recorded during studies of four male subjects. Schematic drawings are presented of the major muscle groups of the lower extremity showing the major mechanics of their functions in the sagittal plane. His explanations of the role these muscles play during normal locomotion are to be commended for their conciseness and clarity.

Joseph (1964) used electromyographic and cinematographic techniques to study the phasic activities and functions of the lower limb skeletal muscles during normal locomotion on a level surface. He observed in a limited investigation that the m. quadriceps femoris showed

several differences in activity for different ways of walking. In quick walking (62 steps/min) its activity in both the stance and swing phases was much more marked but not lengthened in time. In slow walking (36 steps/min) with normal steplengths the activity is very slight but with long steps at the same cadence the activity was very much increased. Similar investigations on the m. hamstrings did not show these differences. Joseph (1964) concluded that simple statements about muscle activity can be made only in relation to walking in which the length of the step and the number of steps per minute are known as well as the sex of the subject, the type of shoes worn and the state of the ground on which the walking is taking place.

Liberson (1965) using techniques of simultaneous accelerography, electromyography, muscle tensiography, electrogoniography and cinematography showed that there existed certain correlations between the variables measured during normal gait. He also found that these correlations between different parameters of gait were affected by certain neurological or orthopaedic diseases. In particular Liberson demonstrated significant correlations between vertical and horizontal accelerograms and muscle action. In this manner it was concluded that both the m. gluteus maximus and m. gastrocnemius contribute to forward acceleration in ambulation.

Battye and Joseph (1966) investigated a group of 14 subjects (8 male and 6 female) with the aid of a telemetering electromyograph during normal walking on a flat surface. The muscles investigated were the m. tibialis anterior, m. soleus, m. quadriceps femoris, m. hamstrings, m. gluteus medius and maximus and m. sacrospinalis. Surface electrodes were used and the signals picked up were amplified before transmission over a radio link between the subject and a stationary receiver. The sites chosen for the electrodes were carefully investigated to reduce or eliminate "pick up" from adjacent muscles and a detailed statistical analysis of the phases of activity of these muscles was presented.

Sutherland (1966) using a combination of cinematography and electromyography studied the phasic activity in the seven plantar-flexor muscles, the m. vastus medialis and m. gluteus maximus for eight normal subjects (one female and seven males) during normal walking on a level surface. The study confirmed the indirect knee-stabilizing function of the ankle plantar-flexors in walking on the level. By combining simultaneous electromyograms and motion pictures of gait the periods of activity of the ankle plantar-flexors and of increasing knee extension and dorsiflexion of the foot were shown to correspond. Only at the end of the period of ankle plantar-flexor action did plantar-flexion of

the foot occur. Knee extension took place after the cessation of activity of the quadriceps muscle and did not appear to be produced by quadriceps action. An alternate hypothesis was offered instead of the theory that related knee extension in the stance phase to movement of the center of gravity in front of the line of support. The hypothesis suggested that knee extension during the stance phase, in ordinary walking on the level, is brought about by the force of the ankle plantar-flexors resisting the dorsiflexion of the ankle, this dorsiflexion being produced by the resultant of the extrinsic forces (kinetic forces, gravity and the floor reaction). The resultant of the extrinsic forces is greater than the intrinsic force, as manifested by the increasing dorsiflexion of the foot which occurs up until heel-off begins. Sutherland (1966) suggests that the restraining function of the ankle plantar-flexors in decelerating forward rotation of the tibia on the talus is the key to their stabilizing action.

Gray and Basmajian (1968) made a comprehensive study of the EMG activities in the muscles of the leg and foot. Using fine wire intramuscular electrodes the various phasic activities were delineated for ten "normal" and ten flatfooted subjects for five different ways of walking. One interesting observation expressed by the authors was that contingent arch support by the muscles rather than

continuous support was the rule with muscles being recruited to compensate for lax ligaments and special stresses during the walking cycle.

Basmajian and Greenlaw (1968) using a combination of electromyography and cinematography studied the functions and phasic activities of the muscles about the hip joint during normal locomotion and also during standing.

Paul (1969) studied the action of some two-joint muscles in the thigh during walking. The phasic activities of these muscles were interpreted in association with the turning moments in the sagittal plane developed between shank and thigh and thigh and trunk as obtained from experimental measurements of normally walking subjects. The periods of phasic activity of relevant muscles, however, were drawn from the University of California Report (1953).

Milner et al (1971a) investigated, using indwelling electrodes, the nature and timing of muscular control exercised by several leg muscles in the course of normal walking by six male subjects at various speeds. The effects on the EMG activities, of imposing the constraint of pace frequency on the walk, were also studied. From their results it was suggested that when the subject was permitted to walk without the imposition of a pace frequency

constraint he selected a walking pace for a set speed in such a manner as to allow for a minimum of muscular activity. Arguing that the EMG is a measure of muscular energy it was suggested that a subject chooses the most comfortable walking speed to minimize "energy consumption" and permit a reasonable propulsion speed. One criticism of their work (which would apply equally well to most other investigators of the EMG activities of the leg muscles during gait) was their use without justification of a low pass filter having a 4.4 msec time constant. The randomities exhibited by such rectified and averaged EMG envelopes are a function of this time constant as will be shown in Chapter 4. In addition, no information was given on precisely where the electrodes were inserted into the muscles. These facts have a bearing on the interpretation of random variations in the EMG activity.

Paul (1971) analysed certain gait parameters during 17 test runs on 14 subjects. In this study the cyclical movements of the limb segments during level walking were measured by cine-photography and ground to foot force actions were measured by a force plate. From this information the moments developed between leg segments were calculated. Surface electrodes were applied over selected groups of muscles and their results were analysed in respect of the phasic activity of the muscles over a specified

threshold value. There was not sufficient information, however, to make a correlation of the values obtained with walking speed. It was concluded that in experiments intended to obtain the relationship between the electrical activity of muscles and the forces developed by the same muscles, a careful recording of potentials from all agonist and antagonist muscles acting at the joint should be carried out and also that the length of the muscle relative to its length in some standard configuration of the limb should be recorded. The phasic activity of the muscles of the leg in locomotion as reported by several experimenters when compared are found to contain discrepancies between the experimenters which may be accounted for by differences in technique and analysis but also may correspond to variations in stride length or walking speed of the subject. Thus all such data should be reviewed with these considerations in mind.

Rozin et al (1971) measured the timing and duration of ground contact, electrogoniometry of the ankle (dorsi- and plantar-flexion), knee (flexion-extension) and hip (flexion-extension and abduction-adduction) joints and the EMG patterns using needle electrodes of 8 ankle and knee muscles in 10 (7 male, 3 female) subjects. The m. hamstrings and m. flexor hallucis longus were not examined for EMG activity because the needle electrode gave rise to pain

and a change in the natural gait pattern. No measurements of walking speed were made. With the exception of the m. peroneus longus, all the muscles examined showed phasic activity during a gait cycle.

Ralston et al (1976) dealt with the relation between the EMG of human m. rectus femoris, the movement of the lower leg (shank) and the force developed at the ankle, during the knee jerk and during voluntary contraction. Through such studies it was hoped that the role of muscle activity in relation to the various phases of the walking cycle might be more fully analyzed. Electrical activity (using both surface and embedded wire electrodes) in the m. rectus femoris, acceleration of the shank and force at the ankle were simultaneously recorded in 2 human subjects during reflex and voluntary extension of the knee. Time lags of the order of 30-40 msec occurred between onset of electrical activity and onset of extension and between cessation of electrical activity and onset of flexion. Time lags of the order of 200-350 msec occurred between cessation of electrical activity and cessation of tension and/or motion. It was pointed out that much of the present evidence on the roles of muscles in human movement such as walking should be reevaluated in terms of tension, rather than in terms of EMG alone since consideration should be given to the duration of contractile activity rather than

merely the duration of EMG activity.

2.3 Anatomical Aspects of the Muscles of the Lower Limb

2.3.1 Introduction

In an effort to keep this thesis as complete as possible it has been decided to include this fairly detailed description of the skeletal system and musculature of the lower half of the body. Most of the content has been taken from Basmajian's text (1970) but detail has been sacrificed for ease in perusal by one not conversant with anatomy.

2.3.2 Anatomical Aspects of Human Locomotion

The skeletal system that is being considered during the process of human locomotion consists of:

- A. The hip bone
- B. The femur or thigh bone
- C. The tibia and fibula
- D. The patella or knee-cap
- E. The bones of the foot

A. The Hip Bone (Fig. 2.2)

The acetabulum is a socket for the reception of the spherical head of the femur or thigh bone and it faces lateralwards, downwards, and slightly forward.

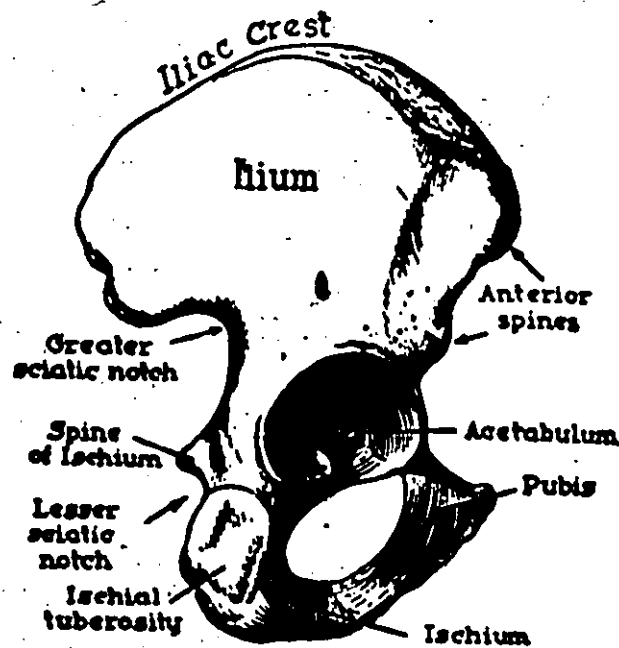


Figure 2.2
Outer Aspect of Right Hip Bone
(From Basmajian, 1970)

B. The Femur or Thigh Bone (Fig. 2.3)

The femur or thigh bone is the longest bone in the body being about 65 cm in length. Its ends are very specialized for the hip and knee joints but the shaft is relatively simple. The shaft slopes downwards and medially while the spherical articular head fits accurately in the acetabulum of the hip bone. As the knee is approached, the cylindrical shaft becomes expanded sideways and a large, smooth, triangular area exists which forms the upper part of the region at the back of the knee.

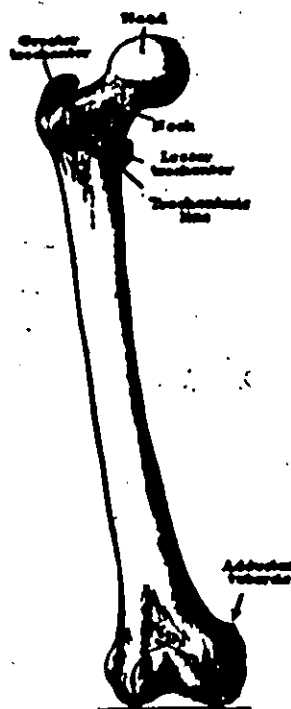


Figure 2.3
Right Femur from in Front
(From Basmajian, 1970)

C. The Tibia (Fig. 2.4)

The strong and massive bone on the medial side of the leg is the tibia. It alone receives weight transmitted to it by the femur and it conveys that weight to the foot. The salient features of the tibia may readily be made out since the bone lies just deep to the skin where, as the shin, it is palpable from knee to ankle. The shaft of the tibia tapers from the expanded upper end until it approaches the ankle when it again expands; the lower end, however, is less expanded than the upper. The lateral bone of the leg, the

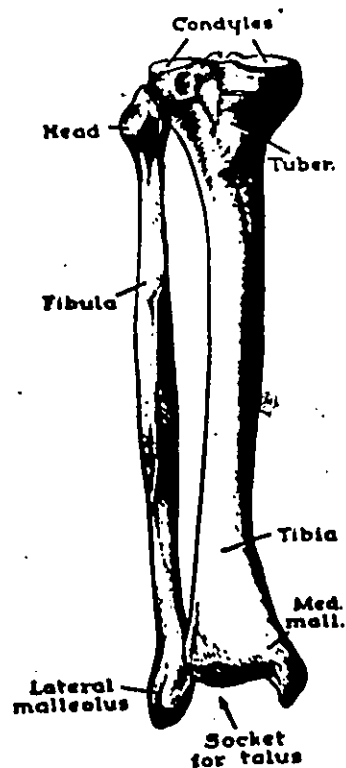


Figure 2.4
Right Tibia and Fibula from in Front
(From Basmajian, 1970)

fibula, is like a long thin stick, its shaft is twisted and is moulded by the origins and dispositions of the numerous muscles that arise from and are in contact with it.

The functions of the fibula are threefold

- (1) to give origin to muscles
- (2) to act as a pulley for tendons passing behind it at the ankle
- (3) to act as a lateral 'splint' for the ankle joint.

Without the fibula the whole security of that joint

is lost.

D. The Patella (Fig. 2.5)

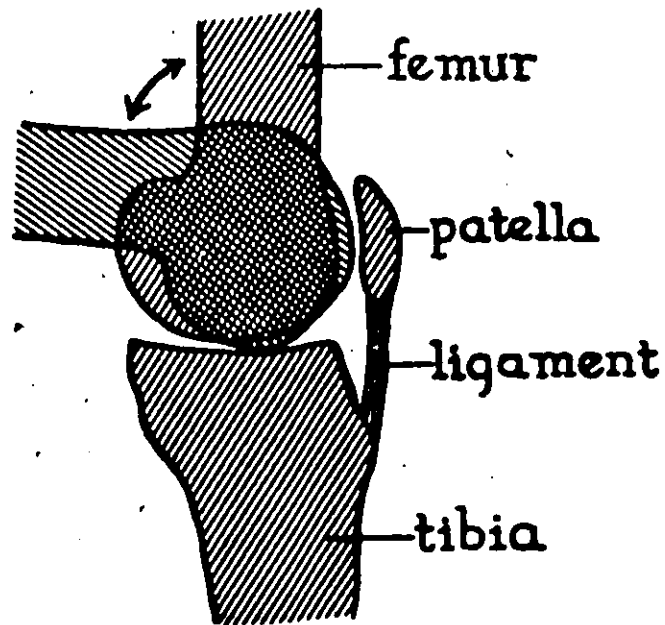


Figure 2.5
Position of Patella during Flexion and Extension of Knee
(From Basmajian, 1970)

The patella or knee-cap is a bone developed in a tendon which is triangular in outline with its apex down. It is thick and more or less flat. Since it lies just deep to the skin its size and shape are readily made out. It is said to enhance the power of the already powerful extensor muscle of the knee, in whose tendon it is developed, by increasing the leverage for that muscle.

E. The Bones of the Foot (Fig. 2.6)

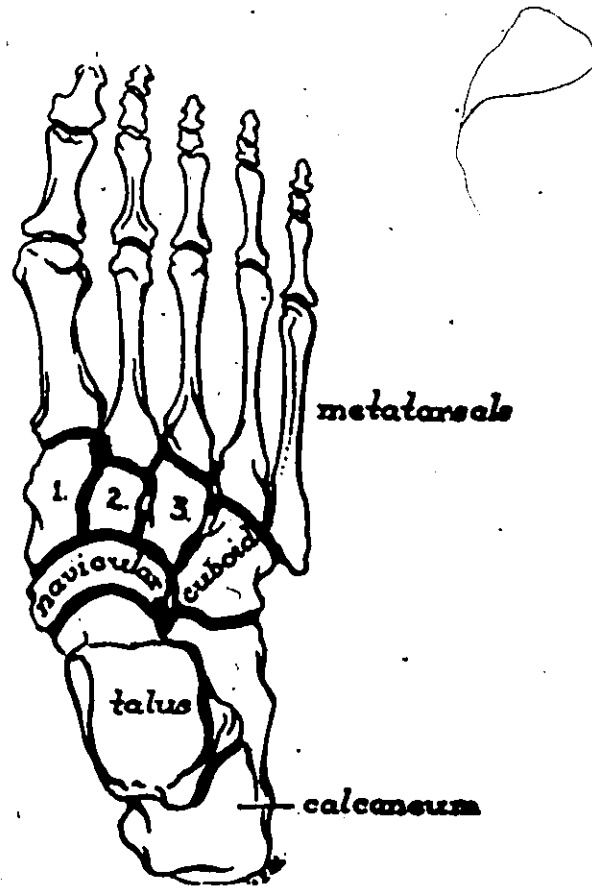


Figure 2.6
 Bones of Right Foot Viewed from Above
 1, 2, 3 = cuneiforms
 (From Basmajian, 1970)

The human foot, in contrast to the hand, has sacrificed all other function to concentrate on the duties of weight bearing and locomotion. The anterior half includes all the metatarsals and phalanges; the posterior half includes all seven tarsal bones. The talus and calcaneus are the largest of the tarsal bones and are concerned with receiving the weight of the body above. The

talus rests on the calcaneus or 'heel-bone' and occupies the socket of the ankle joint. On the upper surface of the talus, i.e., at the ankle joint, occur only the simple hinge movements of flexion and extension. The calcaneus on the other hand, accommodates itself to the irregularities of the ground with which it is in contact and it does so without in any way disturbing the superimposed talus. The posterior third of the calcaneus projects behind the ankle joint as the heel. The heel is a lever whereby the powerful calf muscles can extend the ankle and raise the body on tip-toe. Viewed from above, the bones of the foot may be divided longitudinally into two segments (1) calcaneus, cuboid, metatarsals 4 & 5, (2) talus, navicular, three cuneiforms and metatarsals 1, 2 and 3. There is some functional significance to this arrangement. The lateral segment of the foot consist of a low longitudinal arch supported chiefly by ligaments. The medial segment consists of a high longitudinal arch supported chiefly by ligaments during standing but also by muscles during locomotion. In walking, the weight is first borne by the heel and then is spread forwards along the lateral edge of the foot quickly to the metatarsal heads. The 'push-off' thrust is concentrated at the head of metatarsal 1, accounting for the large diameter of this bone.

2.3.3 The Muscular System

The muscular system pertinent to the process of human locomotion consists of the muscles of the lower limb:

A. The muscles of the hip and thigh.

B. the muscles of the leg.

The lower limb is the limb of stability, its movements are limited, coarse and often stereotyped. The paramount duty of its muscles is locomotion. The most powerful muscles lie alternatively at the back of the hip, at the front of the thigh, and at the back of the leg. The existence in the thigh of so many 'two-joint' muscles is explained by the requirements of the act of walking. Hip flexed and knee extended is the position of the limb when the foot leaves the ground. If, by passing over both joints, certain muscles can perform the two required movements simultaneously, they achieve an economy of effort.

A. The Muscles of Hip and Thigh

These can be subdivided into

- (i) Muscles crossing the front of the hip joint
- (ii) The three gluteal muscles (and the m.tensor fascia lata).
- (iii) The six lateral rotators.
- (iv) Muscles of the front of the thigh.
- (v) Muscles of the medial side of the thigh.

(vi) Muscles of the back of the thigh.

(i) Muscles crossing the front of the hip joint (Fig.2.7)

m.psoas major and m. iliacus.

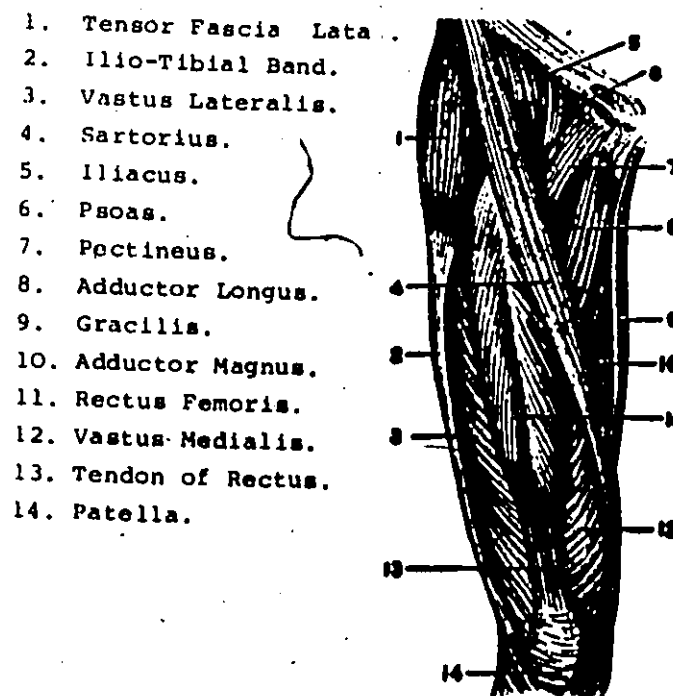


Figure 2.7
 Dissection of Muscles of Front of Right Thigh
 (From Basmajian, 1970)

These two muscles come together, fuse and cross the front of the hip joint close to the head of the femur. Because they share a common tendon of insertion and have a common action, they are often regarded as one - the m. iliopsoas.

(ii) The three gluteal muscles are the m. gluteus maximus, the m. gluteus medius and the m. gluteus minimus. Associated with these muscles is the m. tensor fascia lata. The m. tensor fascia lata is inserted with the m. gluteus maximus into the iliotibial tract of the fascia lata. The m. gluteus medius and m. gluteus minimus except for their origin and insertion onto the femur are identical (for all practical purposes) in action and use.

(iii) The six lateral rotators originate from the back of the hip bone, pass behind the hip joint and all except one crowd to be inserted into the medial surface of the greater trochanter. All six are lateral rotators of the hip and probably do little else.

(iv) The muscles of the front of the thigh (Fig. 2.7)

These are the three vasti and the m. rectus femoris which are grouped together under the name m. quadriceps femoris. In addition there is the long obliquely-running m. sartorius. The m. sartorius originates from the ilium and is inserted on the upper part of the tibia. The m. sartorius is not a powerful muscle and does not seem to play an important role in walking. The m. rectus femoris arises by means of two tendons from a region just above the acetabulum. It runs down the front of the thigh and is

inserted by means of a tendon on the upper border of the patella. The m. rectus femoris is the only member of the quadriceps group that crosses the hip joint and that can, therefore, flex the hip and/or extend the knee. The m. vastus medialis and m. vastus lateralis arise on the back of the upper part of the femur and are inserted into the sides of the rectus tendon and into the patella.

(v) The muscles of the medial side of the thigh (Fig. 2.7)

These consist of the m. gracilis which originates from the pubis and is inserted onto the medial side of the tibia just beyond the knee and adductors (longus, brevis and magnus) which also originate from the area of the pubis and are inserted along the femur.

(vi) The muscles of the back of the thigh (Fig. 2.8)

This group of muscles is known as the hamstrings. They consist of the m. biceps femoris, m. semimembranosus and m. semitendinosus. These are very long and extend from a common origin on the ischial tuberosity to beyond the back of the knee joint.

B. The Muscles of the Leg

The muscles of the leg are divided into four groups

(i) Extensors, in front of the ankle.

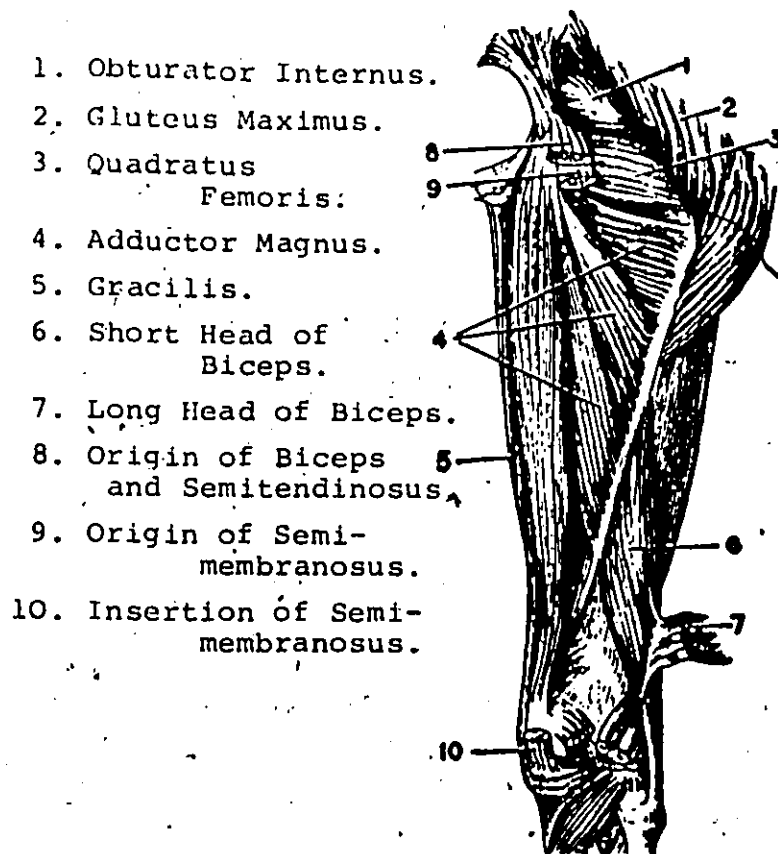


Figure 2.8
Deep Dissection of Muscles of Back of Right Thigh
(From Baemajian, 1970)

- (ii) Peronei.
- (iii) Superficial Flexors, behind the ankle.
- (iv) Deep Flexors.
- (i) Extensors (Fig. 2.9)

The extensor muscles (dorsiflexors) are the m. tibialis anterior, m. extensor digitorum longus, m. extensor hallucis longus, m. peroneus tertius and m. extensor digitorum brevis. The m. tibialis anterior is most important, most powerful and most medial of the group. It

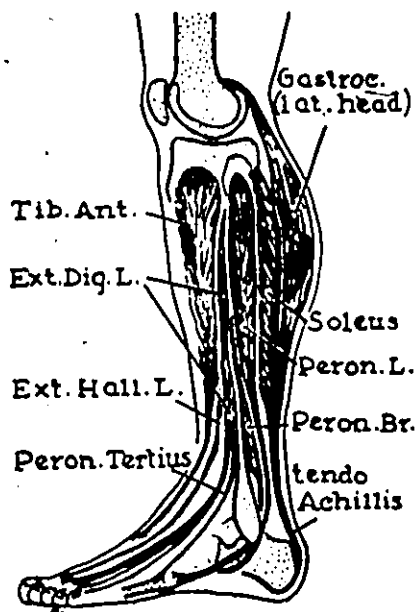


Figure 2.9
Muscles of Left Leg from Lateral Side
(From Basmajian, 1970)

arises from the lateral surface of the tibia and is inserted onto the base of the first metatarsal and to the adjoining medial cuneiform. The m. extensor hallucis longus is a special extensor for the great toe, arising from the front of the fibula and being inserted onto the base of the distal phalanx of the great toe. It assists in dorsiflexion of the ankle. The m. peroneus tertius is the lateral half of the m. extensor digitorum longus and is inserted on the shaft of the fifth metatarsal. The m. extensor digitorum brevis is the only muscle arising on the dorsum of the foot and is connected by means of four slender tendons to the four medial toes.

(ii) The peronei.

The m. peroneus longus and m. peroneus brevis arise from the upper two-thirds and from the lower two-thirds of the lateral side of the fibula respectively and are inserted finally onto the lateral side of the base of the first metatarsal and onto the base of the fifth metatarsal respectively.

(iii) Superficial plantar-flexors. (Fig. 2.9).

These are the m. gastrocnemius and m. soleus. Relatively unimportant is the associated m. plantaris. The m. gastrocnemius crosses two joints and its two bulging medial and lateral heads arise from the back of the femur just above the condyles. These two heads unite to form a single muscle. The m. soleus arises from the back of the tibia and fibula and lies beneath the m. gastrocnemius. The m. plantaris shares its origin with the lateral head of the m. gastrocnemius. All three muscles share a single tendon of insertion (Tendo Achillis) which is inserted into the back of the calcaneus at the back of the ankle joint.

(iv) Deep plantar-flexors

These consist of three muscles; the m. flexor hallucis longus, m. flexor digitorum longus and m. tibialis posterior. The m. flexor hallucis longus arises from the

lower two-thirds of the fibula posterior and is inserted finally onto the distal phalanx of the great toe. The m. flexor digitorum longus arises from the posterior surface of the tibia and is inserted finally by means of four tendons to the four smaller toes. The m. tibialis posterior is the deepest muscle of the leg. It arises from the inner surface of the osseofibrous pocket (a compartment between the tibia and fibula) and is inserted finally into the tuberosity of the navicular.

The Muscles of the Foot

These occur in four distinct layers in the sole of the foot and other than help to maintain the arches of the foot during locomotion the functions and actions of these muscles do not appear to be important in human locomotion.

2.4 The Phasing of the EMG Activity and the Function of the Muscles of the Leg During Normal Locomotion on a Level Surface

The walk cycle as referred to below is based upon a normalized time cycle which starts (0%) and ends (100%) at the heelstrike of the leg considered. HS indicates heel strike. TO indicates toe-off or onset of swing.

2.4.1 Muscles crossing the front of the hip joint:

Iliopsoas

Pl.
Flex. Dors. Flex. Pl. Flex. Dors. Flex.

Hip Extension Hip Flex. Hip Ext.

Knee
Flex. Knee Ext. Knee Flex. Knee Ext.

0 10 20 30 40 50 60 70 80 90 100

HS TO HS

Psoas

1. Close & Todd (1959)
2. Hagy et al (1973)

Iliacus

1. Close & Todd (1959)
2. Battye & Joseph (1966)
3. Paul (1971)
4. Hagy et al (1973)

Function:

The above phasic activity confirms the statement of Basmajian and Greenlaw (1968) that the accepted main action of the iliopsoas is flexion of the hip. Both muscles are often active during lateral rotation of the thigh but not during medial rotation. Liberson (1965) reports contraction of the iliopsoas occurs simultaneously with that of the m.

gluteus maximus of the opposite side.

2.4.2. The three gluteal muscles (and m. tensor fascia lata)

Pl.
Flex. Dors. Flex. Pl. Flex. Dors. Flex.

Hip Extension Hip Flex. Hip Ext.

Knee
Flex. Knee Ext. Knee Flex. Knee Ext.

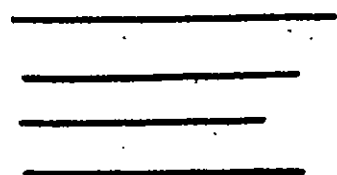
0 10 20 30 40 50 60 70 80 90 100
HS TO HS

Gluteus Maximus



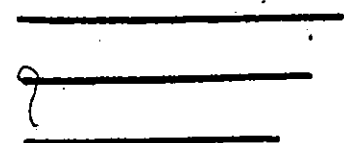
1. Univ. of Calif (1953)
2. Radcliffe (1962)
3. Sutherland (1966)
4. Battye & Joseph (1966)
5. Paul (1971)
6. Hagy et al. (1973)

Gluteus Medius



1. Univ. of Calif (1953)
2. Battye & Joseph (1966)
3. Paul (1971)
4. Hagy et al. (1973)

Gluteus Minimus



1. Univ. of Calif (1953)
2. Battye & Joseph (1966)
3. Hagy et al. (1973)

Pl.
Flex. Dors. Flex. Pl. Flex. Dors. Flex.

Hip Extension Hip Flex. Hip Ext.

Knee
Flex. Knee Ext. Knee Flex. Knee Ext.

0 10 20 30 40 50 60 70 80 90 100

HS TO HS

Tensor Fascia Lata

1. Univ. of Calif (1953)
2. Hagy et al (1973)

Function:

Basmajian (1970) writes that the m. gluteus maximus is an extensor of the hip joint but is used only when the joint has to be extended with power and is also a powerful lateral rotator of the extended thigh. The functions of the m. gluteus medius and m. gluteus minimus are to abduct the thigh (outwards) and the anterior parts of the muscle rotate the thigh medialwards. Basmajian (1973) commented that since the m. gluteus maximus shows activity at the end of swing and at the beginning of stance, it probably contracts to prevent or control flexion at the hip joint. This is contrary to the general belief that its activity is not needed for ordinary walking. The m. tensor fascia lata is a flexor and medial rotator of the hip joint as well as an extensor of the knee joint. Its important use is to brace

the knee so that, in walking, the knee joint can take the weight without "buckling" while the other foot is off the ground and the body is swinging forward.

The above table confirms that the gluteal muscles are essentially hip extensors.

2.4.3 The muscles of the front of the thigh m. quadriceps femoris (m. rectus femoris, 3 vasti, m. sartorius)

Pl. Flex. Dors. Flex. Pl. Flex. Dors. Flex.

Hip Extension Hip Flex. Hip Ext.

Knee Flex. Knee Ext. Knee Flex. Knee Ext.

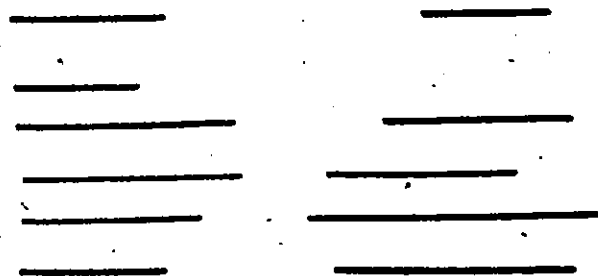
0 10 20 30 40 50 60 70 80 90 100
HS TO HS

Sartorius

- 1. Univ. of Calif (1953)
- 2. Hagy et al (1973)

Rectus Femoris

- 1. Univ. of Calif (1953)
- 2. Close & Todd (1959)
- 3. Radcliffe (1962)
- 4. Battye & Joseph (1966)
- 5. Paul (1971)
- 6. Hagy et al (1973)



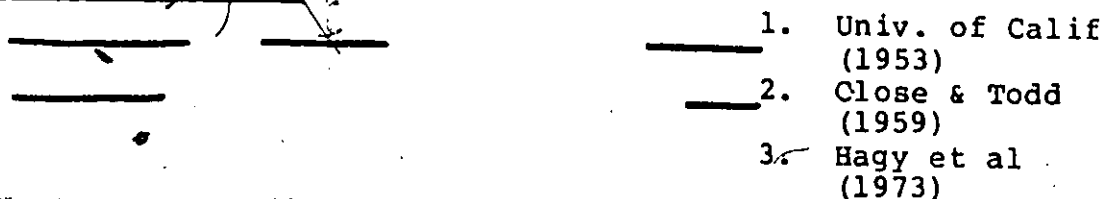
Pl.
 Flex. Dors. Flex. Pl. Flex. Dors. Flex.

 Hip Extension Hip Flex. Hip Ext.

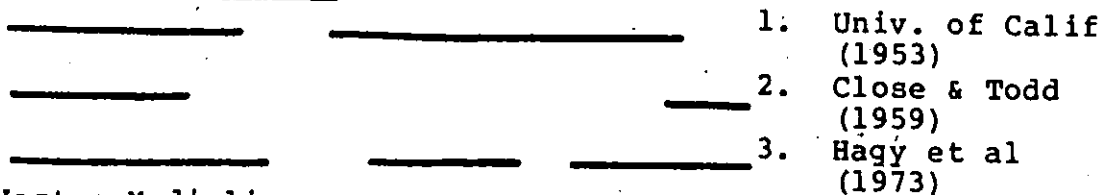
 Knee
 Flex. Knee Ext. Knee Flex. Knee Ext.

 0 10 20 30 40 50 60 70 80 90 100
 HS TO HS

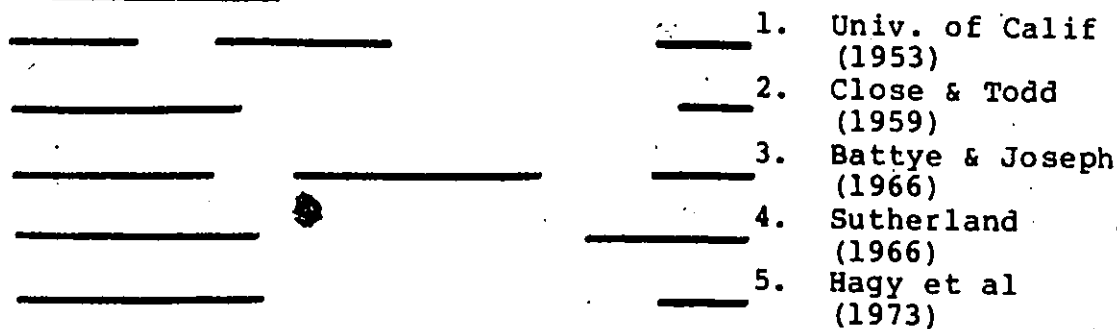
Vastus Lateralis



Vastus Intermedius



Vastus Medialis



Function:

As the above table indicates the most predominant phase occurs at or about the transition from swing to stance. This tends to support the observation of Milner et al (1971a) that a major role of the m. vastus lateralis,

together with other members of the quadriceps group, was to attempt to hold the knee joint rigid while the walker underwent the transition from swing to stance and executed the latter phase. The muscular action in this phase seemed to be responsible for the maintenance of stability of the walk at higher speeds.

Basmajian (1970) comments that the m. rectus femoris is the only member of the quadriceps group that crosses both the hip and knee joints and that can, therefore, flex the hip and/or extend the knee by which means the limb is advanced in walking. The vasti along with m. rectus femoris are the powerful extensor complex of the knee. It appears, however, that knee-locking can be attained merely by contraction of the m. tensor fascia lata. The phasic activity of the m. rectus femoris shown in the above table seems to confirm Basmajian's observation that it is a hip flexor but there is no clear indication of its role as a knee extensor since in general the quadriceps activity has ceased during knee extension. An explanation for this phenomenon is given by Sutherland (1966) and his conclusions are discussed further in the part of this section examining the deep plantar-flexors.

2.4.4 The muscles of the medial side of the thigh
m. gracilis, m. adductor longus, brevis and magnus

Pl.
 Flex. Dors. Flex. Pl. Flex. Dors. Flex.

Hip Extension Hip Flex. Hip Ext.

Knee
 Flex. Knee Ext. Knee Flex. Knee Ext.

0 10 20 30 40 50 60 70 80 90 100
 HS TO HS

Gracilis

1. Univ. of Calif (1953)
2. Hagy et al (1973)

Adductor Longus

1. Univ. of Calif (1953)
2. Close & Todd (1959)
3. Hagy et al (1973)

Adductor Brevis

1. Hagy et al (1973)

Adductor Magnus

1. Univ. of Calif (1953)
2. Close & Todd (1959)
3. Paul (1971)
4. Hagy et al (1973)

Function:

As a group these muscles produce powerful adduction and are quite active during locomotion. Because they are on

Semitendinosus

_____	_____	1. Univ. of Calif (1953)
_____	_____	2. Close & Todd (1959)
_____	_____	3. Battye & Joseph (1966)
_____	_____	4. Hagy et al (1973)

Function:

These muscles extend the hip and/or flex the knee. In walking, as the foot leaves the ground to take a step forwards (i.e. toe-off), the hamstrings contract momentarily in order to take the weight of the partially flexed leg. As soon as hip flexion begins and the limb starts to swing forward, the hamstrings relax and allow knee extension to occur in the advancing limb (Basmajian, 1970).

The above table also seems to confirm the findings of Milner et al (1971a) who reported that the lateral hamstring's activity seems to predominate in the swing phase with some carry over beyond the transition from swing to stance. Since some subjects showed a measure of activity during the stance phase, it would seem that the lateral hamstring serves to assist in supporting and then paying out the flexed fibia at the knee joint during the swing phase.

2.4.6 The extensors muscles of the leg (m. tibialis anterior, m. extensor digitorum longus, m. extensor hallucis longus)

Pl.
Flex. Dors. Flex. Pl. Flex. Dors. Flex.

Hip Extension Hip Flex. Hip Ext.

Knee
Flex. Knee Ext. Knee Flex. Knee Ext.

0 10 20 30 40 50 60 70 80 90 100
HS TO HS

Tibialis Anterior

- _____ 1. Univ. of Calif (1953)
- _____ 2. Close & Todd (1959)
- _____ 3. Battye & Joseph (1966)
- _____ 4. Hagy et al (1973)

Extensor Digitorum Longus

- _____ 1. Univ. of Calif (1953)
- _____ 2. Close & Todd (1959)
- _____ 3. Hagy et al (1973)

Extensor Hallucis Longus

- _____ 1. Hagy et al (1973)

Function:

Basmajian (1970) writes that the m. tibialis anterior dorsiflexes the ankle and inverts the foot. It is used in

walking to bend the foot up and so prevent stubbing of the toes as the advancing limb swings forward. The m. extensor digitorum longus is the extensor of the lateral four toes and helps to dorsiflex the ankle weakly. The m. extensor hallucis longus is a special extensor for the great toe and assists in dorsiflexion of the ankle.

The major activity of the pretibial group occurs during the period the toe is approaching the ground and the foot is becoming plantar-flexed in relation to the tibia. Therefore, the motion which is normally associated with activity of this muscle, dorsiflexion of the foot, not only does not occur but the converse, plantar-flexion, takes place. The muscles are both lengthened, despite their contraction, as they resist the force of the body acting down the tibia about the fulcrum at the heel. Thus the tendency of the forepart of the foot to slap to the ground is controlled while decelerating the conditions wherein muscles are being lengthened against their normal motion of contraction. Work is being done upon the muscles rather than by the muscles upon the skeletal system. The secondary and much smaller peak of contraction at toe-off tries to dorsiflex the foot towards the right angle. Plantar-flexion associated with calf group propulsion has just occurred. Thus maximum clearance is afforded to the toe during the

swing-through period by this lifting action. (Basmajian, 1970)

For a range of speed (2 ft/sec. - 8 ft/sec.), there are essentially two phases of activity in the m. tibialis anterior. One occurs at the transition from stance to swing and the activity invariably straddles the transition point. The other occurs at or about the transition from swing to stance. The former muscle action evidently serves to prepare for and then effect lifting off the toes to clear the ground, while the latter action presumably acts to prevent the foot from slapping down as the transition from swing to stance is made. At higher speeds, activity in the stance phase appears to become more pronounced. Possibly more stabilization is necessitated and thus prolonged muscle activity called for (Milner et al, 1971a). The above observations are confirmed by the phasic activity shown in the table.



2.4.7 The m. peroneus longus and m. peroneus brevis

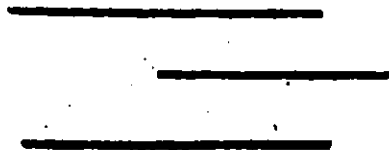
Pl.
Flex. Dors. Flex. Pl. Flex. Dors. Flex.

Hip Extension Hip Flex. Hip Ext.

Knee
Flex. Knee Ext. Knee Flex. Knee Ext.

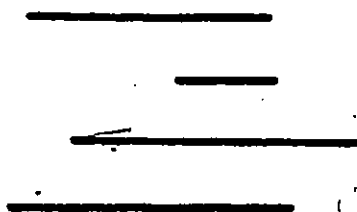
0 10 20 30 40 50 60 70 80 90 100
HS TO HS

Peroneus Longus



1. Univ. of Calif (1953)
2. Sutherland (1966)
3. Hagy et al (1973)

Peroneus Brevis



1. Univ. of Calif (1953)
2. Close & Todd (1959)
3. Sutherland (1966)
4. Hagy et al (1973)

Function:

The peronei evert the foot. The m. peroneus longus is a plantar-flexor of the transverse tarsal joint. (Basmajian, 1970)

The pattern of activity of the m. peroneus longus (as shown in the above table) confirms the findings of many who

have suggested that the m. peroneus longus helps to stabilize the leg and foot during mid-stance. (Basmajian, 1973)

2.4.8 The superficial plantar-flexors (m. gastrocnemius, m. soleus)

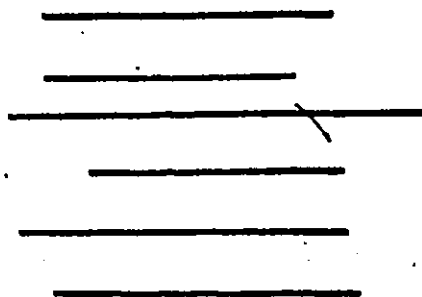
Pl:
Flex. Dors. Flex. Pl. Flex. Dors. Flex.

Hip Extension Hip Flex. Hip Ext.

Knee
Flex. Knee Ext. Knee Flex. Knee Ext.

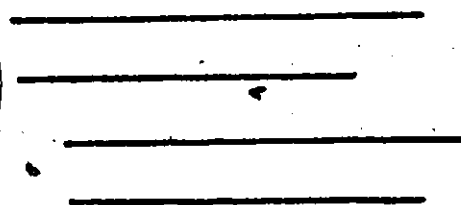
0 10 20 30 40 50 60 70 80 90 100
HS TO HS

Gastrocnemius



1. Univ. of Calif (1953)
2. Close & Todd (1959)
3. Radcliffe (1962)
4. Sutherland (1966)
5. Milner et al (1971a)
6. Hagy et al (1973)

Soleus



1. Univ. of Calif (1953)
2. Close & Todd (1959)
3. Battye & Joseph (1966)
4. Sutherland (1966)
5. Hagy et al (1973)

Function:

The m. gastrocnemius can either flex the knee or plantar-flex the ankle but never both together. The m. soleus plantar-flexes the ankle when the knee is flexed. Both muscles are active during the "take-off" phase of the foot in walking and running. (Basmajian, 1970)

For three subjects at higher speeds the m. gastrocnemius does appear to be active at some part, usually the earlier, of the swing phase. It appears that there is at this stage some antagonistic action with the m. tibialis anterior. The essential action of m. gastrocnemius is certainly to contribute to the lifting of the subject early in the stance phase and aiding in propelling him forward. (Milner et al, 1971a)

The phasic activity of the m. gastrocnemius as shown in the table seems to concur more with Milner's observations rather than that of Basmajian since the m. gastrocnemius is mainly active during the stance period of knee extension and ankle dorsiflexion.

2.4.9 Deep plantar-flexors

(m. flexor hallucis longus, m. flexor digitorum longus and m. tibialis posterior)

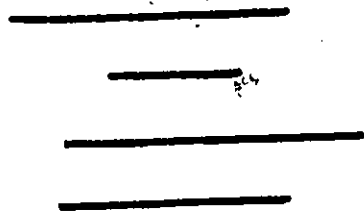
Pl. Flex. Dors. Flex. Pl. Flex. Dors. Flex.

Hip Extension Hip Flex. Hip Ext.

Knee Flex. Knee Ext. Knee Flex. Knee Ext.

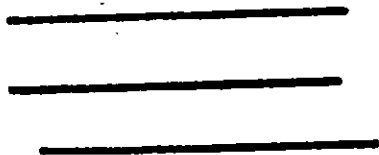
0 10 20 30 40 50 60 70 80 90 100
 HS TO HS

Flexor Hallucis Longus



1. Univ. of Calif (1953)
2. Close & Todd (1959)
3. Sutherland (1966)
4. Hagy et al (1973)

Flexor Digitorum Longus



1. Univ. of Calif (1953)
2. Sutherland (1966)
3. Hagy et al (1973)

Tibialis Posterior



1. Univ. of Calif (1953)
2. Close & Todd (1959)
3. Sutherland (1966)
4. Hagy et al (1973)

Function:

The m. flexor hallucis longus flexes the great toe and assists in plantar-flexion of the ankle. The m. flexor digitorum longus flexes the four smaller toes. The m.

tibialis posterior inverts the foot and plantar-flexes the transverse tarsal joint (Basmajian, 1970). The m. tibialis posterior is an inverter in non-weight-bearing movements of the foot, but its role at "mid-stance" appears to be a restraining one to prevent the foot from everting past the neutral position (between inversion and eversion) (Basmajian, 1973).

With respect to the function of the ankle plantar-flexors, the work of Sutherland (1966) is most important. Sutherland (1966) confirmed the indirect knee-stabilizing function of the ankle plantar-flexors in walking on the level. This had been postulated earlier by Radcliffe (1962). Combined EMG's and motion pictures of gait showed that the periods of activity of the ankle plantar-flexors corresponding with increasing knee extension and dorsiflexion of the foot. Only at the end of the period of ankle plantar-flexor action did plantar-flexion of the foot occur. Knee extension took place after the cessation of activity of the quadriceps muscle and did not appear to be produced by quadriceps action.

Sutherland (1966) believed that knee extension in the stance phase was brought about by the force of the plantar-flexors of the ankle resisting the dorsiflexion of the

ankle. This restraining function of the ankle plantarflexors in decelerating forward rotation of the tibia on the talus was the key to their stabilizing action.

2.5 Conclusions:

It is clear that after a careful examination of the preceding four sections one is in a position to select those muscles that are nominally active during rotations about the hip and knee joint during normal locomotion on a level surface. The information reviewed in this chapter has been published in the form of an educational monograph (Hershler, 1977a). The objective of this thesis is to delineate certain statistical properties of the phasic activity of pertinent skeletal muscles (Chapter 4) as well as examine in some detail certain aspects of the rotations about the hip and knee joints in the sagittal plane (Chapter 5). Chapter 6 is then an initial attempt to model the relationship between EMG patterns of selected skeletal muscles in the leg and these angular rotations. Before proceeding to the actual research it would be pertinent to describe the experimental techniques and equipment used in the locomotion studies outlined in this thesis. This description follows in Chapter 3.



CHAPTER 3

CURRENT EXPERIMENTAL TECHNIQUES AND EQUIPMENT USED IN LOCOMOTION STUDIES

3.1 INTRODUCTION

The purpose of this chapter is to describe some of the current experimental techniques available in the Locomotion Laboratory, Department of Biomedical Engineering, Chedoke Hospital. Some of these techniques were used in the locomotion studies described in this thesis. The first part of the chapter is essentially a description of three techniques for the measurement of certain kinematic variables during gait. These are as follows:

- (a) The stroboscopic flash-photography system
- (b) The electrogoniometer system
- (c) The optoelectronic system.

The advantages and disadvantages of each system have been outlined.

The second part of the chapter examines methods of recording, amplifying and processing EMG (electromyographic) signals. Some of the advantages and disadvantages of using

surface and intramuscular fine-wire electrodes are presented. Appendix 1 contains brief descriptions of two of the computer programs that were used extensively for analysis of EMG signals and angle-angle diagrams.

3.2 MEASUREMENT OF THE KINEMATIC VARIABLES IN GAIT

3.2.1 The Period and Phases of the Walk Cycle

In the study of normal gait it is important to know when heel-strike (HS), heel and toe (HT), toe only (HO) and swing (SW) occur during one complete walk cycle. This is achieved by fitting both shoes of the subject with footswitches at the heel and toe. Each footswitch consists of two brass shim stock contacts (5cm x 5cm x 0.15mm) separated by strips of foam rubber. An additional resistor network (Figure 3.1) is included in such a manner that depression of the heel footswitch creates a dc voltage of approximately $1/3V$, depression of the toe footswitch creates a dc voltage of approximately $2/3 V$ and finally depression of both heel and toe creates a dc voltage of approximately $1V$.

A footswitch voltage pattern can thus be obtained for each shoe indicating the time sequence of ground contact of the extremities of the underside of the foot. Figure 3.2 is the footswitch pattern obtained for a sequence of normal footsteps on a level surface. A single footstep has been

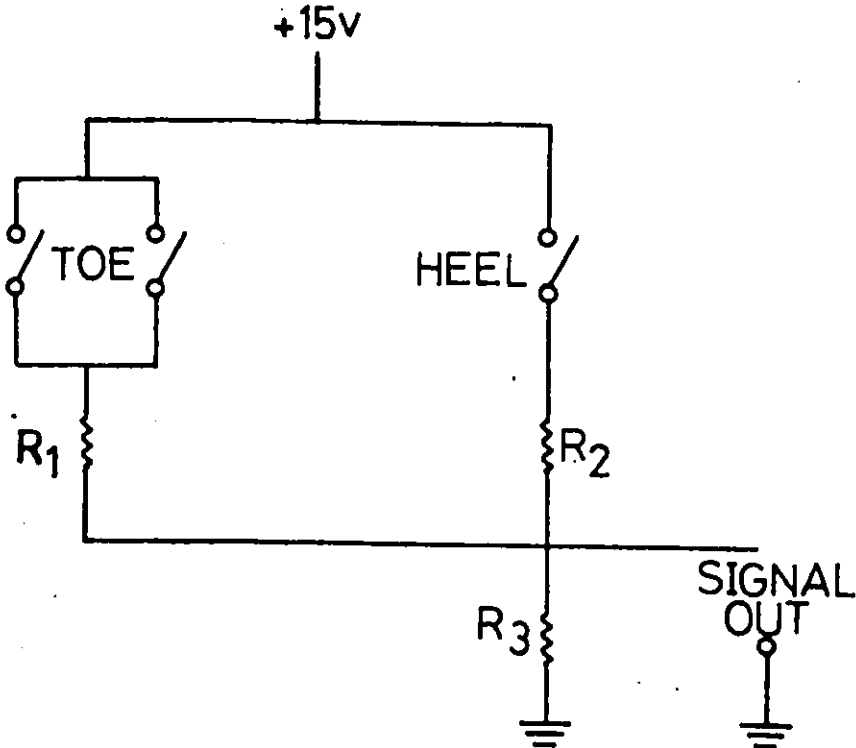


Figure 3.1
Resistor Network for Footswitches

R1 = 330 kΩ

R2 = 680 kΩ

R3 = 1.5 kΩ

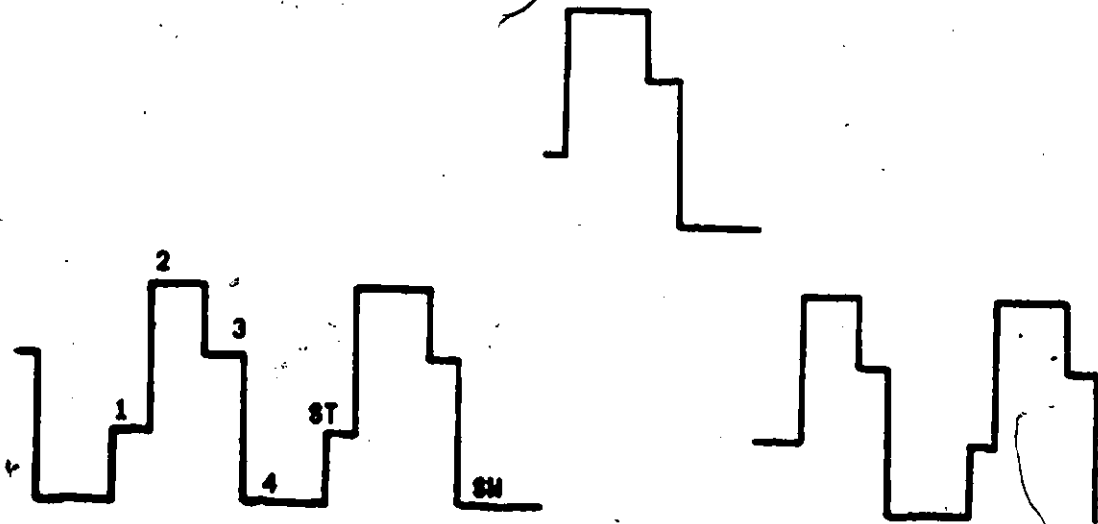


Figure 3.2

Normal Footswitch Patterns

- 1: Heelstrike
- 2: Heel and Toe
- 3: Toe only (heel off)
- 4: Swing
- ST: onset of stance
- SW: Onset of swing

A footswitch pattern for one complete stride on the same leg has been displaced up with respect to the other patterns.

selected from the sequence and is shown displaced with respect to the rest of the patterns. The footswitch patterns of both feet are passed directly into a PDP11/10 computer. A simple pattern recognition algorithm written in Fortran IV enables the period from heelstrike to heelstrike of the same foot as well as the time intervals of the various phases to be easily computed.

In the study of certain types of pathological gait, however, even though the same system of footswitches may be used, it is not as simple to recognize and measure the various phases of the gait cycle. This is due to the fact that, at times, onset of stance (ST) can be caused either with the toe (dropfoot) or the heel and the toe could be making contact with the ground throughout swing (SW) as in the case of toe dragging. Figure 3.3 is the footswitch pattern obtained for a sequence of footsteps of a patient suffering from cerebral palsy (C.P.). A comparison of this figure with the previous one shows how radically the footswitch pattern can change even though the gait of the C.P. patient was fairly repeatable.

An interactive pattern recognition algorithm has been written (de Bruin and Milner, 1977), which enables the user to select single footstep patterns from a sequence of such

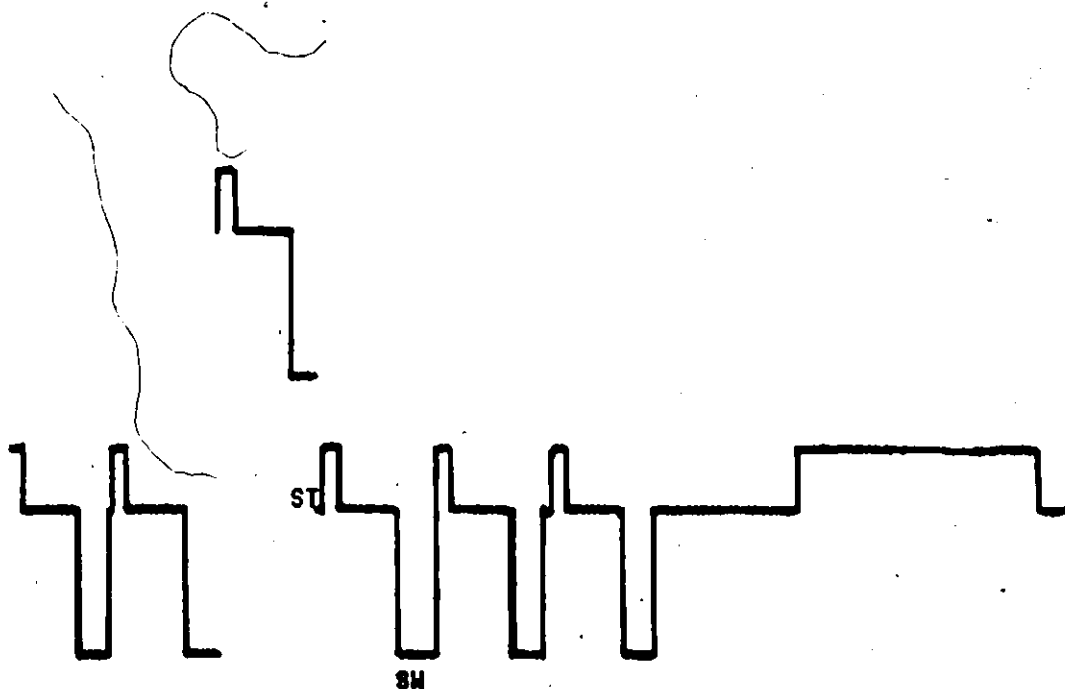


Figure 3.3

Footswitch Patterns for a C.P. Patient

ST: Onset of Stance

SW: Onset of Swing

A footswitch pattern for one complete stride on the same leg has been displaced up with respect to the other patterns. The change in the footswitch pattern on the right indicates that the patient had terminated his walk.

patterns. It is then possible to discriminate between stance and swing and to measure the respective phasic intervals. Temporal stance-swing ratios can thus be computed for both normal and pathological gaits. It should be stressed however, that especially in the case of pathological gait, inspection of the footswitch pattern provides only a limited amount of kinematic information. Further kinematic variables have to be isolated and measured to define the gait completely.

The next section includes a description of a stroboscopic (interrupted-light) flash-photography method

used in the laboratory for gait analysis. Figure 3.4 is a typical strobe photograph of a patient's gait in the saggital plane. It is obvious that visual examination of this "stick-diagram" plus a knowledge of the stroboscopic frequency can give one estimates of the stride period and phases of the walk-cycle. These estimates are subject to large inaccuracies which will be discussed at greater length in the next section. Figure 3.4A is a typical knee angle-hip angle diagram obtained with the stroboscopic method.

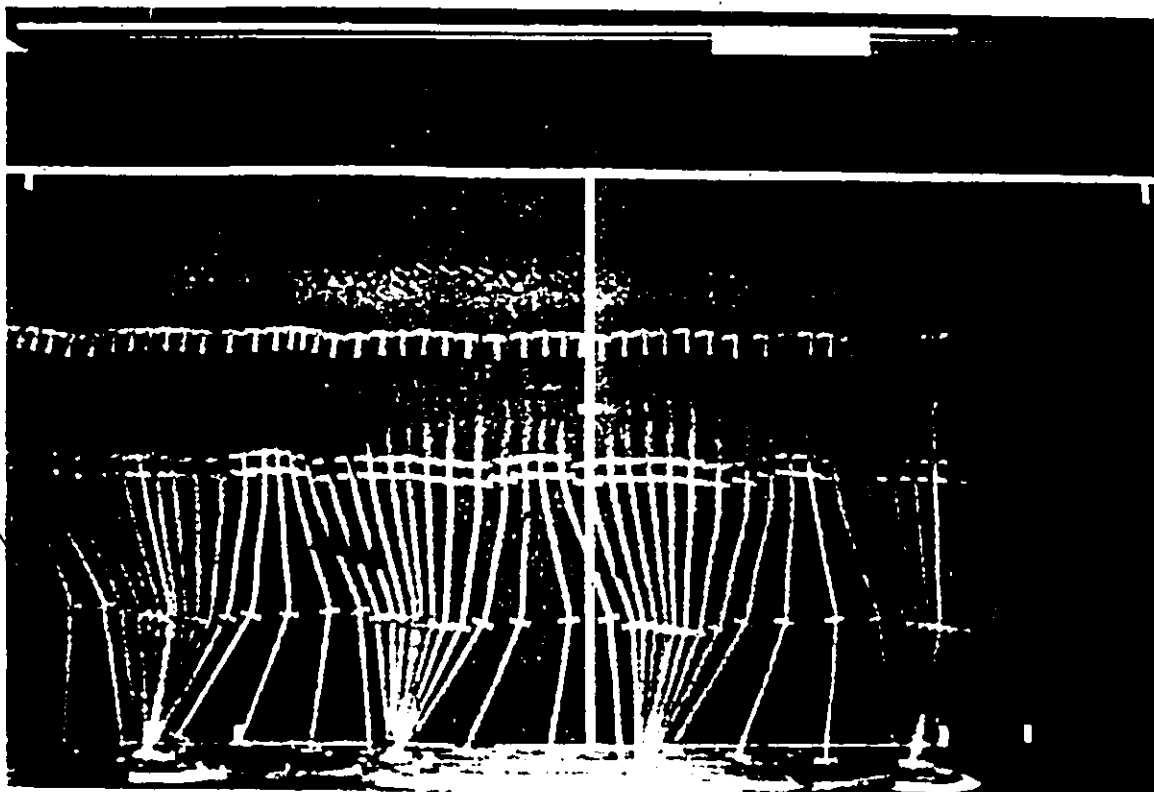


Figure 3.4
A Stroboscopic "Stick" Diagram

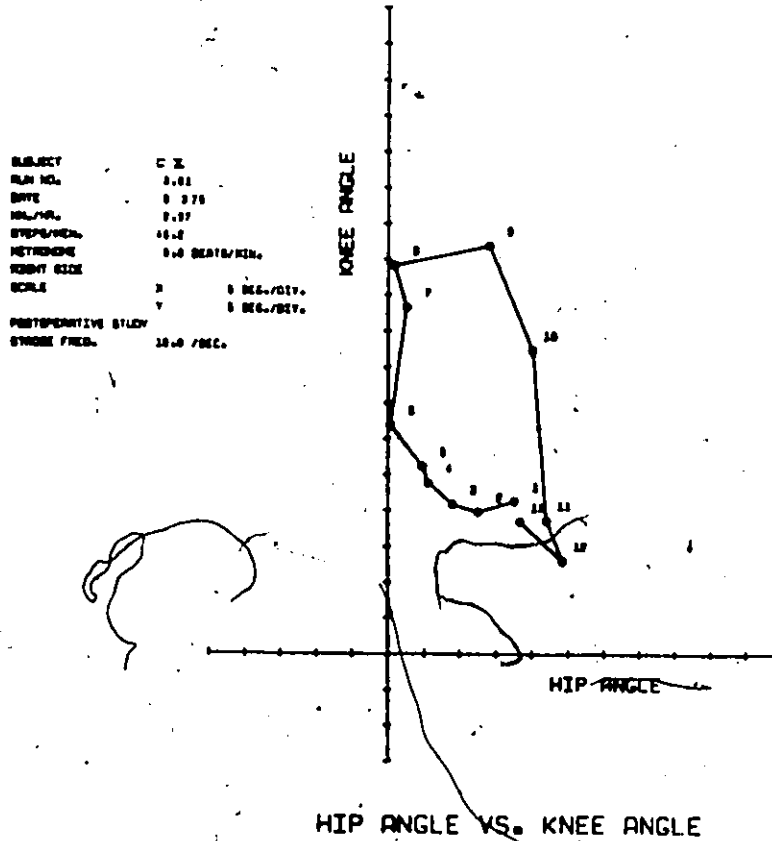


Figure 3.4A.
A Knee-Angle/Hip-Angle Diagram Derived Using the
Stroboscopic Method

The sequence of numbers in this plot reflects the sequence of stroboscopic flashes. Each number is a timing marker and each point is separated from its neighbour by an equal interval of time (1/10 sec.). Point 1 corresponds to the position of the joints described by the first "stick" in Figure 3.4. A fair amount of clinically useful information can be visually extracted from this angle-angle plot. e.g.

- (a) Range of Knee angle flexion = 45°
- (b) Range of Hip angle flexion = 25°
- (c) No hyperextension of the knee. No hip extension
- (d) Flexion contracture of approximately 12° in the knee

In a later chapter of this report an optoelectronic method available in the laboratory for studying gait will be described. By measuring the time between the point of

maximum weight-bearing on the one leg (i.e. when the y-coordinate of the ankle reaches a minimum) and the next point of maximum weight-bearing of the same leg, the period of the footstep can be computed. Figure 3.5 is a "stick"-diagram created from the spatial joint trajectories of a subject's gait using the optoelectronic system. Again one is able visually to estimate the phasic intervals of stance and swing if the "stick" frequency is known. Figure 3.5A is a typical knee-angle/hip-angle diagram obtained with the optoelectronic method.

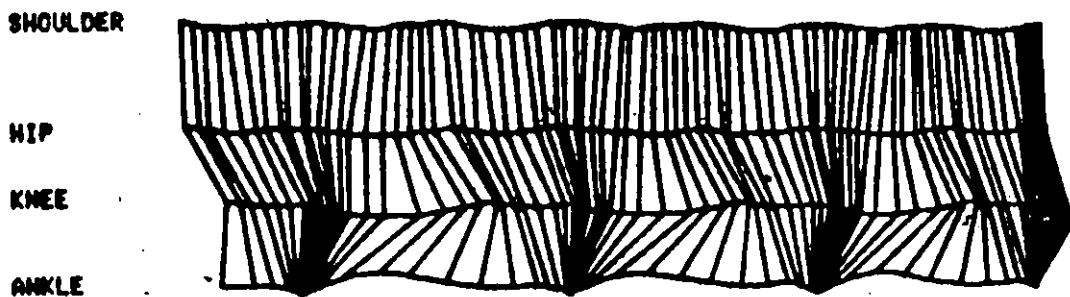
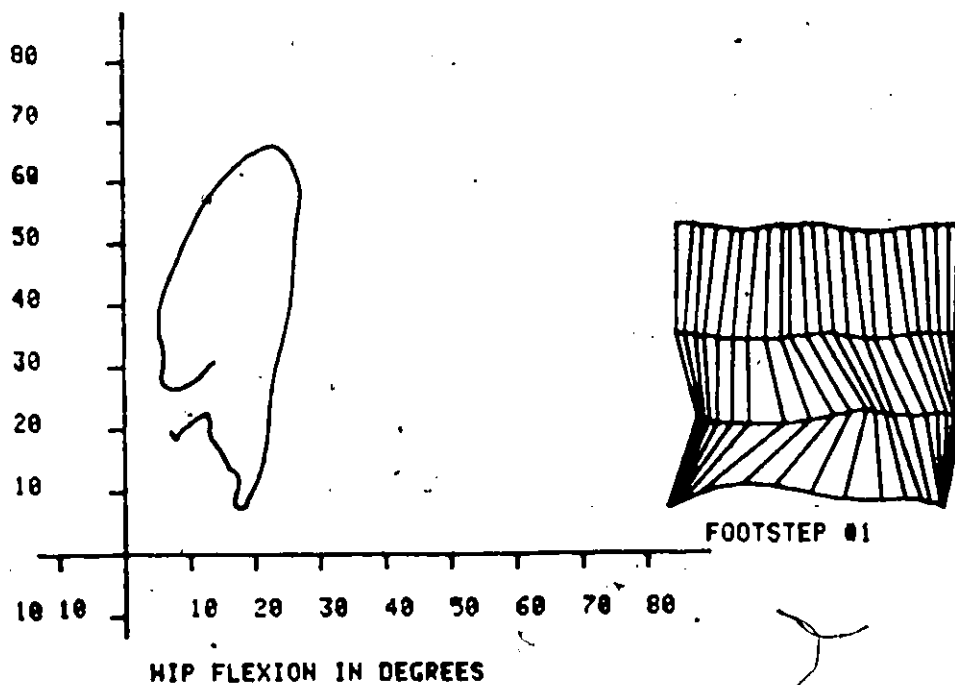


Figure 3.5
 A "Stick"-Diagram Utilizing the Optoelectronic Method
 Normal Female Gait Bare Foot
 Right Leg
 Sticks Displayed at 0.05 second intervals

KNEE FLEXION IN DEGREES



78

Figure 3.5A
A Knee-Angle/Hip-Angle Diagram Derived Using The
Optoelectronic Method
Normal Female Gait Bare Foot
Right Leg
Stride Length = 105.7 cm
Stride Period = 1.1 sec
The "Stick"-Diagram corresponding to the angle-angle
diagram is displayed to the right of the figure

3.2.2 Measurement of Spatial and Angular Information

3.2.3 The Stroboscopic Flash-Photography System

A system utilizing interrupted-light photography or stroboscopic photography is available in the Locomotion Laboratory. This system is a duplication of that reported by Milner et al (1973). Here consecutive phases of locomotor action are exposed upon a single film frame (Figure 3.4). This "stick"-diagram demonstrates sequential actions of a particular motion and thus the trajectories traced out in space and time of selected points on the

subject's body can be obtained. From the trajectories of the shoulder, hip, knee, ankle and toe the angular variations about the hip, knee and ankle joints can be deduced.

The disadvantages of this method are that only the motions and angular variations in the sagittal plane can be obtained. Also relevant data have to be digitized manually from the exposed film or negative. Although we have available for our use an x-y digitizer in the Department of Mechanical Engineering, McMaster University (Ruscom Logics* Limited Graph Digitizer Model 77), the selection of the points to be digitized still has to be done manually and this leads to a great amount of time wastage as well as introducing greater possibilities of human error. Other disadvantages of this method are that the patient or subject has to be dressed in a close-fitting black cat-suit (Figure 3.6) and has to walk in a darkened room illuminated only by the stroboscopic flashes. These constraints could have unsettling effects on certain patients. In addition, the use of the CDC 6400 computer for data processing and hard copy output is expensive. (Approximately \$6/photograph including graphical output.) The advantage of this system is its simplicity and the various elements of the system will now be described in detail.

*Ruscom Logics Limited, 62 Alness Street, Downsview 463, Ontario

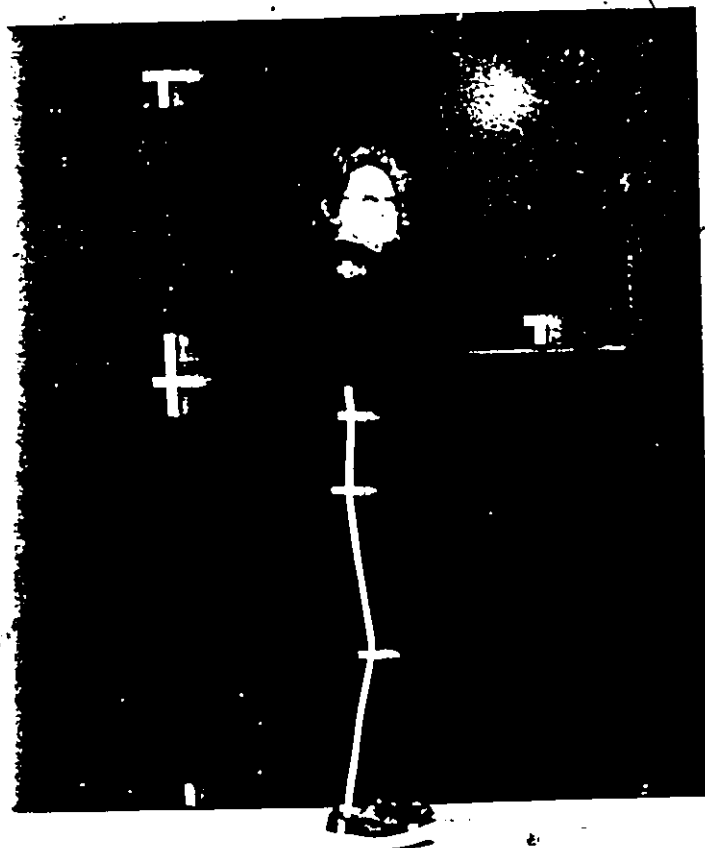


Figure 3.6
Patient Dressed in Black Cat Suit
White Tape is Attached to Selected Anatomical Landmarks

The Walkway

The subject walks a distance of approximately 8 metres along a straight line. The perpendicular distance from the straight line to the location of the camera is about 3.5 metres. The strobe light source is mounted directly above the camera. A suitable black background (5m x 3m piece of styrofoam painted black) with white markers located at fixed intervals on the backdrop enables scaled measurements to be made from the film records (Figure 3.7).

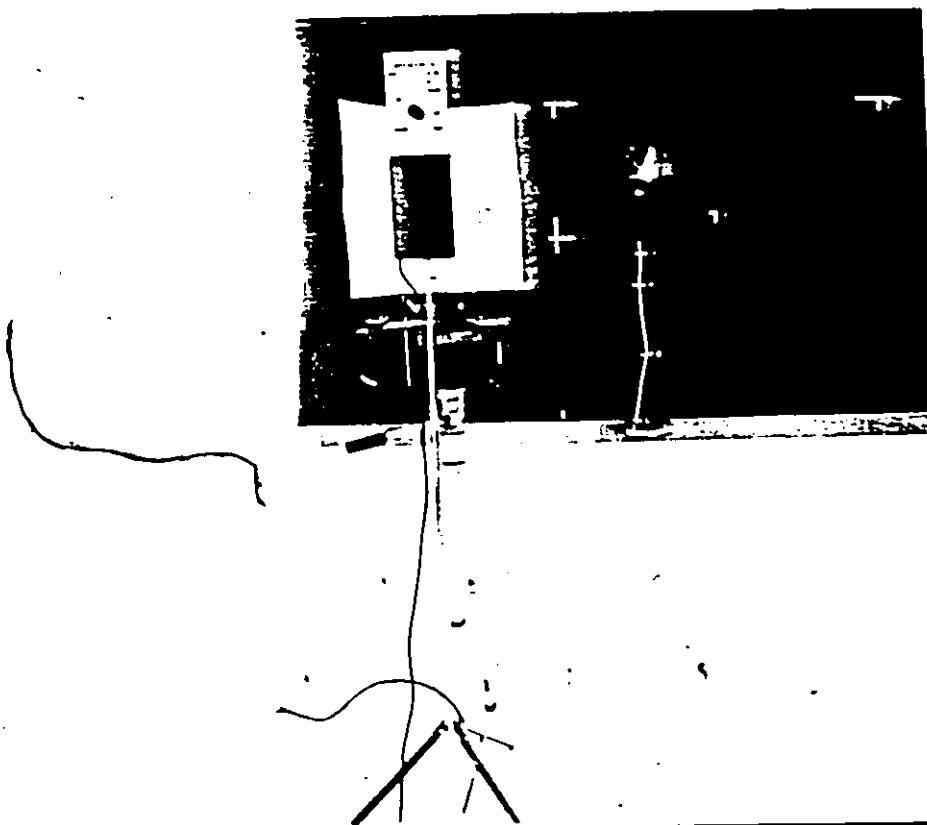


Figure 3.7
Stroboscopic Flash-Photography System Including
Patient, Background, Walkway, Camera and Stroboscope

The Camera (Figure 3.7)

The camera being used is a Mamiya Universal Press with a Polaroid back, a 100 mm lens and a maximum aperture opening of $f3.5$ ($+32$). For Polaroid film type 107 the usual settings of the camera are $f22$ and shutter set at B.

The Stroboscope (Figure 3.7)

The stroboscope flash system that is available is a Honeywell Cronoscope (modified) with an adjustable flash

rate. The fixed rates available are 2, 5, 10, 12.5, 15, 17.5 flashes/second.


Subject Preparation

The subject wears a black cat-suit with long sleeves. Small strips of white masking tape are placed over the appropriate joints while longer strips are adhered to the body of the subject so as to connect one joint with the other. (Figure 3.6)

An internal progress report (Hershler, 1976) has been compiled which describes the above system in even greater detail and contains both diagrammatic and written information on the sequences followed by the human operator in extracting data from a photograph. Also included in this progress report are copies of a number of typical output plots. A listing of the Fortran IV program for the CDC 6400, a corresponding flow-chart and the programmed deck of cards are available in the Locomotion Laboratory for any interested user.

The advantages and disadvantages of this system can be summarized as follows -

Advantages

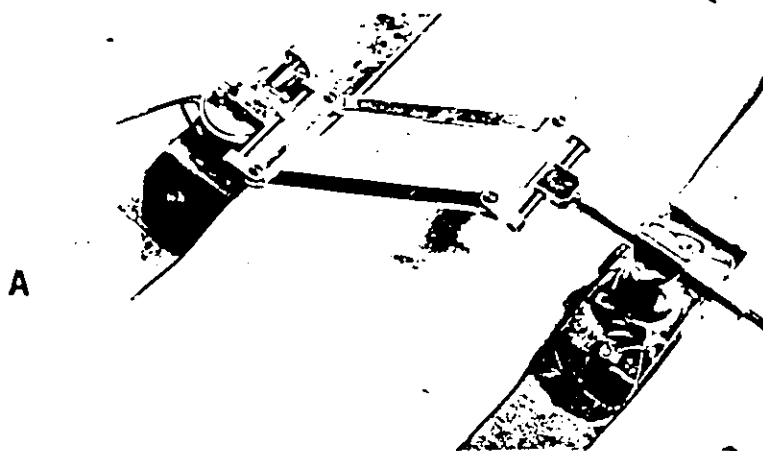
- 
- 1) Provides a simple and relatively inexpensive method of measuring spatial and angular information.

Disadvantages

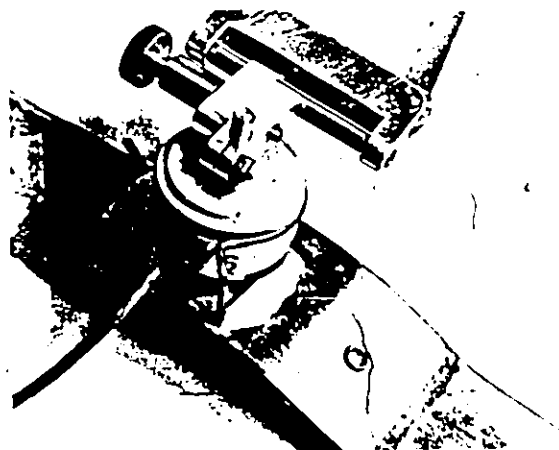
- 1) Does not detect high frequency perturbations in the gait ($>7/\text{sec}$)
- 2) Stroboscopic flashes and tight clothing affect natural gait.
- 3) Long data processing time, involving substantial manual interaction with associated errors.
- 4) Computer time expense
- 5) 2 - dimensional (sagittal) information only.

3.2.4 The Electrogoniometer System

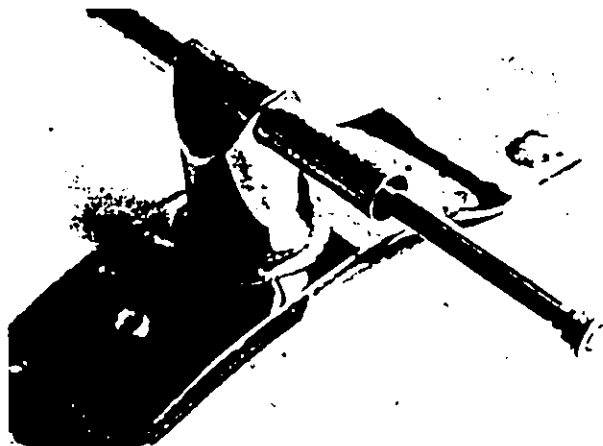
The electrogoniometer used in the Locomotion Laboratory is a device which measures joint angles in one plane. It was developed by members of the Bioengineering Department after a design of Lamoreux (1971) and consists of a linear (1% error) potentiometer attached to a specially designed parallelogram linkage (Figure 3.8). The linkage allows for measurement of angular motion in one plane while compensating for motions in the other planes. Joint movement involves motions in three dimensions and anatomical



A



B



C

Figure 3.8

Self-aligning Electrogoniometer System

- A: Parallelogram linkage
- B: Potentiometer and fixing screw
- C: Bearing rod and bushed tube

joints are bumpy and irregular in shape. This new design of linkage is self-aligning and non-restrictive therefore providing an accurate measurement of the sagittal plane joint angle during movement.

The electrogoniometer system is secured to the appropriate limb segments about each joint with the aid of elastic velcro straps. A simple electronic circuit (Figure 3.9) sends current through an umbilical wire which is supported overhead by runners on a tension cable. As the joint angle changes, the resistance of the potentiometer varies linearly which causes a corresponding change in the voltage across the potentiometer. This analogue voltage is then fed to the acquisition and display system which consists of a PDP11/10 minicomputer and which includes multi-channel input and output analog signal facilities and magnetic disk and tape storage systems. A Tektronix 7613 storage oscilloscope with a 7A18 dual trace amplifier is used for general display of the acquired angle data while a Tektronix 4006-1 graphics terminal with ancillary hard-copy unit is used to record the data in a more permanent form. (Figure 3.10)

Calibration:

Each attached electrogoniometer system is calibrated

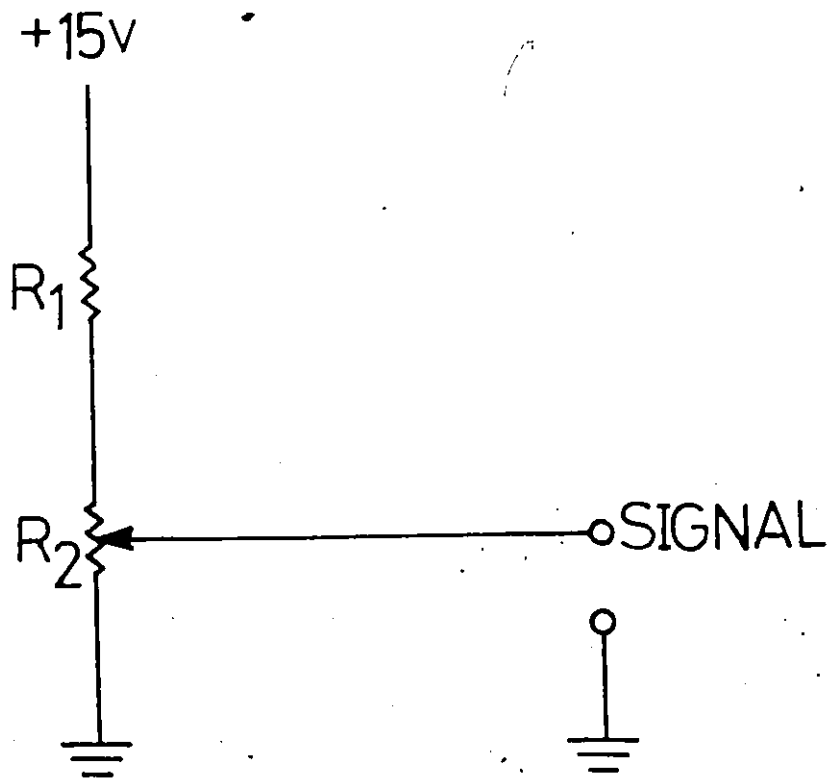


Figure 3.9
 Circuit Diagram For Electrogoniometer System
 $R_1 = 100 \text{ k}\Omega$ $R_2 = 10 \text{ k}\Omega$

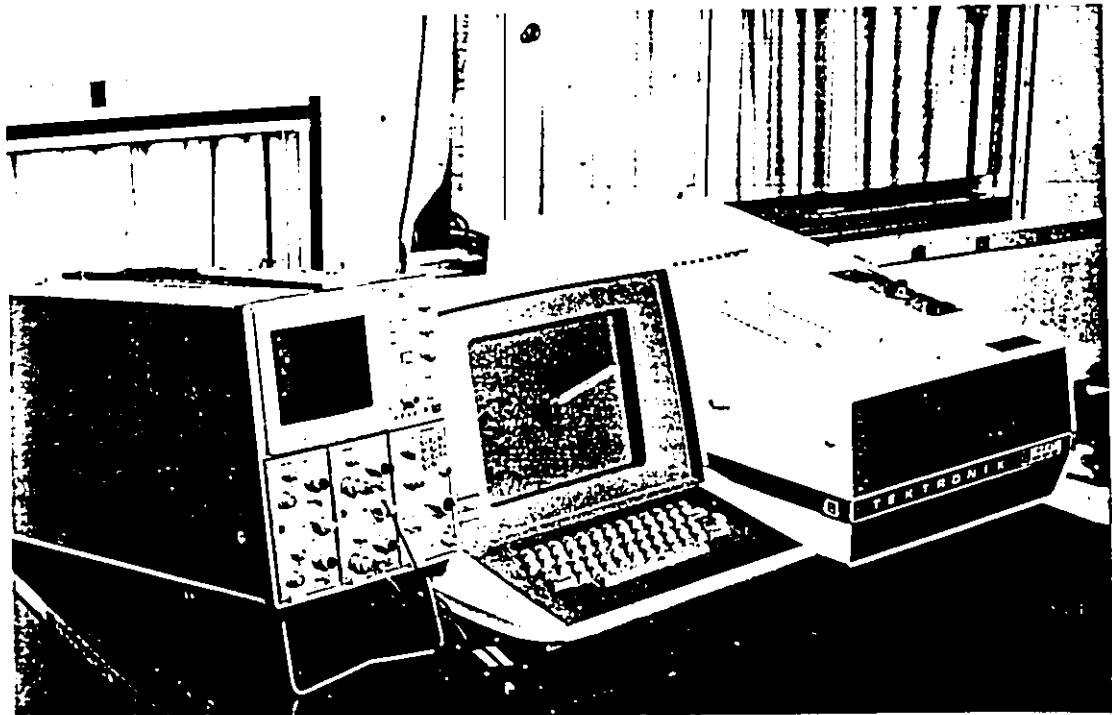


Figure 3.10
 Display Devices
 A: Tektronix 7613 Storage Oscilloscope
 B: Tektronix 4006-1 Graphics Terminal
 C: Ancillary Hard-Copy Unit (Tektronix)

on the patient's body using two selected angles in the range of movement. For each of these angles the corresponding electrogoniometer voltage is acquired and stored by the computer. After final acceptance of the calibration information, the gait study proceeds with the patient walking the length of the walkway. When the subject has attained a relatively constant velocity, the computer is remotely triggered to begin acquisition and collection of the data. These methods were developed by de Bruin and Milner (1977).

As the patient walks there is a shift of the entire electrogoniometer system about the joint due to movement of the muscle bulk under the velcro straps. This slippage affects the calibration of the electrogoniometer system. Certain subjects were calibrated before and after some experiments to obtain an estimate of calibration error. The maximum change in calibration values that ever occurred to any such subject was 20%. It was adjudged that observer error would account for less than half that range with the main source of error due to slippage of the electrogoniometer system on the limb during the experiment.

Figure 3.11 is a complete electrogoniometer system fitted about the knee joint of a patient. Referring to

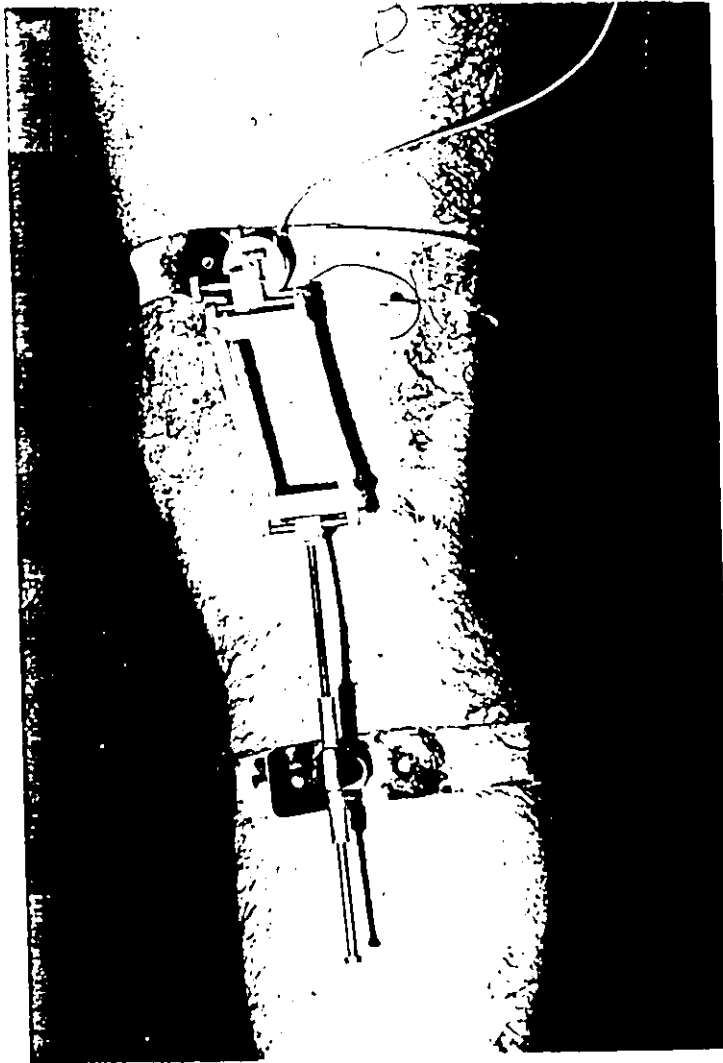


Figure 3.11
Electrogoniometer System Attached About the Knee

Figure 3.8 a breakdown of the components of the electrogoniometer system can be listed:

- (a) The potentiometer is a Bourns* Model 6538 servo mount precision potentiometer (10 k Ω). (Figure 3.8A, B)

* Bourns Inc. Trimpot Products Division.
1200 Columbia Ave., Riverside California. 92507

- (b) The parallelogram linkage is made of 2024T351 aluminium (Figure 3.8A)
- (c) The bearing rod and bushed aluminium tube are made of 2024T351 aluminium. (Figure 3.8C)
- (d) The fixing screws are 18/8 stainless steel (Figure 3.8B)

The advantage of using an electrogoniometer system to measure joint angle is that an analogue signal is obtained which can be relayed directly to the data acquisition system. If desired, the analogue output can be passed through appropriate differentiating circuits so that angular velocity and angular acceleration curves can be obtained. Differentiation, however, does increase the noise associated with the signal so that additional smoothing and filtering techniques might have to be employed.

The various advantages and disadvantages can be summarized as follows:

Advantages

- 1) Analogue signal output allows for continuous monitoring and is conducive to digital processing and subsequent

Disadvantages

- 1) Only angular information in one plane is obtained.
- 2) Large calibration error during an experimental run due to slippage of electro-

- storage in computer.
- 2) Rapid and inexpensive method
- 3) Necessary to attach instrumentation to the body segment which may modify the gait.
- goniometer system.

3.2.5 The Optoelectronic System

An optoelectronic system which obtains virtually on-line the spatial trajectories of the joints during gait has been developed for this Locomotion Laboratory by Brugger and Milner (1977). At the present time the system only tracks moving objects in one plane but the system is being extended to monitor 3-dimensional motion. The optoelectronic system includes a two-dimensional charge-coupled device (CCD) in the form of 190 x 244 array image sensor* which is used for the tracking of body motions. Interfacing circuitry was developed to link the CCD - image sensor to a PDP11/10 minicomputer to enable virtual on-line tracking of illuminated "labels" on a moving object. Essentially the interface consists of counters for equivalent x and y coordinates coupled with a marker detector to decide on the presence or absence of illumination at a particular location. Figure 3.12 is the CCD camera while Figure 3.13 shows the various "labels" in the form of small incandescent light sources attached to the joints of a particular

* CCD 211 Fairchild semiconductor, Palo Alto, California
94304

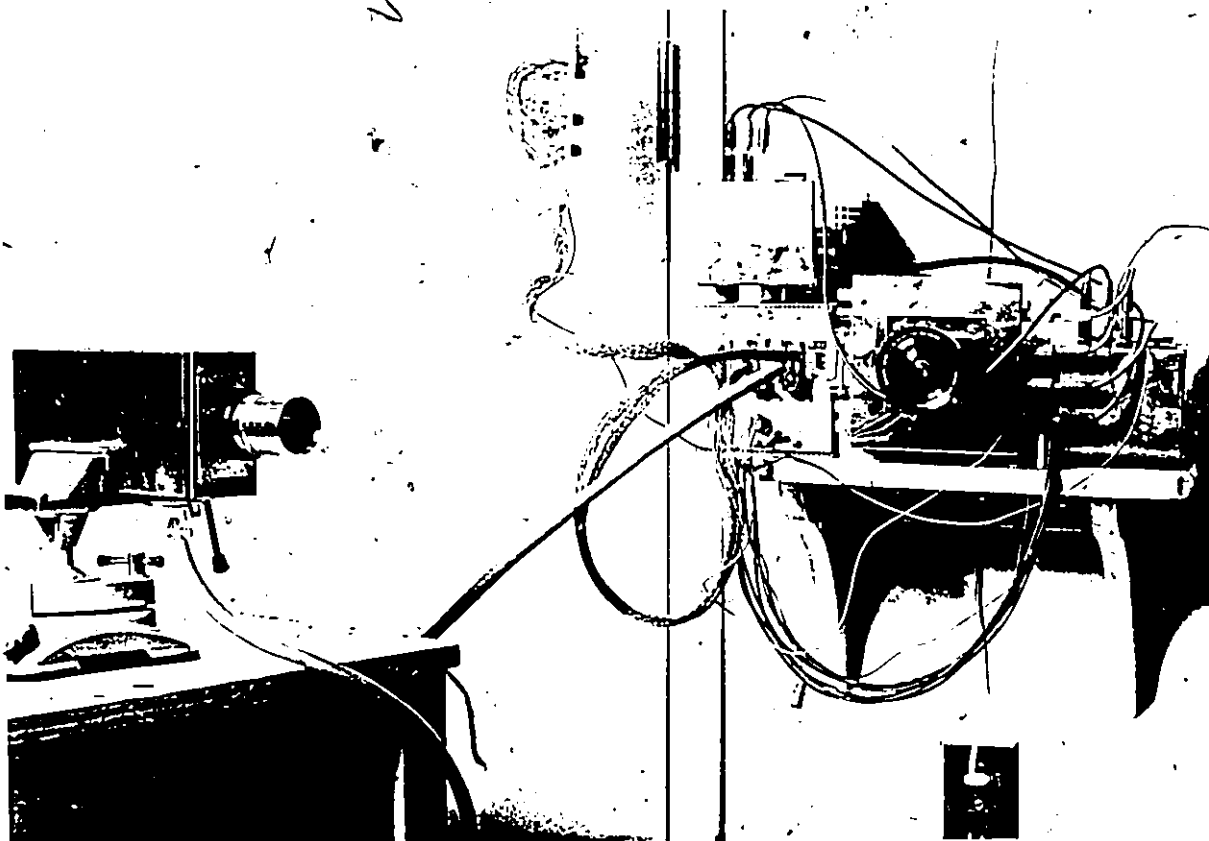
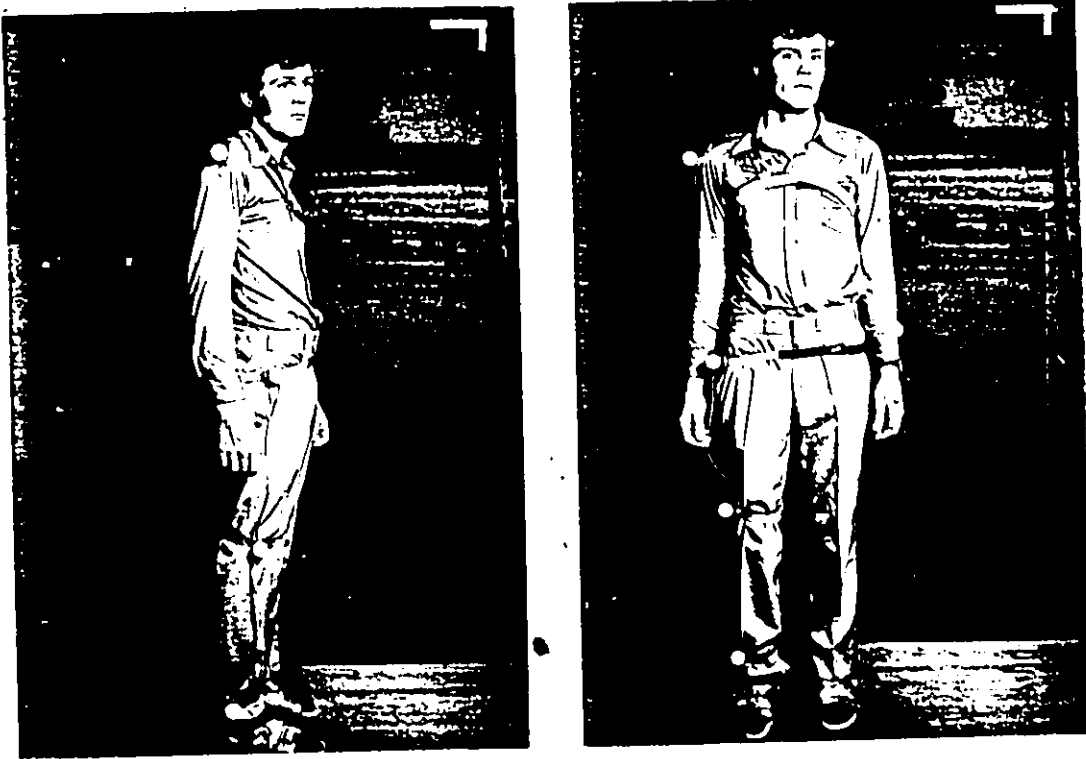


Figure 3.12
The Optoelectronic System

subject. Software routines have been developed by Brugger (1977) to extract and display pertinent kinematic information. Figure 3.5 shows the shoulder, hip, knee and ankle trajectories of a walking subject for three strides ("stick"-diagram). Additional software to separate the footsteps, calculate angles, and analyse the angle-angle diagrams have been developed for use with this system (Hershler, 1977b). Appendix 1 contains a brief description of the program which analyses the angle-angle diagrams.



A.

B

Figure 3.13
Light Sources Attached to Pertinent Anatomical Landmarks
on Body of Subject

A: Lateral View

B: Frontal View

The advantages and disadvantages of this opto-electronic system as compared with the stroboscopic flash-photography and electrogoniometer systems can be summarized as follows:

Advantages

- 1) Provides a rapid, online and accurate method of acquiring and displaying pertinent kinematic information during a gait study.
- 2) With two CCD cameras, 3-dimensional body tracking can be achieved.
- 3) Patient can walk in normal clothes and ambient light.
- 4) The illuminated "labels" attached to appropriate body points do not affect the patient's gait.
- 5) Variable frame rate depending on type of motion studied, 20 - 350 frames/sec.

Disadvantages

- 1) The number of elements in the CCD image sensor defines the resolution (at present image sensors with large numbers of elements are expensive). A centroid technique which averages over the image area improves resolution.
- 2) The swinging arm might obstruct the illuminated "label" for a period of time which could be too large (in the case of pathological gait) for even the extrapolation algorithm to correct.
- 3) The absolute resolution is related to the field of view which is determined by the type of lens and subject-lens distance. The

- 6) Easy to interface with digital computers. present system in these laboratory conditions can only allow for a maximum of 3 successive footsteps.
- 7) Pre-processing by system allows usage of slow minicomputers. 4) The illuminated "labels" cannot be too close or on top of each other in which case the detection algorithm is unable to separate them.
- 8) A large number of "labels" can be detected on the horizontal limited only by the software detection algorithm.

3.3 MEASUREMENT OF THE ELECTROMYOGRAPHIC (EMG) SIGNAL

3.3.1 Monitoring of the EMG signal

Monitoring of the EMG signal from the skeletal muscles is accomplished with the aid of disposable surface electrodes produced by Becton-Dickinson* (Figure 3.14).

These surface electrodes are used for the recording of the electrical activities of surface muscle groups only. Surface electrodes were chosen over fine-wire intramuscular electrodes for the following reasons:

- (1) Fine-wire electrodes are indwelling and hence invasive. Surface electrodes can be quickly applied, are non-invasive and relatively safe to the subject.

* Becton Dickinson - Division of Becton Dickinson and Company, Rutherford, New Jersey, U.S.A.

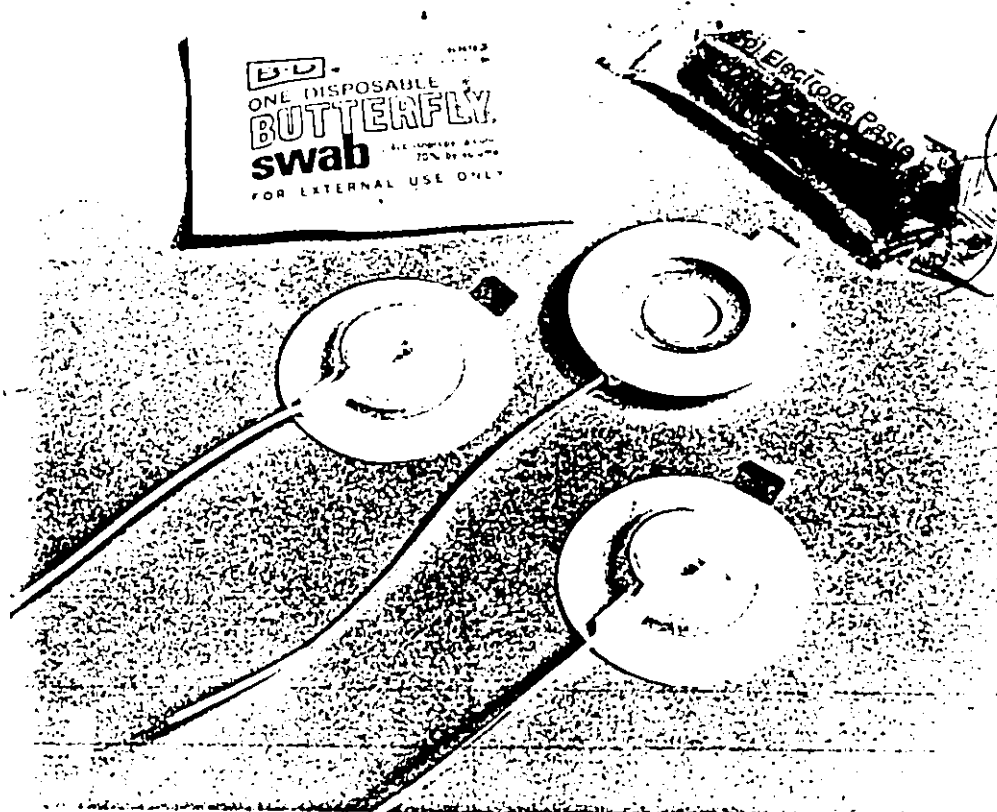


Figure 3.14
Surface Electrodes, Alcohol Swab and Electrode Paste

(2) Fine-wire electrodes can be the cause of some discomfort in certain subjects. The amount of pain may depend partly on the site of implantation (Babb and Dymond, 1975) or the type of hypodermic needles used for the insertion (Jonsson et al, 1968). The latter showed that there existed a positive correlation between the occurrence of bleeding on insertion or removal and the presence of reported pain. This insertion trauma can be minimized by using needles which are small and sharp.

Part of the pain was also due to the type of fine wire used. Jonsson et al (1968b) demonstrated that at least in some cases inserting fine wires caused more pain than a control in which the hypodermic needle was inserted without wires, then removed. It was found by the author of this thesis that during repeated locomotion studies of one subject when the m. rectus femoris contracted and "bunched" up pain was caused in the region of the fine wire electrode inserted into that muscle.

(3) The fine-wire electrodes had to be sterilized before use and because the metal surface of the wire tip oxidized with the air, the fine wire tissue-electrode interface had to be stabilized by passing a DC current in both directions through the wire. This was time-consuming and troublesome.

(4) Migration of the fine-wire electrodes can occur as a result of muscle contraction (Jonsson and Bagge, 1968a). Also with lead migration the bipolar leads could change in relation to each other which changes the characteristics of the bipolar recording. Scott and Thompson (1969) suggest a possible solution by twisting the leads together and with the insulation twisted off at different points (i.e. not both at the tips), even though the pair of leads might move, the exposed recording areas should remain in a constant relation to each other.

(5) Horning et al (1972) recommended the use of surface electrodes for measuring the latency of evoked muscle response except in cases where the muscle is atrophic or where it lies deep to other muscles. Superficial intramuscular placements resulted in latencies that were much longer.

(6) Because of low frequency signal artifact (40 Hz) a high pass filter with a low cut-off at 40 Hz was needed.

It was recognized, however, that if the EMG's of deeper lying muscle groups were desired indwelling intramuscular electrodes would have to be utilized and hence solutions found for some of the above problems. For the purposes of this thesis it was considered sufficient to work only with the EMG's of the surface musculature. The EMG recorded with surface electrodes is more representative of the activity of the surface musculature. In order to obtain the equivalent representation with fine wire electrodes, a multiple set of such electrodes would have to be utilized.

To reduce tissue-electrode impedance, the skin is thoroughly cleaned with alcohol swabs before applying the surface electrode. Also the electrode was pre-gelled with Becton-Dickinson electrode paste before being adhered to the skin surface. The active part of the surface electrode was

thus "floating" on a skin-electrode interface consisting of electrode paste and any other chemicals remaining on the skin surface. This minimized the occurrence of signal artifact due to the movement of skin under the electrode. The impedance of the surface electrodes was found to vary with frequency in the range of 30 k Ω (at 10 Hz) to 7 k Ω (at 1.3 kHz).

3.3.2 Amplification and Processing of the Raw EMG Signal

The various systems for amplification and processing of the EMG signal were developed by members of the Biomedical Engineering Department. The raw EMG signal (containing frequencies from dc upto at most 500 Hz for the type of surface electrodes used) was pre-amplified by means of a differential amplifier. The components were enclosed in a hobby-grade clearcasting resin* so that the amplifier could be easily attached to any part of the body without impediment. Spiral springs attached to the amplifier allow the electrode wire ends to be clamped firmly. (Figure 3.15) Figure 3.16 is a circuit diagram of the differential amplifier. The following table summarizes the characteristics of a typical differential amplifier used in locomotion studies:

* Lewiscraft Toronto Canada.

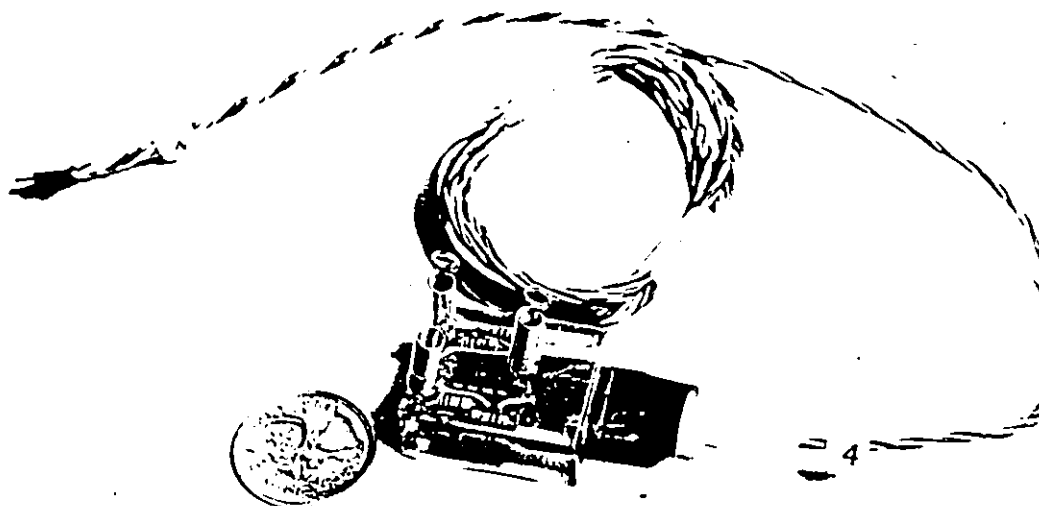


Figure 3.15
The Pre-Amplifier

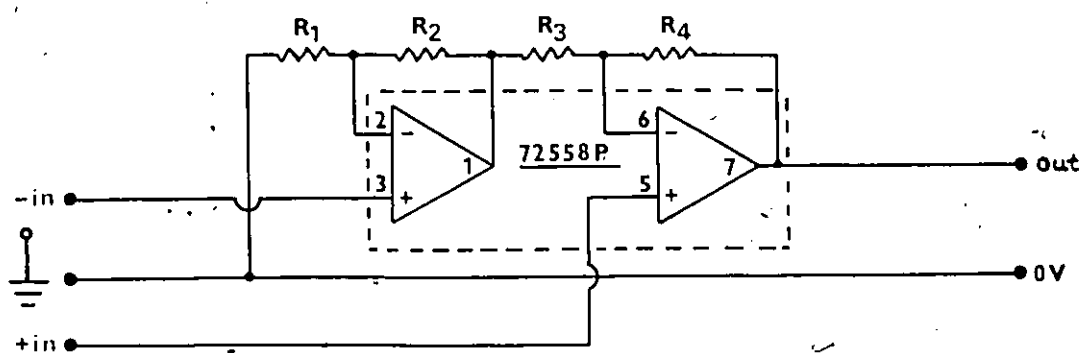


Figure 3.16
Circuit Diagram For the Differential Amplifier
 $R_1 = R_4 = 100 \text{ k}\Omega$ 1% $R_2 = R_3 = 1 \text{ k}\Omega$ 1%

Table 3.1Characteristics of a typical differential amplifier

Common Mode Gain (Balanced): = 1/80

Common Mode Gain (Unbalanced): = 1/50

Difference Gain: 100

Common Mode Rejection Ratio: 8000

Input Impedance: 1.2 M Ω

Output Impedance: 450 Ω

Lower 3 db point: 0.4 Hz

Upper 3 db point: 20 kHz

Gain x Bandwidth: 2 x 10⁶ Hz

The raw EMG signals, after being passed through a high pass filter (low cut-off 7 Hz 3 db point and 12 db/octave slope) to eliminate motion artifacts, could be further amplified so that finally the EMG signals were sampled at a rate of 1 kHz, digitized and stored in the PDP 11/10 minicomputer. Figure 3.17 is a circuit diagram of the high pass filter and amplifiers. It should be noted that the analogue EMG signals were transferred from the outputs of the differential amplifiers to the high pass filters and amplifiers by means of umbilical wires similar to those transferring the electrogoniometer and footswitch signals mentioned before. At any one time a maximum of eight analogue signals could be monitored and transferred to the

computer.

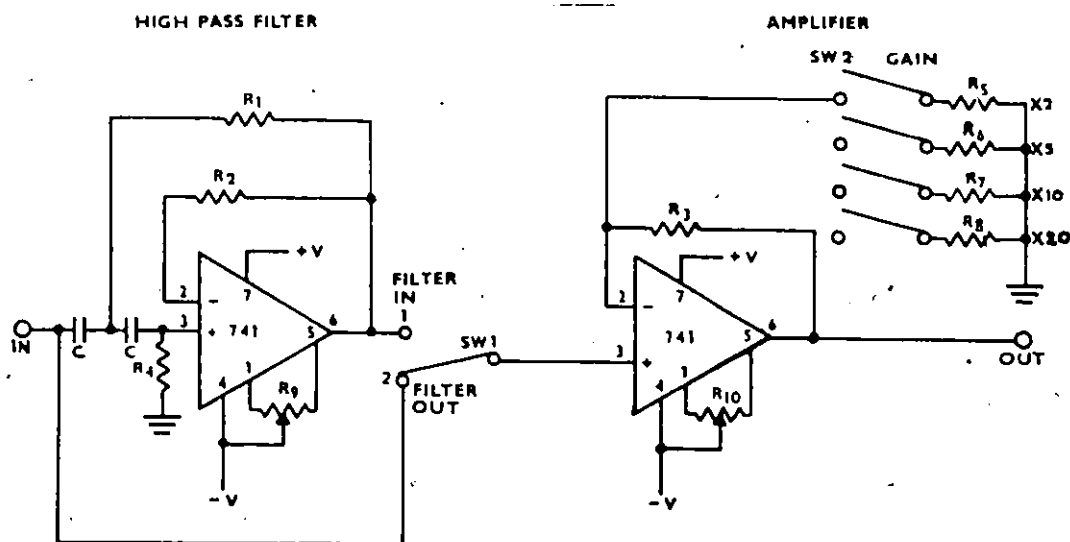


Figure 3.17

Circuit Diagram For High Pass Filter and Amplifiers

$R1 = R3 = R5 = 100 \text{ k}\Omega$

$R8 = 5.24 \text{ k}\Omega$

$R2 = R4 = 22 \text{ k}\Omega$

$R9 = R10 = 10 \text{ k}\Omega$

$R6 = 24.9 \text{ k}\Omega$

$C = .1 \text{ }\mu\text{F}$

$R7 = 11 \text{ k}\Omega$

$V = 15 \text{ V}$

In addition to the display system which includes the Tektronix storage oscilloscope and Tektronix graphics terminal with ancillary hardcopy unit, there exists also a visicorder with ultra-violet paper output upon which the analogue signals can be displayed in hard copy form. The visicorder available in the Locomotion Laboratory is a Honeywell* Fibre-Optic CRT Visicorder Model 1858 which had the capability of displaying 8 channels of information - 6

* Honeywell Test Instruments Division, P.O. Box 5227,
Denver Colorado, U.S.A.

EMG channels (or electrogoniometer) and 2 footswitch channels. In addition to high pass filtering and amplification the EMG signals could be passed through a rectifier and averager which would result in EMG envelopes which followed the peaks of the rectified signal. (The time constant of the rectifier averager is 4.84 msec). Figure 3.18 is a circuit diagram of the rectifier and averager available in the Locomotion Laboratory.

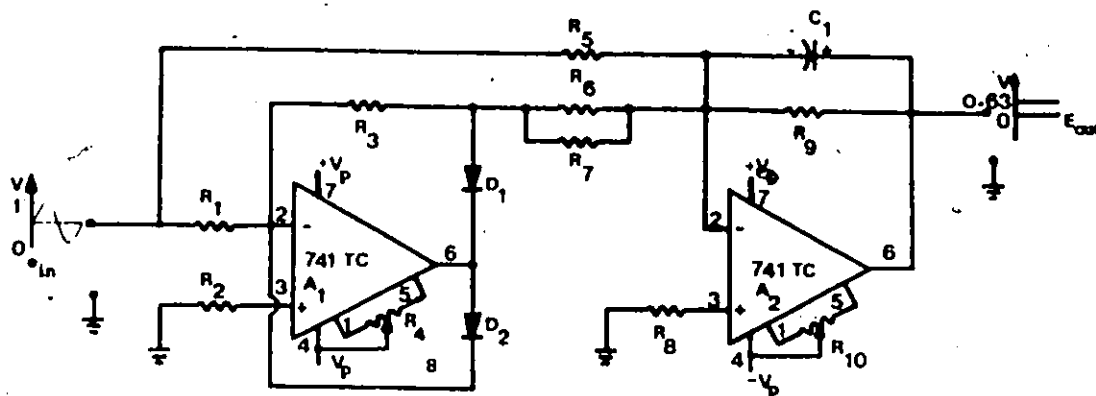


Figure 3.18
Circuit Diagram of the Rectifier and Averager
Used in the Locomotion Laboratory

$R_1 = R_3 = R_5 = R_6 = R_7 = R_9 = 22 \text{ k}\Omega$

$R_2 = 15 \text{ k}\Omega$

$R_4 = R_{10} = 10 \text{ k}\Omega$

$R_8 = 6.8 \text{ k}\Omega$

$V_p = 15 \text{ V}$

$C_1 = .22 \text{ }\mu\text{F}$

All resistors 10%, 1/4W

D1, D2 silicon signal diodes (1N4154 or equivalent)

3.3.3 Storage of the EMG Signals

After digitization of the analogue EMG signals, the sampled data could be stored either on the RK11 disks of the PDP 11/10 minicomputer or on magnetic tape.

3.3.4 Analysis of EMG Signals

A large quantity of software has been written by the author of this thesis in both Fortran IV and Macro assembly languages (RT11 version) for analysis and display of the EMG and electrogoniometer signals. Appendix 1 contains flow-charts of two of the programs available. Listings of these programs which include self-explanatory comments are available in the Department of Biomedical Engineering, Chedoke Rehabilitation Centre, Hamilton, Ontario. Additional software relating to different aspects of the analysis and display of these signals has been developed by de Bruin and Milner (1977). The contents of this chapter have been published in the form of a progress report (Hershler, 1977b).

CHAPTER 4

AN OPTIMALITY CRITERION FOR PROCESSING ELECTROMYOGRAPHIC (EMG) SIGNALS RELATING TO HUMAN LOCOMOTION

4.1 Introduction

4.1.1 Major Concerns

This thesis is concerned with endeavours to model the functional relationships between the EMG activities in pertinent skeletal muscles and the resulting limb angular rotations during normal human locomotion. Prompted by this concern, and the need for consistency and repeatability in EMG measures, it was considered essential to study the characteristics of observed electromyographic signals and to seek appropriate consistency and repeatability criteria.

Fundamental reasons for pursuing such a study are the following:

(1) In order to assess surface electromyographic signals which vary with time, an objective, accurate and consistent description is needed.

(2) Such a description should be universally

accepted to enable comparisons of results from different laboratories to be made.

(3) Even though it is impossible to exactly repeat two or more consecutive cycles of normal gait both kinematically and electromyographically this is of minimal concern since all that is required is to extract from the EMG signals, consistent and reliable information that the gait cycles have in common.

In this chapter only the rectified and averaged EMG signal has been considered. Attention is confined to this type of signal processing for the following practical reasons:

(a) The resulting envelope $E(t)$ following from the rectified and averaged EMG signal retains the essential phasic and amplitude information or activity (i.e. it can be considered to be physically meaningful).

(b) $E(t)$ can be obtained with suitable equipment usually readily available to most gait laboratories.

(c) The descriptor $E(t)$ seems to be universally accepted in most laboratories interested in surface electromyography.

(d) de Bruin (1976) has shown that the rectified and averaged EMG signal is as sensitive to changes in muscular contraction (isometric) as any other commonly considered

amplitude processor.

This chapter reports reliability results for processed signals derived from arrays of surface electrodes on the m. vastus lateralis for four normal subjects and on the m. rectus femoris for two normal subjects walking under controlled repeatable gait conditions at a maximum of three different speeds along a level walkway.

A reliability criterion is defined consisting of a variance ratio which measures the repeatability of an EMG signal over a given number of identical footsteps.

4.1.2 Reliability

Following the convention of Viitasalo and Komi (1975) reliability is defined to be the repeatability of measurements within a test session and constancy to be the repeatability of measurements between different test days.

Based on the results of this study, the following conclusions are drawn:

(1) The reliability varies as a function of speed of walking.

(2) Using arrays of identical electrode pairs on the muscles indicated it was found that the reliability under

identical experimental conditions varied depending upon the positions of the electrode pairs upon the muscles.

(3) At any one speed of walking, the reliability varies as a function of the processor. (The processor yielding the rectified and averaged signals was adjusted to provide different degrees of smoothing).

While a range of EMG processors can be specified with which the most reliable EMG information can be obtained, the choice of an optimal EMG processor would be governed by two conditions:

(a) The processed signal is obtained as quickly as possible and

(b) The processed signal contains the most consistent and reliable information over the number of footsteps analysed.

(4) The relative comparisons of reliability with respect to speed of walking, type of processing and electrode position were found to be independent of the numbers of footsteps used as long as the same numbers of footsteps were used throughout the analysis. Different numbers of footsteps used in the analysis might give different absolute results but relative comparisons remain identical.

(5) Ascertaining an area of the muscle which is of a constant reliability with respect to identical electrode

pairs could facilitate a comparison of different types of electrodes.

4.2 Background

Komi and Buskirk (1970) have examined the reproducibility of electromyographic measurements with surface electrodes and intramuscular wire electrodes. Results were reported for repeatability of measurements with surface electrodes in submaximal and maximal isometric and maximal isotonic contractions of the m. biceps brachii. Similar results were reported for intramuscular wire electrodes. In this chapter dynamic conditions have been examined.

In the study by Komi and Buskirk (1970) only one electrode site on the muscle was chosen and they did not examine the variations in repeatability with electrode position (for the same type of electrode). It is considered that comparisons between the reliability of two different types of electrodes are difficult to make if reliability is a function of placement position of the electrodes on or in the muscle.

One question, too, the sensitivity of the "integrated" EMG (IEMG) to determine the reliability of the

measurements since such a measure quantifies the area under the rectified EMG signal and tends to mask phasic information.

Viitasalo and Komi (1975) investigated the reliability and constancy of certain EMG signal measures (including IEMG) where the EMG signal was recorded using surface electrodes during constant maximal and submaximal contractions (apparently under isometric conditions) of the m. rectus femoris. The above remarks are applicable as well to this paper.

Jonsson and Reichmann (1968c) studied the repeatability in electrical activity of the m. brachioradialis using inserted wire electrodes during isometric and isotonic contractions. While these authors asked pertinent questions regarding repeatability in various circumstances, they do not appear to have provided quantitative answers.

Grieve and Cavanagh (1974) have also expressed an interest in whether EMG signals exhibit any repeatability during gait. They reported that a quantitative analysis of EMG signals was made either from bipolar pairs of surface electrodes with 5cm spacing overlying various muscle groups of the lower limb, or from pairs within a 3 x 4 rectilinear

array of electrodes (5 cm spacing) over one region of the limb. These authors found that differences in intensities and temporal patterns exist for different positions of the electrode pairs on the various muscle groups tested. Also the standard deviations were less over the array of electrodes placed on the quadriceps compared with the array placed on the medial side of the thigh. Although these results were interesting, the authors did not appear to have a sufficiently sensitive criterion to make an objective assessment of variations in reliability with electrode position and, as the authors admitted, their findings did not lead to any generalization. They also suggested that the integral of the full wave signal (FWRI) could be used to describe the EMG.

(The FWRI is not to be confused with the IEMG which is a continual evaluation of the area under the signal whereas the FWRI evaluates the area for discrete epochs of the signal.)

The FWRI was determined either in successive samples of 50 msec following heelstrike or samples equal to 5% of the walking cycle. The FWRI was taken about the mean base line of voltage in each sample. The authors base their choice of a 50 msec sample duration on their assumption that the frequency ranges of the displacements of the body and their time derivatives which are of interest to the

kinesiologist, extend at least from 0 to 20 Hz.

By using successive 50 msec samples to determine the FWRI, Grieve and Cavanagh transformed a continuously varying rectified signal into a histogram of discrete levels. In the work reported here, however, an optimal percentage length of the walk-cycle is determined for use in the averaging process. Also the averaging process involves the use of a moving window of given length shifted along the original signal to obtain a continuous signal which is in a form amenable to further signal processing. The use of a moving window has the advantage that better use is made of the time history of the signal being processed.

Kramer et al (1972) investigated the effects of a change in electrode position on the EMG amplitude. The voltage distribution across the m. triceps brachii, which emerged from amplitude measurements on the electromyogram obtained during repeated isometric muscle contractions under identical conditions, showed that reduction in amplitude of about 25% occurred at a distance of only about 3 cm from the assumed muscle midpoint. Further results confirmed that differences occurred between voltage values derived simultaneously from the midpoint to those from neighbouring points on the muscle. The following points should be

considered in relation to the work of Kramer et al (1972).

(1) The authors used a RLC filter (time of rise 50 msec; time of fall 150 msec) to rectify and smooth the electromyogram. If however the characteristics of the filter were changed this would change the mean values obtained as well as the standard deviations about the mean for the number of identical contractions performed.

(2) It should be recognised that it is the variance about the mean for identical contractions that will give information on the repeatability of the EMG signal. In Kramer et al (1972) which gives information on the standard deviations about the means, it is noteworthy that the points furthest from the mid-point indicate better reproducibility even though the highest voltage value is obtained at the mid-point (even considering the fact that as the mean decreases so does the variance). Figure 4.1 is drawn from the aforementioned paper.

Elliot and Blanksby (1976) investigated the reliability of average integrated electromyograms during running. Cross-correlation was employed to analyse the average integrated electromyogram for one trial of each selected muscle with a repeated trial which was not controlled other than by standardizing the speed of running.

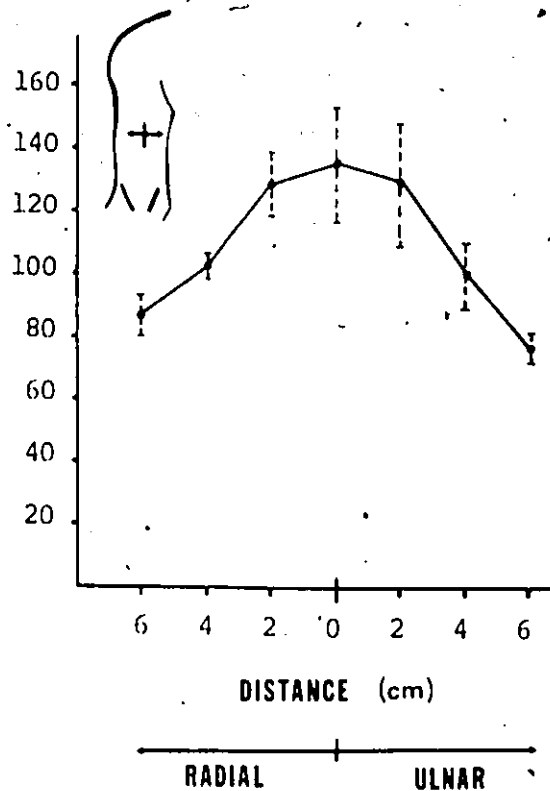


Figure 4.1
 Influence of placement of electrodes on the derived electrical muscle activity. Variation of the exploring electrode perpendicular to the course of the fibres. Unipolar lead (from Kramer et al, 1972)
 Abscissa: Distance of exploring electrode from midpoint of muscle in cm.
 Ordinate: Mean electrical muscle activity in μV

The following points, however, should be considered in relation to their work:

(1) The final average integrated electromyogram is a function of the initial smoothing performed on the raw EMG. Elliot and Blanksby (1976) used a RC smoothing circuit evidently with a time constant of 200 msec. No mention was made of the possibility of using a shorter time constant and

as will be shown later, a time constant of 200 msec is needlessly too large since it smooths out valuable repeatable information from the EMG.

(2) The effects on the results of changing the electrode position and type of electrode were not considered.

From the foregoing, it does not appear that information on the processing of EMG signals is sufficiently comprehensive to provide ready answers to the following questions:

(A) What is the optimal form or measure of the EMG signal which can be used in the description and modelling of a biological phenomenon such as gait and what is the best criterion for optimality?

(B) Does the EMG signal in whatever state it is observed vary significantly with electrode type, orientation and position in or on a muscle and what is the best criterion for making a decision on electrode type or position?

In order to find an answer for question (A) which in turn could throw some light on question (B), a statistical criterion has been devised. This criterion is a variance ratio which measures the reproducibility or repeatability of

the EMG signal for a given number of footsteps. As the results of this thesis will show, the variance ratio will enable the observer to choose an optimal EMG signal processor. The exact choice of such a processor is governed by two conditions.

(1) The processed signal is obtained as quickly as possible and

(2) The processed signal contains the most consistent and reliable information over the number of footsteps analysed.

The criterion also enabled an optimal electrode position on a muscle to be found.

4.3 Optimality Criterion

The optimality criterion put forward by Hershler and Milner (1976) measures the repeatability of a signal over a given number of identical footsteps. (See Figure 4.2) This repeatability can be evaluated independently of the peak amplitude of the particular signal by the following variance ratio:

$$VR = \frac{\sum_{i=1}^k \sum_{j=1}^n (X_{ij} - \bar{X}_i)^2 / k(n-1)}{\sum_{i=1}^k \sum_{j=1}^n (X_{ij} - \bar{X})^2 / (kn-1)} \quad (4.1)$$

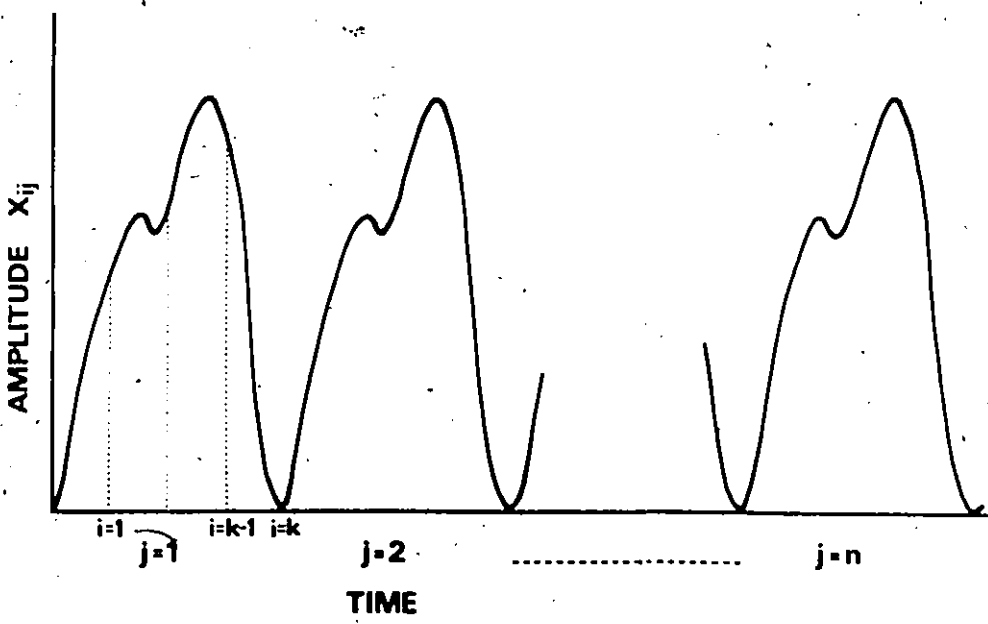


Figure 4.2
 A repetitive time varying signal
 k = Total number of points in a signal period
 n = Total number of signals being analysed

where k = no. of time points and n = no. of footsteps and where X_{ij} is the actual value of the j^{th} EMG signal at time point i and \bar{X}_i is the average of the EMG values at time point i averaged over j realizations of the experiment (in the case of gait j realizations would be j identical footsteps), \bar{X} is the grand mean of the average EMG signal:

$$\bar{X} = \frac{1}{k} \sum_{i=1}^k \bar{X}_i$$

Intuitively one can see that for an EMG signal completely irreproducible over-j footsteps $\bar{X}_i \neq \bar{X}$ and both

the numerator and denominator are estimates of the same variance with the result that $VR \rightarrow 1$. Similarly for an EMG signal completely reproducible over j footsteps the numerator $\rightarrow 0$ as $X_{ij} \rightarrow \bar{X}_i$ so that with the denominator always non-zero (i.e. the EMG signal is never purely a constant dc signal) $VR \rightarrow 0$. It is to be stressed that such a determination of the repeatability of a signal by means of the VR can be applied to any repetitive signal.

An analogy to this variance ratio can be found in statistical texts considering the analysis of variance e.g. Wonnacott and Wonnacott (1969). An estimate of the analytical error variance (mean square between steps) is generally given by:

$$\sum_{i=1}^k \sum_{j=1}^n (X_{ij} - \bar{X}_i)^2 / k(n-1)$$

where there are k samples (observations within a step) and n repeat analyses (steps) on each, and the "total sum of squares" of all the observations about the grand mean \bar{X} is given by

$$\sum_{i=1}^k \sum_{j=1}^n (X_{ij} - \bar{X})^2$$

with $(nk-1)$ degrees of freedom. The variance ratio introduced here is merely the ratio of the mean square

between steps to the total sum of squares.

In the account of the experimental procedure which follows, an attempt is made to address the questions (A) and (B) posed earlier on.

4.4 Experimental Procedure

Electromyographic signals were acquired for six ambulatory subjects constrained to walk in a particular way at two or three different speeds. The EMG signals were recorded from four pairs of surface electrodes placed along the length of the m. vastus lateralis (or m. rectus femoris). Prior to application of the electrodes, the skin was thoroughly cleaned with alcohol. The surface electrodes used were those produced by Becton - Dickinson*. The distance between the centres of each electrode in a pair was 4.6 cm. Before each experiment a polaroid photograph of the muscle and attached electrodes was taken (see Figure 4.3). In this manner a permanent record of the position of each electrode on the muscle was retained.

Controlled gaits at selected speeds were analysed. Before each experiment stride length markers on the walkway were adjusted to match with the most natural walk of each subject.

* Division of Becton Dickinson and Company, Rutherford, New Jersey, U.S.A.

stride periods coupled with known constant stride lengths. Each subject performed the various constrained walks several times during which data relating to an appropriate number (typically 5) of footsteps in the steady state were recorded. In effect, each footstep constituted a separate realization of the experiment.

In each experimental run, the raw EMG signals were passed through identical differential amplifiers (gain 100, input impedance $1M\Omega$) and high pass filter (low cut-off 7 Hz 3db point and 12db/octave slope) to eliminate cable-motion artifact. The upper limit of the frequency response was 2kHz (3db point), well above the nominal 250 Hz bandwidth of these surface EMG signals. The pre-conditioning system was designed such that no signals with frequency components > 500 Hz were sampled. Finally the analogue EMG signals were sampled at a rate of 1 kHz, digitized and stored in a PDP11/10 computer. More details concerning the experimental techniques involved in the recording and processing of EMG signals can be found in Chapter 3.

4.5 Computer Processing

The stride period (heel strike to heel strike interval of the same foot) was computed for each footstep digitized. Only those footsteps with stride periods within 40 msec of the average stride period were retained. (40 msec is arbitrary and can be made smaller the more

repeatable the gait becomes). The five most repeatable footsteps were then normalized to the average stride period. This was achieved by expanding the shorter footsteps (with the aid of linear interpolation of data points along the entire length of the signal) and compressing the longer footsteps (by uniformly deleting data points along the length of the signal). At a sampling frequency of 1 kHz and typical footstep periods varying between 1.0 and 1.5 seconds the degree of signal manipulation at worst involved the ~~deletion or addition~~ of 40 points in 1000 points.

Full wave rectification of the EMG signals was simply achieved by taking the absolute value of the digitized data points.

Smoothing of the EMG signals was achieved digitally. A selected boxcar window (i.e. a weight of one is given to each sample in the window) was shifted along the length of the signal from point to point. Each point in the original EMG signal corresponding to the middle of the window was replaced by the average value of the points in the window. Since gait is a cyclic process, in order to start and end the window-averaging process, a suitable number of data points from the end of the EMG signal were appended to the beginning and conversely from the beginning of the EMG

signal, data points were appended to the end.

Changing the length of the window simulated changing the time-constant of a hardware averager. Any given window length was found to be approximately 4 times the RC time-constant of the corresponding hardware rectifier-averager with a configuration as in Figure 3.18.

Changing the shape of the window (e.g. Gaussian windows) did not effect the statistics. The algorithm is hardly affected by the word size of the computer since changing from single precision to double precision only changed the sixth decimal place by 1 digit. Thus error due to round-off could be discounted.

Middle window averaging is preferred since this eliminated phase delays due to window length. End window averaging other than introducing time delays still gave the same relative statistical results.

4.6 Results and Discussion

4.6.1 Processed Signals

Figures 4.4 and 4.5 show typical EMG signals recorded from two different sites on the m. vastus lateralis. Also

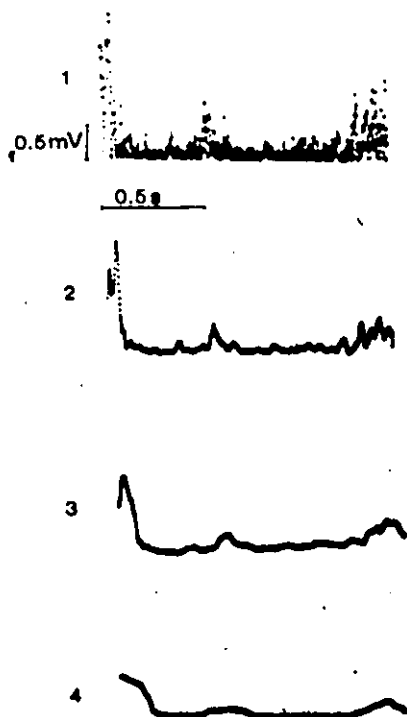


Figure 4.4
EMG signal processing for Subject C (m. vastus lateralis)
Top electrode position

- 1: Full wave rectified EMG signal (FWR)
- 2: FWR + 16 msec window length averaging
- 3: FWR + 50 msec window length averaging
- 4: FWR + 150 msec window length averaging

shown are the results of various modes of processing. The effects of smoothing using different window lengths are clearly depicted as are the variations produced in the signals for different electrode placements on the given muscle.

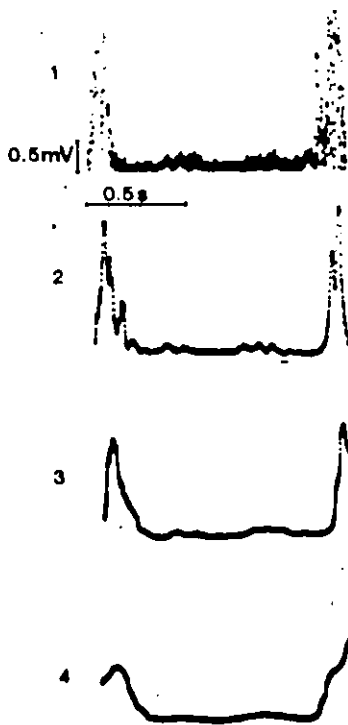


Figure 4.5
EMG signal processing for Subject C (m. vastus lateralis)
Lowest electrode position

- 1: Full wave rectified EMG signal (FWR)
- 2: FWR + 16 msec window length averaging
- 3: FWR + 50 msec window length averaging
- 4: FWR + 150 msec window length averaging

4.6.2 Repeatability Curves

Figure 4.6 shows a representative set of repeatability curves for different electrode positions on the m. vastus lateralis of subject F. The ordinate reflects the variance ratio as described by equation 4.1, whilst the abscissa depicts the window lengths which were selected for digital processing of the acquired EMG data. The electrode positions indicated in Figure 4.6 are described fully by Figure 4.3. The shape of the repeatability curve with

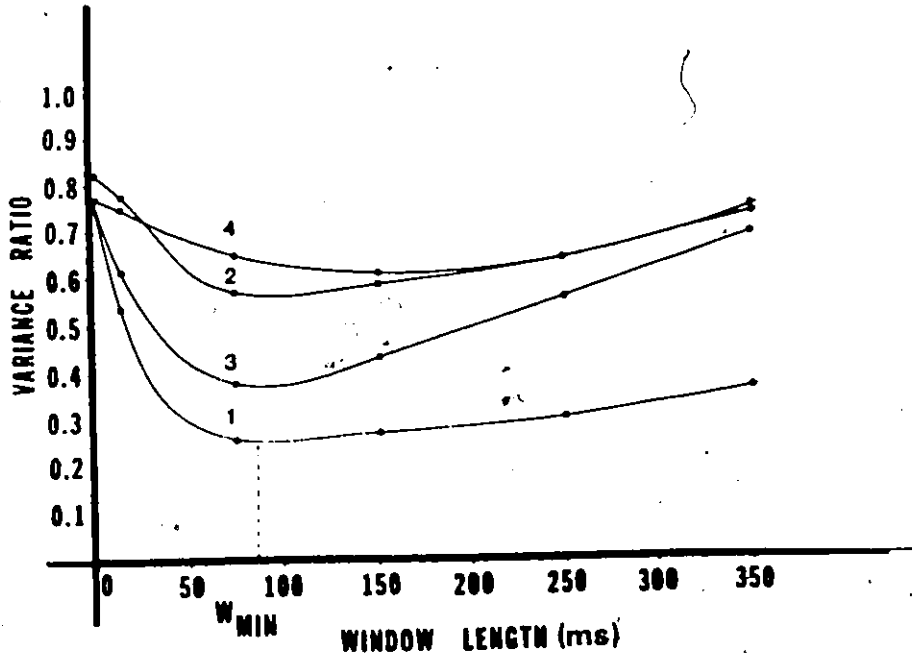


Figure 4.6
 Repeatability curves for different
 electrode positions Subject F
 Speed of walking = 140.0 cm/sec
 Stride length = 150.0 cm
 No. of footsteps = 5
 1: Top
 2: Middle
 3: Lower middle
 4: Lowest

increases in window length is of interest. The trends exhibited by all such curves were constant for all the subjects tested. The general characteristics exhibited by repeatability curves can be briefly summarized as follows:

Beginning with narrow windows and increasing the window size, the curve descends with a sharp negative slope until it reaches a minimum (In Figure 4.6 curve #1 reaches its minimum at a window length W_{min} of approximately 84

msec). After the minimum the curve ascends with a gradual positive slope.

One can rationalize the shape of the repeatability curve by taking recourse to Figure 4.7 which is a plot of both the numerator and denominator of VR as a function of window length. For the range of window lengths $W \leq W_{\min}$ randomities are being smoothed out of the rectified EMG signals in such a way that the resulting envelopes become as repeatable as is possible (i.e. the variance ratio VR finally reaches a minimum). Note that the numerator of VR decreases more rapidly than the denominator over this range. After this point, as the smoothing increases with increasing window length ($W > W_{\min}$) the numerator of the variance ratio remains constant while the denominator tends to decrease further until finally reaching a constant level. Thus the repeatability curve tends to ascend for $W > W_{\min}$ as more and more repeatable phasic information is being smoothed out of the the EMG signals.

4.6.3 Selection of Processor

The optimal processor would thus lie in the vicinity of the minimum corresponding to a window length W_{\min} . In Figure 4.6 curve #1 the minimum occurs at approximately 84 msec. Recognizing the gradual rise in variance ratio for

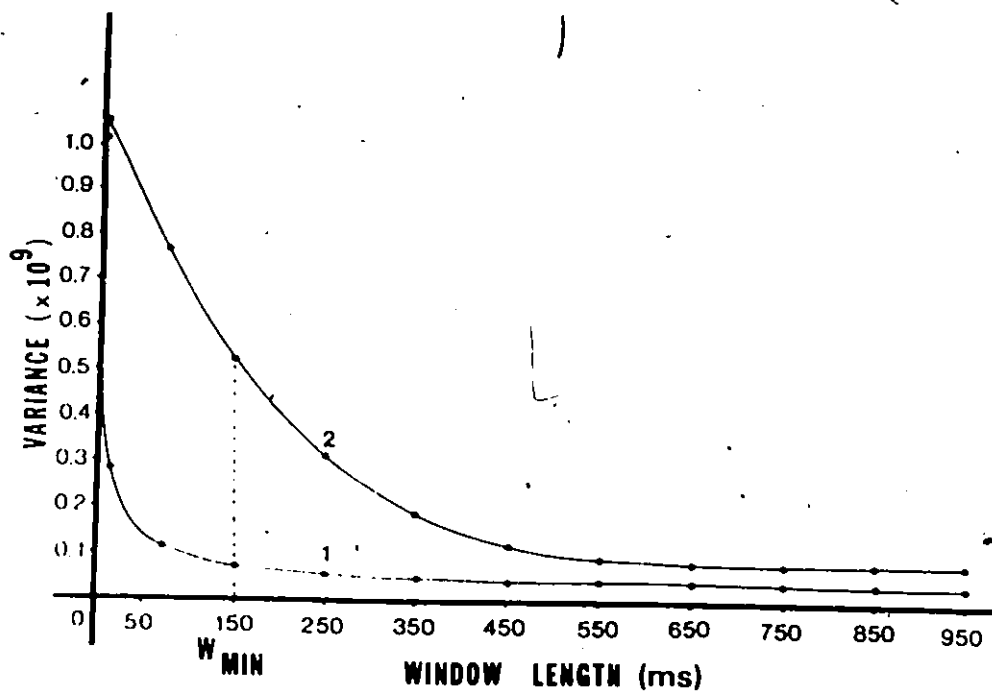


Figure 4.7
 Numerator and denominator of the variance ratio
 as a function of window length Subject B
 Speed of walking = 83.3 cm/sec
 Stride length = 150.0 cm
 No. of footsteps = 5
 1: Numerator of variance ratio
 2: Denominator of variance ratio

windows exceeding W_{\min} the choice of a particular processor would be governed by two practical conditions. The processed signal should be:

- (a) obtained as quickly as possible and
- (b) contain the most consistent and reliable information over the number of footsteps analysed.

In Figure 4.6 curve #1, an obvious choice for an optimal processor would be a rectifier-averager with a RC time constant of approximately $84/4 = 21$ msec (as mentioned before the window length of a given digital rectifier-averager is approximately 4 times the RC time constant of the corresponding hardware rectifier-averager).

4.6.4 Electrode Position

Clearly from Figure 4.6, repeatability curve #1 is associated with the optimal electrode position since the EMG signals associated with that particular electrode pair are the most reliable over the entire range of processors.

4.6.5 Walking Speed

Figures 4.8 and 4.9 show variations in repeatability for three different speeds of walking in the cases of subjects A and D. Interestingly in both cases (but to a greater degree with D) the most comfortable gait speed in the range selected (as assessed by the subject) was associated with the most repeatable curve.

These results suggest that a subject is unable to walk repeatably to the same degree at different speeds. It is interesting to note that in previous work (Milner et al, 1971a) it was concluded that the most comfortable walking

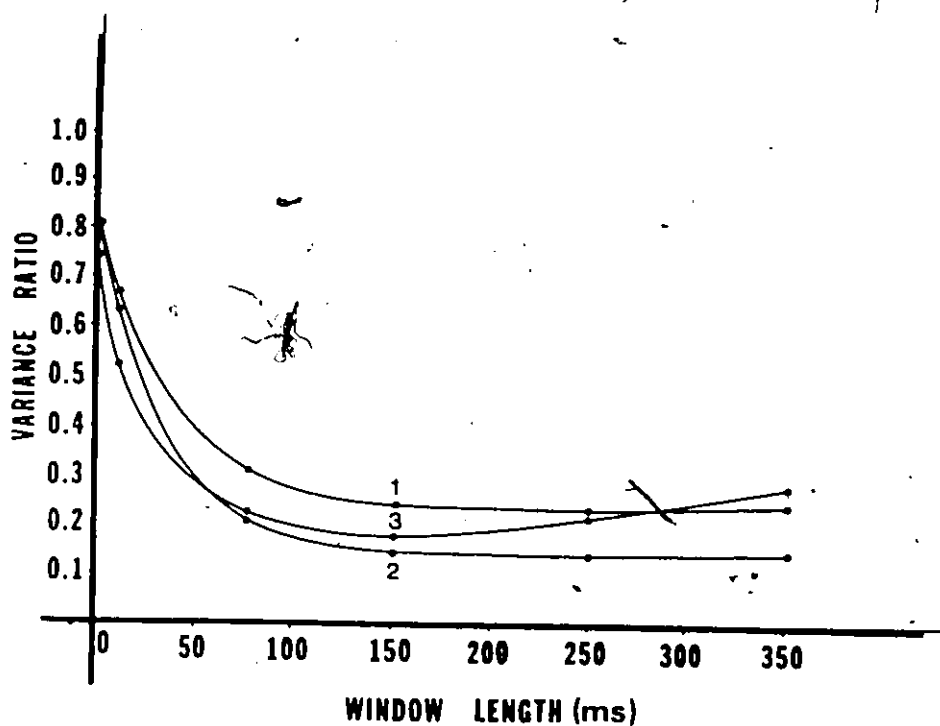


Figure 4.8
Repeatability curves for different speeds of walking
Subject A

Stride length = 120 cm

No. of footsteps = 5

1: Speed of walking = 70.5 cm/sec

2: Speed of walking = 96.7 cm/sec

3: Speed of walking = 100.9 cm/sec

speed would be such as to minimize "energy consumption" and also permit a reasonable propulsion speed. The above results lead one to speculate on the possibility of a maximization of the phasic repeatability of electromyographic activity concomitant with a minimization of energy consumption. Further work in this area seems warranted.

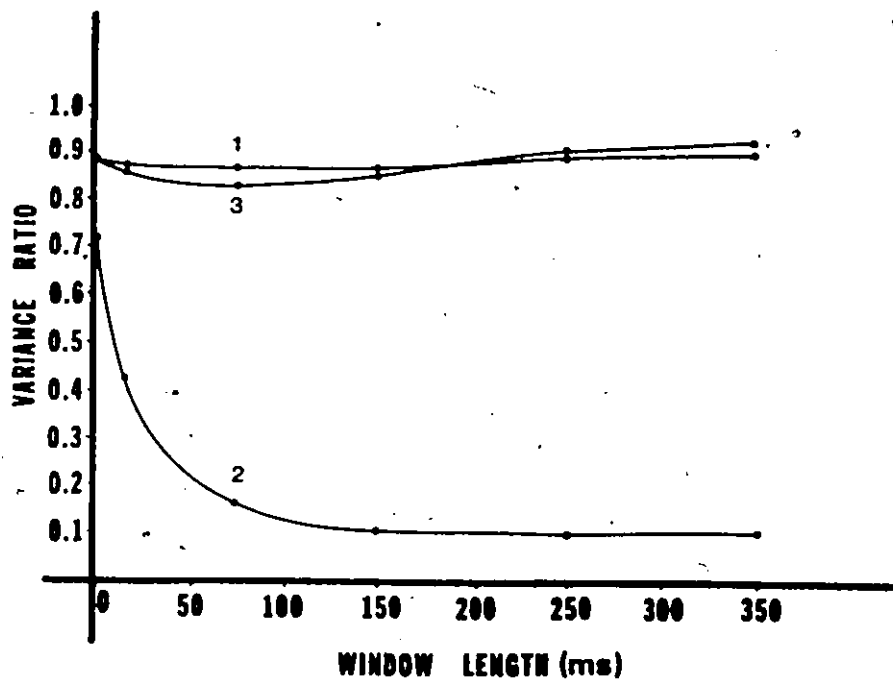


Figure 4.9
Repeatability curves for different speeds of walking
Subject D

Stride length = 112 cm

No. of footsteps = 5

1: Speed of walking = 63.8 cm/sec

2: Speed of walking = 90.3 cm/sec.

3: Speed of walking = 96.8 cm/sec

4.6.6 Optimal Electrode Sites and Walking Speeds

Table 4.1 records the optimal electrode positions and optimal processor ranges for the six different subjects over a range of speeds. Examination of the table shows that generally the optimal electrode position stays practically constant as the walking speed changes. In only one subject F did it change quite dramatically.

TABLE 4.1

Optimal electrode positions and processor ranges for
six different subjects

rf = m. rectus femoris

vl = m. vastus lateralis

See Figure 4.3 for key for electrode position on muscle

SUBJECT	MUSCLE	STRIDE LENGTH (cm) Heel-strike to Heel-strike	SPEED (cm/sec)	OPTIMAL ELECTRODE POSITION	OPTIMAL WINDOW LENGTH RANGE (msec)	W _{MIN} (msec)
A	rf	120	70.5	Middle	200-300	250
			96.7	Lowest	200-300	250
			100.9	Lowest	125-175	150
B	rf	150	83.3	Lowest	125-175	150
			126.0	Lowest	125-300	235
C	vl	112	73.6	Lowest	16-150	83
			88.1	Lowest	250-350	300
			116.0	Lowest	16-75	40
D	vl	112	63.8	Lower		
				Middle	100-200	150
			90.3	Lower		
				Middle	150-350	250
		96.8	Lower			
			Middle	50-100	75	
E	vl	90	62.7	Lowest	16-75	40
			82.5	Lower		
				Middle	100-250	175
F	vl	150	96.9	Top	140-160	150
			111.4	Lowest	250-450	350
			140.0	Top	75-100	84

4.6.7 Window Length and Walking Speed

The optimal window length range for processing varies as a function of the speed of walking. One interesting observation is that for three of the four subjects for which three speeds were analyzed a smaller window length was needed to reach maximum reliability for the slow and fast speeds than for the medium gait speed.

4.7 Conclusions

The variance ratio as defined in this chapter emerges as a useful descriptor of repeatability of the electromographic signals. The characteristics of this ratio have been explored and experimental data pertinent to electrode placement and walking speed variations discussed and described.

4.7.1 Potential Uses:

It is evident that using the criterion described in this paper one is in a position to ascertain an area of the muscle which is of a constant reliability with respect to identical electrode pairs. This knowledge could facilitate a comparison of different types of electrodes. It is germane to speculate at this point that the determination of such an area (independent of the type of electrode used) could in fact support the view that certain regions of a

given muscle predominate over the remainder of the muscle for a given motion. Karlsson and Jonsson (1965) showed with the aid of electromyography that the rostral part of the m. gluteus maximus behaves differently from the remainder of the muscle during abduction although both parts of the muscle were equally active during extension of the thigh. Further work correlating function with statistical reliability seems warranted.

The results of this chapter also bear comparison with the work of Norman et al (1977). They were interested in determining how short a sample of EMG could be processed and still yield a relatively stable number representative of motor unit activity. Rectified integrals of varying time durations were calculated from the same sample of raw EMG interference patterns. Coefficients of variation of these integrals were studied as the index of relative stability of the information contained within each integral. Their plots of coefficient of variation against integration time (msec) are very similar to the plots shown in Figure 4.6. Norman et al (1977) in fact commented that the "elbow" in their curves occurred at an integration time in the region of 50 to 75 msec which is comparable to the value (84 msec) of W_{min} in Figure 4.6.

Having determined the optimal type of electrode, electrode position and form of processing for a number of synergistic muscle groups one could use the same criterion to give a weighting to the contributions of different muscle groups involved in the same motion.

The criterion described in this paper is also currently being explored in the Laboratory as a means of making quantitative decisions on the choice of the best processed form of the EMG signal when used as a control mechanism for functional electrostimulation of skeletal muscle for a given desired motion.

The contents of this chapter have been published in the form of a progress report (Hershler and Milner, 1977a) and have been accepted for publication in IEEE Transactions on Biomedical Engineering.

CHAPTER 5

QUANTITATIVE ANALYSES OF ANGLE-ANGLE DIAGRAMS

IN THE ASSESSMENT OF LOCOMOTOR FUNCTION

5.1 The Quantification of Angle-Angle Diagrams

5.1.1 Introduction

A number of authors have used the angle-angle diagram representation of data in which two selected lower limb joint angle variations are plotted against each other for corresponding instants of time. In this chapter a brief review of previous work which utilizes these diagrams is presented. Also included is a discussion of the limitations of visual inspection of the diagrams as well as a delineation of a number of key parameters which are of value in interpreting and assessing the diagrams and making the data from them amenable to statistical analyses. Physical interpretations of the selected factors are rendered where possible (interpretations include aspects regarding range, coordination and overall control). Finally the results of experiments conducted with 5 normal subjects, an above-knee

(A/K) amputee and a cerebral palsied (C.P.) patient using an implanted cerebellar stimulator are presented.

This chapter includes a further in-depth analysis and interpretation of the results associated with the same C.P. patient. The discussion presented at this stage is of a multidisciplinary character and is the combined work of a number of individuals including the author of this thesis. The joint efforts of this group has resulted in the publication of this work in the form of a monograph (Milner et al, 1977). It was gratifying to note that the ideas on quantification of angle-angle diagrams, suggested by this author in section 5.1 were utilized extensively in this work.

Essentially, the subjects were fitted with electrogoniometers to measure hip angle and knee angle histories in the sagittal plane during locomotion. Also, footswitches were fitted to measure heel and toe contact times. All of the acquired data were sampled by and stored in a mini-computer (PDP11/10) which was programmed to produce pertinent displays and to compute relevant factors. Major attention was focussed on the areas of angle-angle diagram loops, their perimeters and a dimensionless ratio P_A defined as the ratio of perimeter/square root (area) and which

appears useful as a quantifier of the shape of the angle-angle diagram. Variations of these three parameters as a function of walking speed for the normal subjects and the A/K amputee are presented and discussed. In the case of the C.P. patient the temporal variations in angle-angle diagrams and pertinent parameters were studied with the implanted cerebellar stimulator both on and off. In the light of the work presented in this chapter, it appears that the quantitative analyses, when coupled with a visual display of pertinent angle-angle diagrams, render a more complete assessment of locomotor function. In addition, extraction of appropriate parameters makes possible statistical analyses associated with locomotor performance.

5.1.2 Background

For the benefit of the readers of this thesis, certain relevant papers included in the general background review of gait (Chapter 2) are further discussed. Their efforts are indicated in what follows.

Grieve (1968) stressed two important points with respect to an improved understanding of gait. Firstly, he argued that gait studies based upon the whole range of walking speeds would go further towards an understanding of the walking mechanism than a further elaboration of the

fixed-cadence approach. Secondly, he proposed a new format for presentation of joint angle histories. He suggested that since its clinical acceptability depends upon information being presented in a palatable form, the joint angles of the lower limb be plotted against each other. These angle-angle diagrams present walking cycles in cyclic loops with the further attraction that various gaits produce characteristic, easily recognisable, loops. While Grieve confined his attention to normal gait, other authors have utilized the representation as well. Lamoreux (1971) using exoskeletal goniometric devices measured several kinematic variables on normal subjects and paid particular attention to the effects of changes in walking speed on these variables. Among the variables measured were hip and knee joint rotations in all three planes. He found it advantageous to display some results in the form of knee-angle/hip-angle diagrams. Milner et al (1973) followed on Grieve's suggestions and used knee-angle/hip-angle diagrams to assess locomotor function. Using a stroboscopic photographic method to acquire the relevant data, they showed that a normal subject exhibited characteristic angle-angle diagrams for five different speeds. They analysed pre-operatively the gait of 5 patients suffering from unilateral osteoarthritis of their hips. The shapes and positions of their angle-angle diagrams differed from normal and those for the

affected side differed radically from the ones on the contra-lateral side. It was clear that this method of representing the data was extremely useful because of the large amount of information conveyed in a simple manner and in view of the distinct angle-angle patterns obtained for the patients tested. Milner et al (1974) followed the latter study with a post-operative one on the same patients. From an examination of the pre-operative and post-operative angle-angle diagrams it was seen that there had been a dramatic change in the post-operative condition. The shapes and positions of the left and right side patterns were very similar post-operatively. Smith et al (1976) used the same approach as Milner et al (1973, 74) to assess pre- and post-operatively 12 patients undergoing the Attenborough knee-joint replacement. The results clearly demonstrated that angle-angle diagrams enhanced the objective assessment of the operative procedure. Paul (1976) recognised the value of angle-angle displays for measuring changes in patient performance corresponding to surgery and post-operative treatment.

5.1.3 On Angle-Angle Diagrams

Recognising the comments of previous workers, it is considered that angle-angle diagrams have facilitated the introduction of measures of objectivity in the clinical

assessment of gait. It is important to note that these diagrams can have a number of attributes for single and multiple loops.

Single Loops: These reflect kinematic data for a single footstep as follows:

(1) Data are presented in a clinically acceptable form which usually represents temporal and angular data allied simultaneously with two joints.

(2) Various gaits present characteristic easily recognizable loops.

(3) The position of the angle-angle diagram relative to a set of mutually perpendicular axes conveys information concerning limitations in the ranges of motion.

(4) The overall ranges of motion are readily appreciated.

(5) It is possible to conveniently annotate angle diagrams to reflect the occurrences on the contralateral limb (i.e. footswitch information).

Multiple Loops: These depict kinematic data for more than one footstep. Sequential loops render a visual impression of the repeatability of gait and the same format is utilized in conveying the information, rather than lengthy tracings. Thus the presentation is concise.

5.1.4 Limitations of Visual Inspection

It is recognised that there are certain limitations regarding the information which can be derived only from a visual inspection of either single or multiple loops.

Single Loops

Easy comparison between two single loops necessitate the generation of the two loops using the same set of axes. The aspects which might be compared are:

- (1) Ranges
- (2) Shape of closed loop
- (3) Size (area) of closed loop
- (4) Perimeter or length of pattern which delineates the closed loop.
- (5) Position of centroid

With the exception of (1), the remaining components require substantial effort and time commitment for their determination unless automated techniques, e.g. the computer, are invoked. A visual inspection is unable to discern combined joint angular changes which might reverse direction for a short time along their original paths.

Multiple Loops

The same issues regarding single loops apply. In addition, with multiple loops:

(1) Their presentation suffers the disadvantage that other information (temporal, contralateral limb performance) confuse rather than clarify.

(2) Where the perimeters of the individual loops intersect or come close together it is not always possible to follow each loop with certainty through its complete cycle.

(3) quantification of the repeatability of gait derived from multiple loops necessitates measurements of the ranges of variability in the parameters either allied with selected localized zones of a set of angle-angle diagrams or of each loop in its entirety. This would, in general, be a laborious, time-consuming task.

5.1.5 Key Factors

From the foregoing discussion, it is apparent, that there is a need to extract relevant numbers with corresponding physical interpretations from the diagrams. these numbers should enable the various identifiable aspects of the angle-angle diagrams to be amenable to unambiguous and rigorous statistical analyses. A fundamental question is: "What are the key parameters that should be extracted from the angle-angle diagram?" The answer to this question is not only important for the quantification of angle-angle diagrams but is also important for the establishment of

ground rules for visual examination of the diagrams. It is considered that the following factors (not listed in order of importance) are of value in interpreting angle-angle diagrams:

- (1) Area, A , of closed loop.
- (2) Perimeter, P , of the boundary of a closed loop.
- (3) Shape of the closed loop.
- (4) Pattern of the boundary of the loop (P affords a measure of the length of this pattern, but derivatives will provide directional information).
- (5) Ranges of the angular variations.
- (6) Time t (and direction of the traverse of the loop).
- (7) Position of the centroid and orientation of the diagram with respect to the coordinate axes.
- (8) Higher order derivatives about the loop.
- (9) In the case of multiple loops, variability of selected parameters in the ranges traversed by the diagrams in selected localized zones.
- (10) Segmenting the loops into pertinent zones, e.g. swing and stance phases, all of the factors listed above can be determined for such segments. It may also be convenient to segment according to intersections which the loop makes with itself.

5.1.6 New Directions

In this chapter attention is paid to the first three key factors indicated above by making a detailed examination of the area A , and perimeter P and their combination expressed through a dimensionless ratio $P_A = P/\sqrt{A}$. This latter ratio appears to yield a useful description of the shape of the closed loop. In the main attention is confined to the properties of the overall angle-angle diagram.

The area A , perimeter P and perimeter/ $\sqrt{\text{area}}$ (P_A) have been computed for individual knee-angle/hip-angle diagrams in the sagittal plane for both legs of 5 normal subjects (2 male, 3 female) walking at 4 different speeds on a level surface. The same study was repeated on an above-knee (A/K) amputee on both legs at 4 different walking speeds. Three separate studies were performed on a Cerebral Palsy (C.P.) patient who had an implanted cerebellar stimulator. The same parameters were extracted from the knee-angle/hip-angle diagrams in the sagittal plane of one leg for a number of conditions with the stimulator on and off.

5.1.7 Physical Interpretation of Variables

Area

A typical knee-angle/hip-angle diagram in the sagittal plane is shown in Figure 5.1A. Figure 5.1B defines

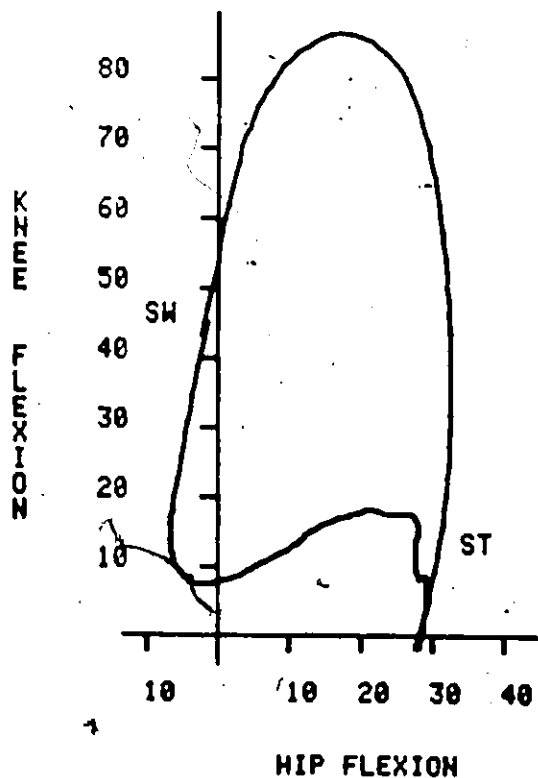
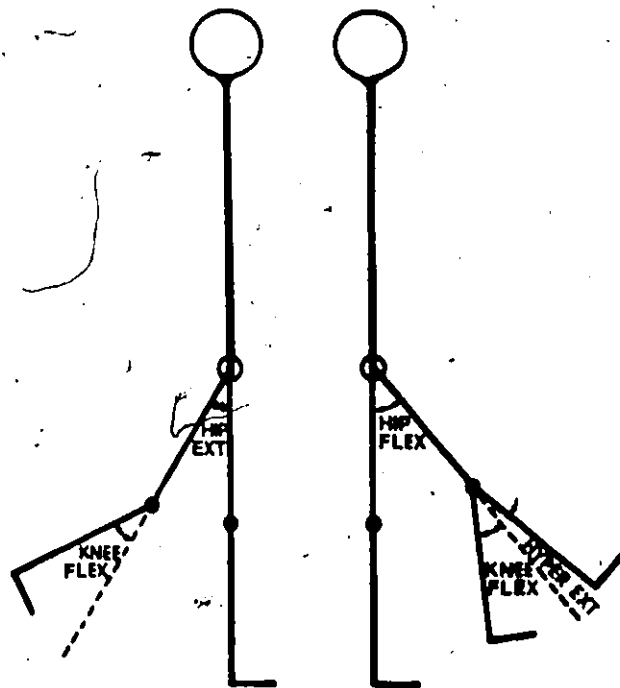


Figure 5.1A

A typical normal knee-angle/hip-angle diagram. Subject A. ST indicates onset of stance and then "reading" the loop in a clockwise direction SW indicates onset of swing.

the knee and hip angles. An examination of Figure 5.1A reveals the range of knee flexion - hyperextension along the Y-axis as well as the range of hip flexion - extension along the X-axis. Clearly, the area of any such diagram is a function of both knee and hip angles and is expressive of the total conjoint range of angular motion experienced at the hip and knee joints during one complete gait cycle. By conjoint range we mean the mapping of all possible



DIRECTION OF FLEXION AND EXTENSION

Figure 5.1B

angle-angle points during a gait cycle.

When segments of the diagram which contribute to the whole are examined, it is noteworthy that when area is contributed it implies that simultaneous rotations have occurred about the hip and knee joints (See Figure 5.2 and note that there is no area contributed along segment AB of loop 3).

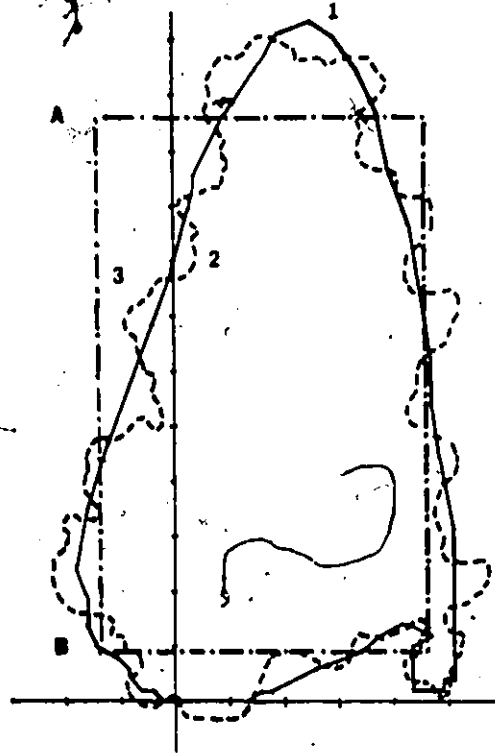


Figure 5.2

- Three superimposed angle-angle diagrams
- 1: Solid line: Normal angle-angle diagram
 area = 1452.0 (degrees)²
 P = 170 degrees
 P_A = 4.46
 - 2: Dashed line: Jerky and uncoordinated motion
 area = 1452.0 (degrees)²
 P = 230 degrees
 P_A = 6.03
 - 3: Dot-dashed line: Angle-angle diagram with rectangular segments
 area = 1452.0 (degrees)²
 P = 156.8 degrees
 P_A = 4.11

Abscissa: Hip angle 10°/division
 Ordinate: Knee angle 10°/division

Perimeter

With changes in the angle at either joint there is a corresponding change in the perimeter of the angle-angle diagram. If any angular variation is jerky (uncontrolled or incoordinate) the perimeter of the angle-angle diagram will be lengthened in spite of the fact that conjoint range or bound area may stay approximately constant (See Figure 5.2, loops 1 and 2). Although the perimeter is a function of both the knee and hip angles, a change in only one of the angles (keeping the other constant) could increase the perimeter without contributing to the area. In this case (See Figure 5.2, loop 3) the angular changes might occur in discrete jumps parallel to either axis resulting in an angle-angle diagram with rectangular segments. This would be a reflection of a robot-like gait in which only one joint angle changes while the other is maintained fixed. The perimeter would change accordingly with again possibly no increase in the conjoint range. The perimeter would seem to provide a reflection of the coordination between the two joints during gait.

Perimeter/ $\sqrt{\text{area}}$ P_A

The dimensionless ratio P_A suggests itself as a quantifier of the shape of the angle-angle diagram for a given value of the ratio knee angle range/hip angle range.

P_A was chosen to be the perimeter/ $\sqrt{\text{area}}$ instead of $\sqrt{\text{area}}/\text{perimeter}$ in order to achieve more sensitivity in distinguishing between different shapes. In order to better appreciate the relationship between P_A and shape we have examined a number of well known geometrical shapes and plotted P_A versus length/breadth (rectangle, parallelogram, rhombus and square) and P_A versus major axis/minor axis (ellipse and circle). Figure 5.3 shows graphically the various relationships. It is clear that for a given ratio of length/breadth (or major axis/minor axis) a given value of P_A can be associated with a particular geometrical shape. However, the absolute value of P_A does not always necessarily uniquely specify a particular geometric shape. In particular, see Figure 5.3 where curves 2 and 3 intersect. Such intersections may possibly occur with other shapes. Thus it can be concluded that P_A has potential value in reflecting relative changes in shape relating to those encountered in, say, angle-angle diagrams.

It should be noted that if the shape of the angle-angle diagram stays constant the value of P_A will also stay constant in spite of the fact that the area of the diagram might change dramatically. For the situation where the ranges of angular motion stay constant but the limb movements are uncoordinated and jerky as compared with

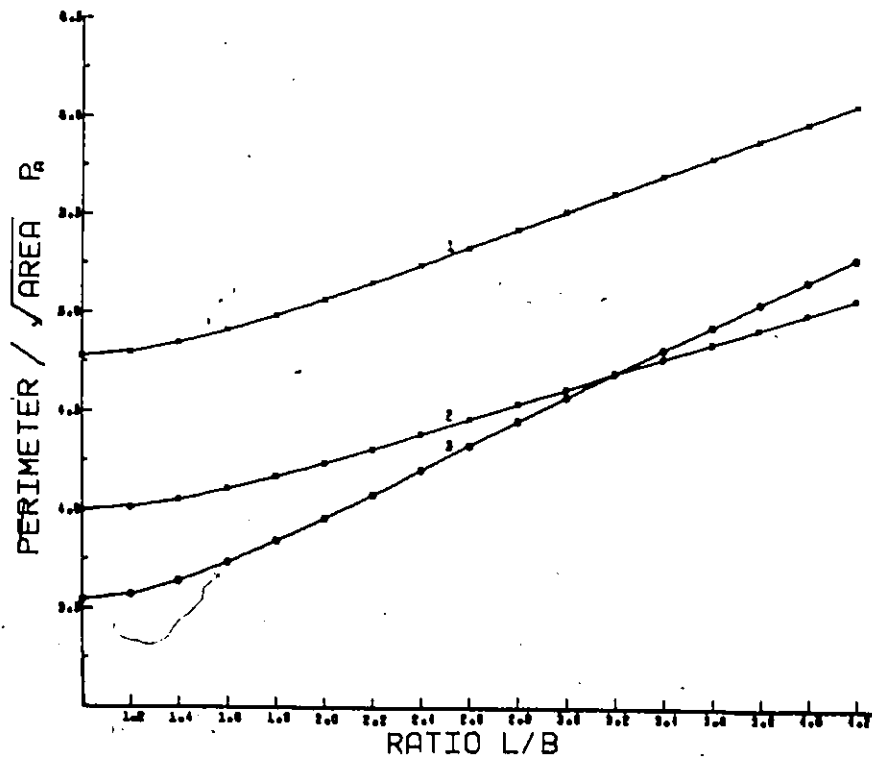


Figure 5.3
 P_A versus L/B for
 1: rectangles ($L/B = 1.0$, curve tends to a square)
 2: parallelograms subtending angles of 45°
 ($L/B = 1.0$, curve tends to a rhombus)
 3: ellipses ($L/B = 1.0$, curve tends to a circle)

L is length of larger side in the case of rectangles and parallelograms and length of major axis in the case of an ellipse.

B is length of smaller side in the case of rectangles and parallelograms and length of minor axis in the case of an ellipse.

normal locomotion, the ratio P_A would tend to increase.

Conversely where the gait is such that angular changes occur in discrete jumps as compared with normal locomotion, P_A would tend to decrease (assuming a constant range of

motion). This is illustrated by Figure 5.2. Here we show three superimposed angle-angle diagrams. The diagram drawn with a solid line (loop 1) represents a typical normal angle-angle diagram similar to the one shown in Figure 5.1 ($P_A = 4.46$). The angle-angle diagram drawn with dashed lines (loop 2) represents a hypothetical motion of equal range to that of the normal but with limb movements that are uncoordinated and jerky ($P_A = 6.03$). The third superimposed and hypothetical diagram drawn with dot-dashed lines (loop 3) represents an equivalent range motion but where the gait is such that one of the joint angles is kept constant while the other varies resulting in an angle-angle diagram with rectangular segments ($P_A = 4.11$).

5.1.8 Experimental Procedure

Hip and knee angle histories were collected from all subjects including 5 normals, an A/K amputee and a C.P. patient using electrogoniometer measuring systems based on the design of Lamoreux (1971). Figure 3.11 is a typical electrogoniometer attached about the knee of a subject. The hip and knee angle information were obtained from electrogoniometersystems at the hip and knee joints usually of both sides of each subject by sampling the corresponding voltage signals at 200 Hz and storing the digital information in a PDP 11/10 computer. Footswitches located

under the heel and toe of the shoes on both sides and in all cases enabled the times of the various gait phases (swing and stance) to be computed. The average speed over a measured distance was determined by timing the walk of each subject. Four metronome frequencies (56, 66, 88 and 112 beats/min.) were used for those subjects for which four speeds of walking along a level surface were prescribed. These resulted in very slow, slow, medium and fast walks for each subject. These constraints were imposed with a view to creating fairly repeatable stride periods. Each gait cycle could then be uniquely identified by the average speed and period.

Each attached electrogoniometer was calibrated using two selected angles in the range of movement. For each angle the corresponding electrogoniometric voltage was acquired and stored by the computer. Following final acceptance of the calibration information, each subject was allowed to walk the length of the walkway at his (or her) most comfortable cadence for each of the required experimental conditions. When the subject appeared to have attained a relatively constant velocity, the computer was remotely triggered to collect 10 seconds of data sampled at 200 Hz. the analog data were then displayed oscillographically for verification and acceptance.

Above-Knee Amputee

In the case of the A/K amputee, in addition to the first study, which was concerned with the effects of walking speed on both legs, a second study was carried out. This study examined the effects of changing the alignment on the prosthesis and allowing the patient to walk at his most comfortable speed. Given that "medial whip x° " means that an external rotation of x° with respect to correct alignment was applied to the prosthesis below the knee, in such a way that, during the forward swing of the prosthetic leg, the prosthetic heel rotated medially towards the other foot (medial whip) the three new settings examined were:

- (1) Medial whip 2° unpractised gait
- (2) Medial whip 2° practised gait
- (3) Medial whip 15° practised gait

C.P. Patient

A 33 year old male with spastic cerebral palsy capable of independent gait was chosen for this study. A cerebellar stimulator was implanted two and a half years ago and coupled to platinum disc electrodes in a silicone coat mesh located over the anterior lobes of the cerebellar cortex. Stimulation was with 200 Hz bipolar rectangular pulses with less than $.45 \mu C/mm^2$ of charge delivered per phase. Previous studies of the effects of cerebellar stimulation on

this patient include H reflex responses, V₁ and V₂ late responses, somatosensory evoked potentials, and visual evoked potentials (Upton and Cooper, 1976); more recent investigations have included brain stem evoked potentials and respiratory studies (Table 5.1).

TABLE 5.1

C.P. patient neurological data

Patient D.A.	H			V ₁			V ₂			SSEP			VEP		
	R	L	B	R	L	B	R	L	B	R	L	B	R	L	B
Male. 33 Cerebral Palsy															
Effect	+	+	+	+	+	+	+	+	+	+	+	+	0	0	0
Times seen	3			3			3			3			3		
Patient D.A.	BSEP			Sleep/Awake Respiration			Gait			EEG			Poly- graph		
	R	L	B				R	L	B	R	L	B	R	L	B
Male. 33 Cerebral Palsy															
Effect	0	0	0			0			+	0	0	0	+	+	+
Time seen	1					4			2	2			2		

This table summarizes the results of various neurophysiological investigations in the 33 year old cerebral palsy patient. Note the effects of right-sided (R), left-sided (L) and bilateral (B) cerebellar stimulation (CS) at

200 Hz on H reflexes in soleus/gastrocnemius muscles (H), V₁ and V₂ late responses, somatosensory evoked potentials after median nerve stimulation (SSEP), visual evoked potentials after flash stimulation (VEP), brain stem evoked potentials, after click stimulation (BSEP), respiratory studies (RESPIRATION), gait studies (GAIT), electroencephalogram (EEG) and polygraphic recordings of involuntary movement and muscle tone (POLYGRAPH). A significant reduction in amplitude (+), a significant effect (+) and no effect (0) are shown. A blank space indicates that the test was not performed.

The patient has been seen on numerous occasions (TIMES SEEN) for the different tests and the results have been remarkably consistent over the course of 14 months with no apparent change in thresholds of stimulation two and a half years after implantation of the stimulator. The correlation between the results of studies of reflexes, late responses and evoked potentials with the gait analysis would indicate that the physiological responses may be used to predict clinical effects. However, in some other patients reflex effects of CS could be detected in the absence of clinical response and clinical effects could be detected in the absence of measurable changes in reflexes or late responses; further studies will be required to assess the

most valuable objective measurements which will allow "biocalibration" of stimulators and prediction of clinical outcome of cerebellar stimulation.

Following on a number of pilot experiments to determine suitable subsequent strategies, three experiments were performed in which electrogoniometric data were gathered only on the left side and they are reported here.

Experiment I was preceded by five hours with the stimulator off. Electrogoniometers were placed on the appropriate joints as described above, the stimulator was turned on and data were collected for traverses along the walkpath at times 0, 3, 5, 14 and 21 minutes later. The patient was not told whether the stimulator was active or not and no results were displayed to him during the testing.

Experiment II began after 25 minutes of stimulation. The stimulator was turned off and data collected at times 0, 2, 4, 6, 8, 10 and 12 minutes later. Experiment III was done with the stimulator off following two months of uninterrupted stimulation. Data were obtained at times 0, 2, 4, 6, 8, 10, 12, 14 and 20 minutes later.

Before each experiment the patient was told to walk

at a comfortable pace and rest stations were set up at each end of the walkway.

Calibration Error

Several subjects were calibrated before and after the experiment to obtain an estimate of calibration error. The maximum change in calibration values that ever occurred with any subject was 20%. It was estimated that observer error would account for less than half that range, with the main source of error due to slippage of the electrogoniometer system on the limb segments during the experimental run. In order to estimate the effects of calibration error on the quantitative results, one set of experimental data, (C.P. patient, experiment III) was analyzed again under the following conditions:

- (1) Hip angle only reduced by 20%
- (2) Knee angle only reduced by 20%
- (3) Hip and knee angles both reduced by 20%

In each case the effect of the error was to reduce area and perimeter in such a way that the ratio P_A remained essentially unchanged both in magnitude and trend. The maximum changes in area and perimeter were approximately 30% and 20% respectively but even though the area and perimeter changed in each case, their trends remained constant.

Footswitch Information

With the aid of a pattern recognition algorithm implemented interactively on the PDP 11/10 computer (de Bruin and Milner, 1977) the various footswitch patterns were separated into individual footsteps (Figure 3.2) and the associated hip and knee angle information written into separate records on disk. The various data records were then amenable to quantitative analysis and the parameters A, P and P_A were computed.

Methods of Computation

The computer programs (Hershler, 1977b) were written in Fortran IV language and realized the following functions:

- (1) The x,y coordinates of the points where the angle-angle diagram intersects itself were computed. These loop intersects (if any existed) divided the larger angle-angle diagram into a number of smaller loops.
- (2) The area of each individual loop was computed using an analytic formula from Edgett et al (1960).
- (3) The total bound area of the angle-angle diagram was obtained by summing the areas of the individual loops. The error associated with the computation of the area was found to be $< 1\%$.
- (4) The perimeter of the angle-angle diagram was computed by successively adding the distance between two adjacent

points as one moved around the loop. The error associated with the computation of the perimeter was found to be $< 2\%$.

5.1.9. Results and Discussion

Normal

Figure 5.4 is a plot of 4 successive knee-angle/hip-angle diagrams for one of the normal subjects. In this figure, ST represents onset of stance that occurs normally at heelstrike. "Reading" the loops in a clockwise direction brings one to SW which is onset of swing occurring at the toe-off. Following heelstrike there is a small amount of hyperextension followed by a rapid knee flexion and extension which shows up as a "kink" in the loop and which is due to the shock absorbed at the knee joint during the initial weight-bearing phase of stance. The hip extends throughout this manoeuvre. In the latter part of stance the knee begins a smooth, rapid flexion that will reach a peak in mid-swing phase, when knee extension begins in preparation for the next heel strike. The hip flexes continuously but relatively slowly during this change from knee flexion to extension during swing phase giving the top of the diagram a peaked appearance. These knee-angle/hip-angle diagrams are typical of all the normal subjects studied and show smooth control through swing and back to

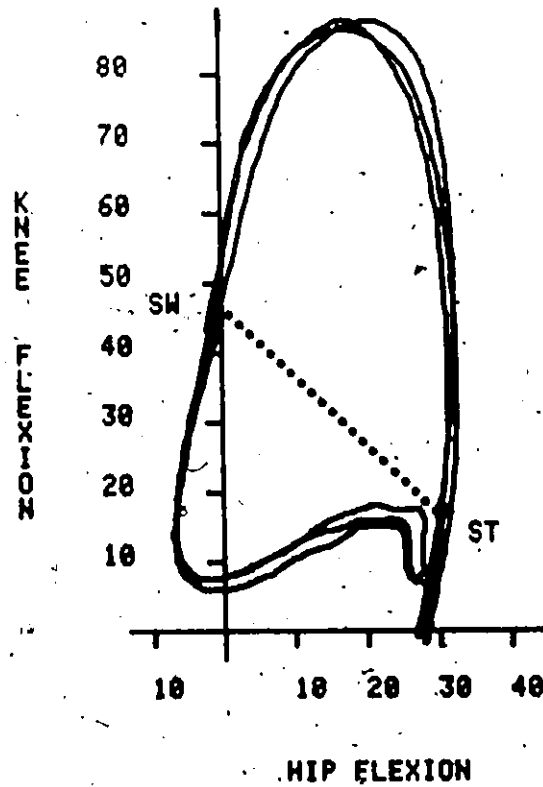


Figure 5.4

Three superimposed angle-angle diagrams for normal Subject A (Female: height 5'3"; weight 115 lb.; walking speed .95 m/sec). Note the high repeatability in both shape and size (area). Dashed line divides any loop into a stance segment and a swing segment.

stance. This is indicated by the smooth rounded appearance of the corresponding segments of the loops. The abrupt change in the shape of the loop following the onset of stance (ST) again shows the nature of the control mechanism that allows the subject to absorb rapidly the impulsive shock at the knee and hip joints. Note the repeatability in

both shape and area. Figure 5.5 consists of plots (for the right leg of normal subject A) of total area, perimeter and P_A versus walking speed respectively. Drawn through the experimentally measured points in each case is the best linear fit as determined by the least squares method. Table 5.2 contains the values of the y-intercepts and slopes for the best linear fits of area, perimeter and P_A versus walking speed for all five normal subjects. Examination of this table indicates that both area A and perimeter P have a close linear relationship to walking speed while P_A is essentially constant with walking speed for both legs of all normal subjects tested. Significantly, the repeatability associated with each of the gait parameters examined was high for all the normal subjects tested. This is shown by the widths of the standard deviations in Figure 5.5.

With the aid of a planimeter (for measurement of areas) and a calibrated wheel (for measurement of perimeters) area A and perimeter P were measured for the stance (ST - SW - ST) and swing (SW - ST - SW) segments of 3 angle-angle diagrams representing 3 footsteps of the right leg of a normal subject. For each angle-angle diagram the ratios (area in the stance segment)/(area in the swing segment) and (perimeter of stance segment)/(perimeter of swing segment) were computed. Also, P_A for the stance and swing segments

Figure 5.5

Plots of area, perimeter and P_A versus average walking speed for the right leg of normal subject A. Drawn through the experimentally measured points in each case is the best linear fit as determined by the least squares method.

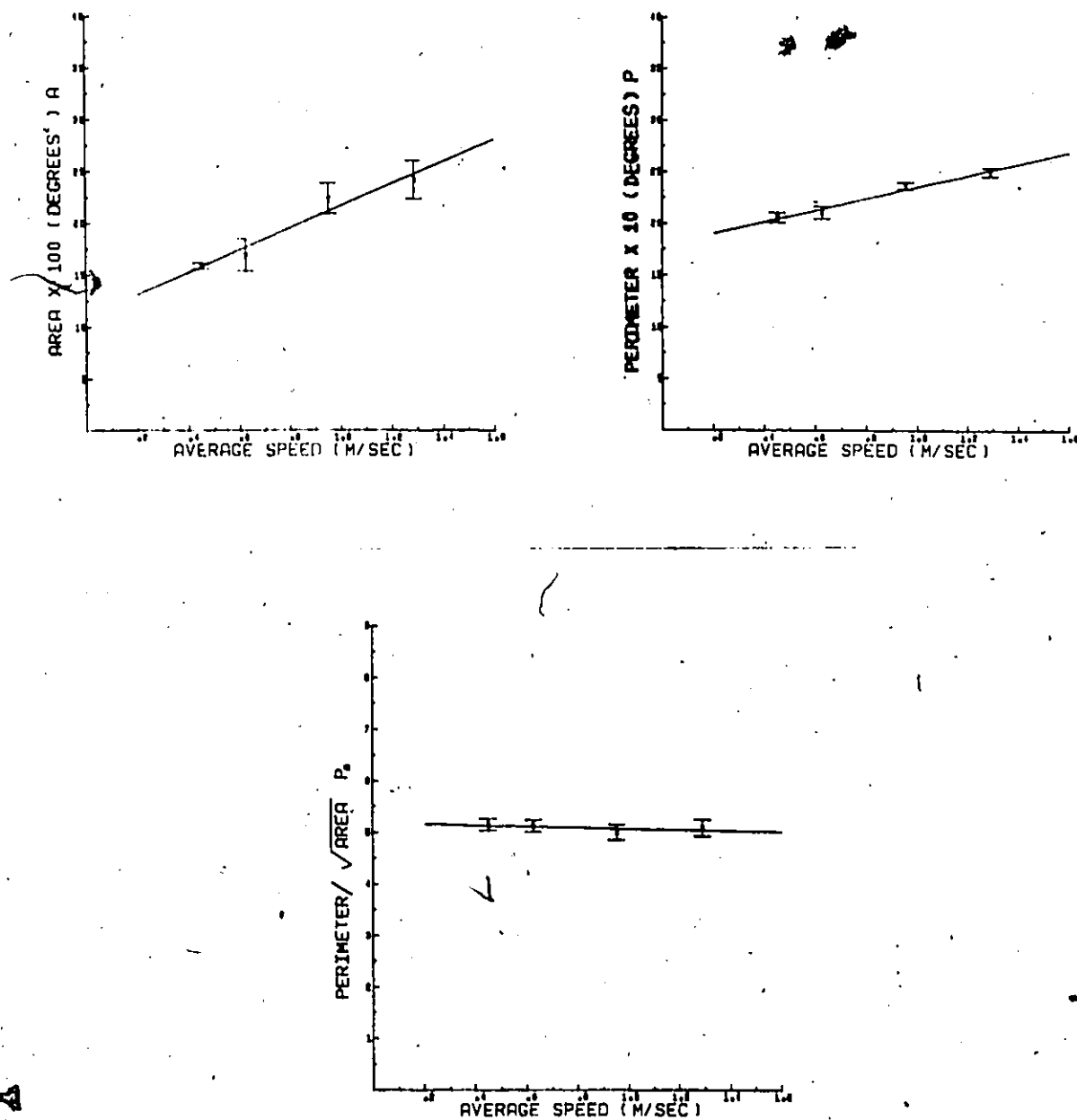


TABLE 5.2
Best Linear Fits for Normal Gait

<u>Subject</u>	<u>Leg</u>	<u>Area versus</u> <u>Walking Speed</u>		Coefficient* of Determination
		(degrees) ² Y-intercept	(degrees) ² m/sec Slope	
A	Right	1093.57	1073.73	.95
	Left	1124.73	1748.45	.96
B	Right	-17.41	3038.55	.99
	Left	716.99	1654.33	.89
C	Right	1283.79	1206.69	.83
	Left	786.17	1106.58	.91
D	Right	1595.33	1246.90	.98
	Left	1351.57	876.4	.99
E	Right	1353.45	297.57	.66
	Left	1546.57	748.43	.67

* The coefficient of determination =

$$\frac{\sum (y_i^{\text{fit}} - \bar{y})^2}{\sum (y_i^{\text{exp}} - \bar{y})^2}$$

gives the fraction of the variance of the experimental data explained by the fitted curve.

TABLE 5.2 (continued)

<u>Subject</u>	<u>Leg</u>	<u>Perimeter versus</u> <u>Walking Speed</u>		Coefficient of Determination
		(degrees) Y-intercept	(degrees) m/sec Slope	
A	Right	178.95	56.6	.97
	Left	169.51	73.51	.98
B	Right	174.03	110.6	.98
	Left	169.31	113.76	.98
C	Right	181.23	51.56	.95
	Left	149.67	47.54	.92
D	Right	159.30	96.15	.98
	Left	145.87	76.0	.95
E	Right	144.42	38.46	.96
	Left	134.99	89.33	.99

TABLE 5.2 (continued)

<u>Subject</u>	<u>Leg</u>	<u>p_a versus Walking Speed</u>		Coefficient of Determination
		Y-intercept	(m/sec) ⁻¹ Slope	
A	Right	5.19	-.10	.33
	Left	4.60	-.04	.01
B	Right	6.27	-.88	.92
	Left	5.81	.07	.01
C	Right	4.47	.36	.52
	Left	4.42	.66	.05
D	Right	4.00	.78	.87
	Left	4.11	.04	.49
E	Right	3.95	.55	.68
	Left	3.57	1.10	.76

were computed individually and these ratios are shown in Table 5.3.

TABLE 5.3

Stance/swing ratios for area and perimeter of angle-angle diagrams taken from a normal subject

<u>Footstep</u>	P_A (Stance)	P_A (Swing)	$\frac{\text{Stance Area}}{\text{Swing Area}}$	$\frac{\text{Stance Perimeter}}{\text{Swing Perimeter}}$
1	4.72	4.08	0.54	.85
2	6.26	4.11	0.34	.88
3	5.17	4.38	0.48	.82

This type of segmental analysis gives additional information. The above results seem to indicate that for normals conjoint angular motion is shared in the ratio 1:2 (approximately) between the stance and swing phases of a footstep. Intuitively it can be considered that more control and coordination would be called for during stance than during swing on the side being studied. The value of the stance/swing perimeter ratio together with that for the stance/swing area ratio indicates that a substantially greater amount of perimeter is associated with the stance segmental area. This is further supported by the fact that P_A (stance) is substantially greater than P_A (swing) while the stance perimeter is fairly close in value to the swing perimeter. The implication of this interpretation lends

support to the above intuitive view. It is of interest to compare these data with those for the A/K amputee and we do this later.

A/K Amputee

Figures 5.6, 5.7 are multiple plots of knee-angle/hip-angle diagrams for the left (prosthetic) and right legs respectively of the A/K amputee. Figure 5.8 consists of area, perimeter and P_A versus walking speed for the left (prosthetic) leg while Figure 5.9 contains corresponding plots for the right leg. Figure 5.10 is a plot of P_A versus walking speed for both legs of the A/K amputee with each measured point representing a different alignment of the prosthesis. Table 5.4 contains the values of y-intercepts and slopes for the best linear fits of area, perimeter and P_A versus walking speed for both legs of the A/K amputee. It is pertinent to note in Figure 5.6 the following points:

(1) Lack of "shock absorber" effect after heelstrike (ST) "reading" the loop in a clockwise direction (i.e. no flexion nor extension of the knee occurs after heelstrike). The knee is locked.

(2) Brief flexion followed by substantial extension of hip after heelstrike with the knee locked in position.

(3) With the knee locked, the hip extends until onset of swing (SW). The control exhibited by the A/K

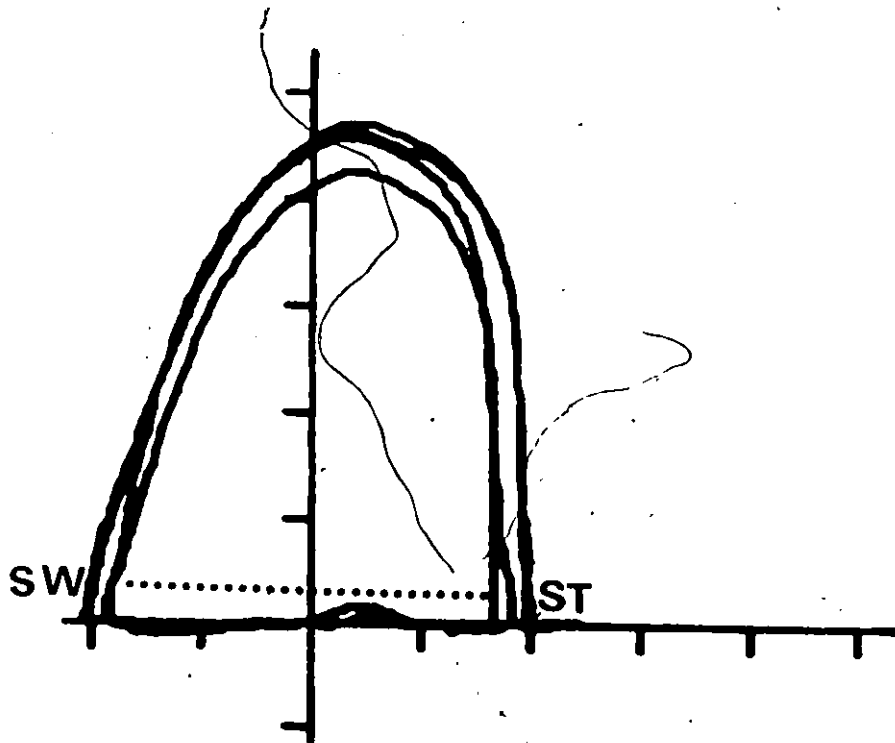


Figure 5.6
Four superimposed angle-angle diagrams for the left
(prosthetic) leg of the A/K-amputee

Note: (i) lack of "shock absorber" effect after heel-strike (ST) reading loop in a clockwise direction (i.e. no flexion nor extension of the knee occurs); (ii) Brief flexion and extension of the hip after heel-strike with the knee locked in position; (iii) Symmetric flexion and extension of the knee and hip.

Ordinate: Knee Angle 10°/division

Abscissa: Hip Angle 10°/division

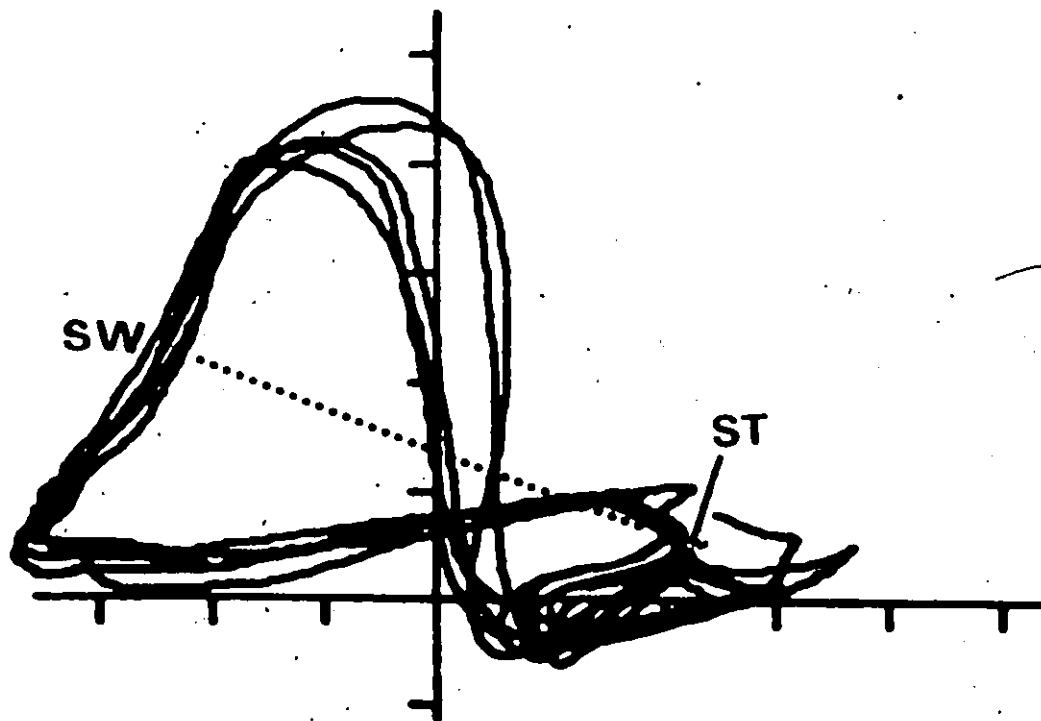


Figure 5.7

Five superimposed angle-angle diagrams for the right leg of the A/K amputee

Note: (i) Extreme complexity of loop shape compared with prosthetic side and with normals; (ii) Large amount of hip extension; (iii) Right leg seems to be compensating in a fairly repeatable yet highly abnormal manner for the prosthetic leg on the contralateral side.

Ordinate: Knee angle 10° /division
 Abscissa: Hip angle 10° /division

Figure 5.8
 Plots of area, perimeter and P_A versus average walking speed for the left (prosthetic) leg of the A/K amputee. Drawn through the experimentally measured points in each case is the best linear fit as determined by the least squares method.

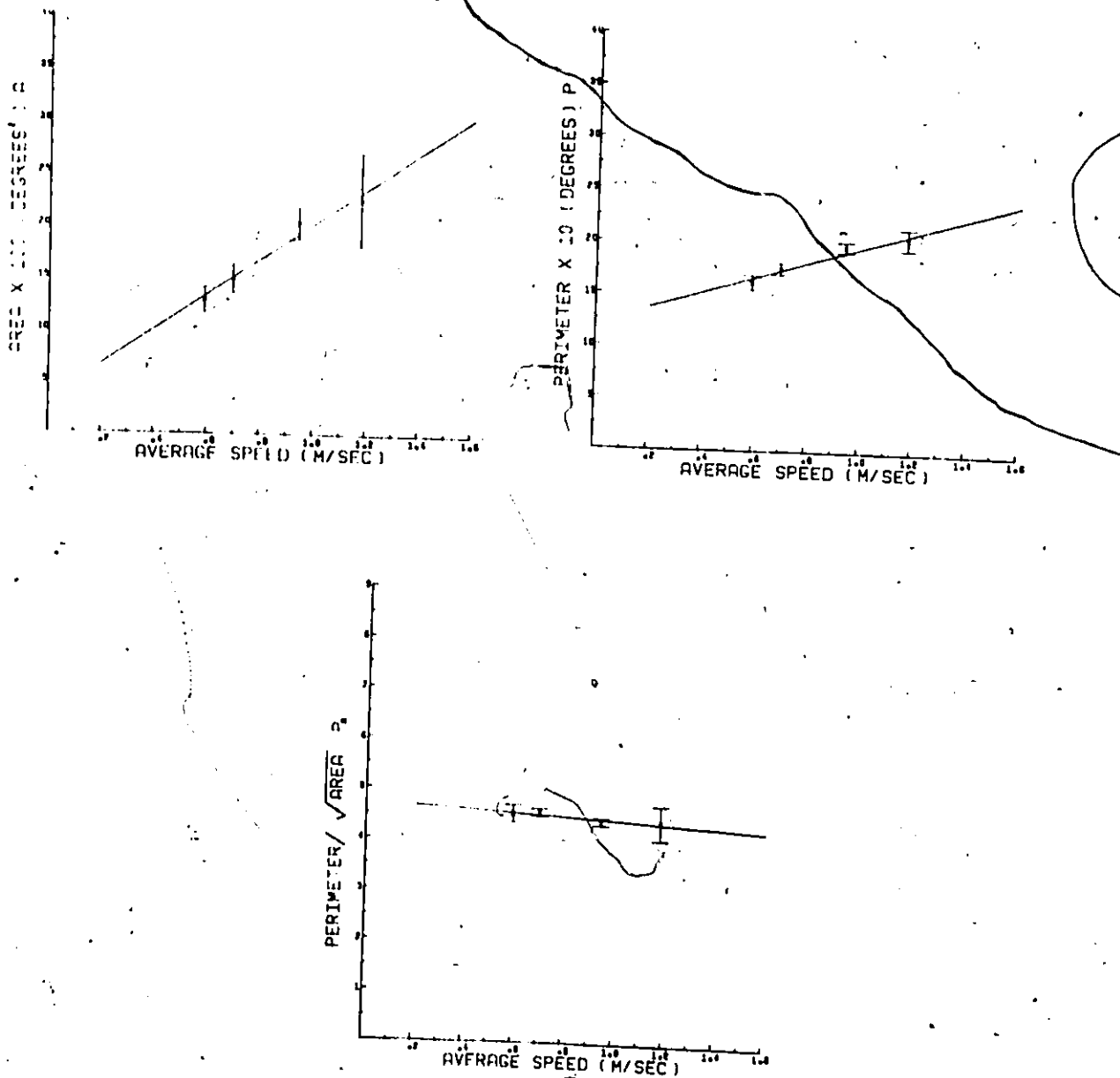


Figure 5.9

Plots of area, perimeter and P_A versus average walking speed for the right leg of the A/K amputee. Only the area plot shows the best linear fit.

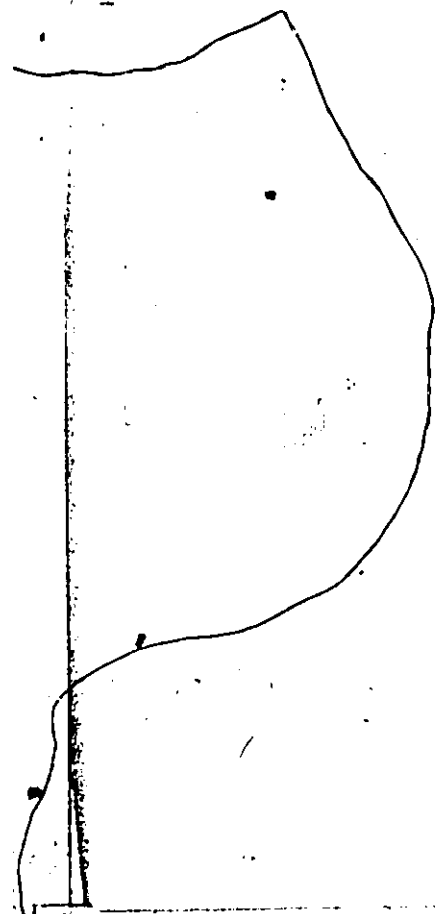
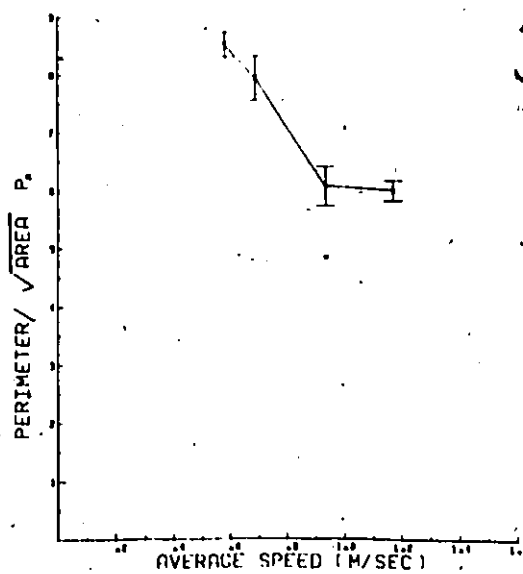
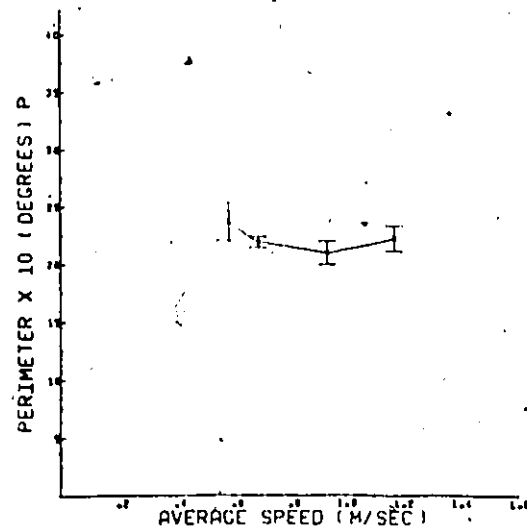
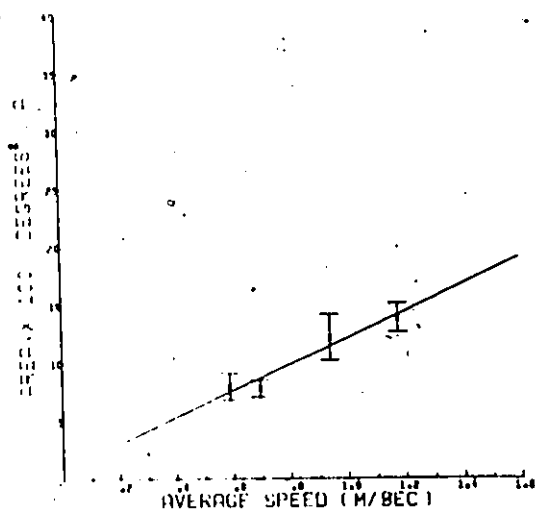


Figure 5.10

Plot of P_A versus average walking speed for both legs of the A/K amputee with each measured point representing a different setting of the prosthesis. The unlabelled point is the normal setting.

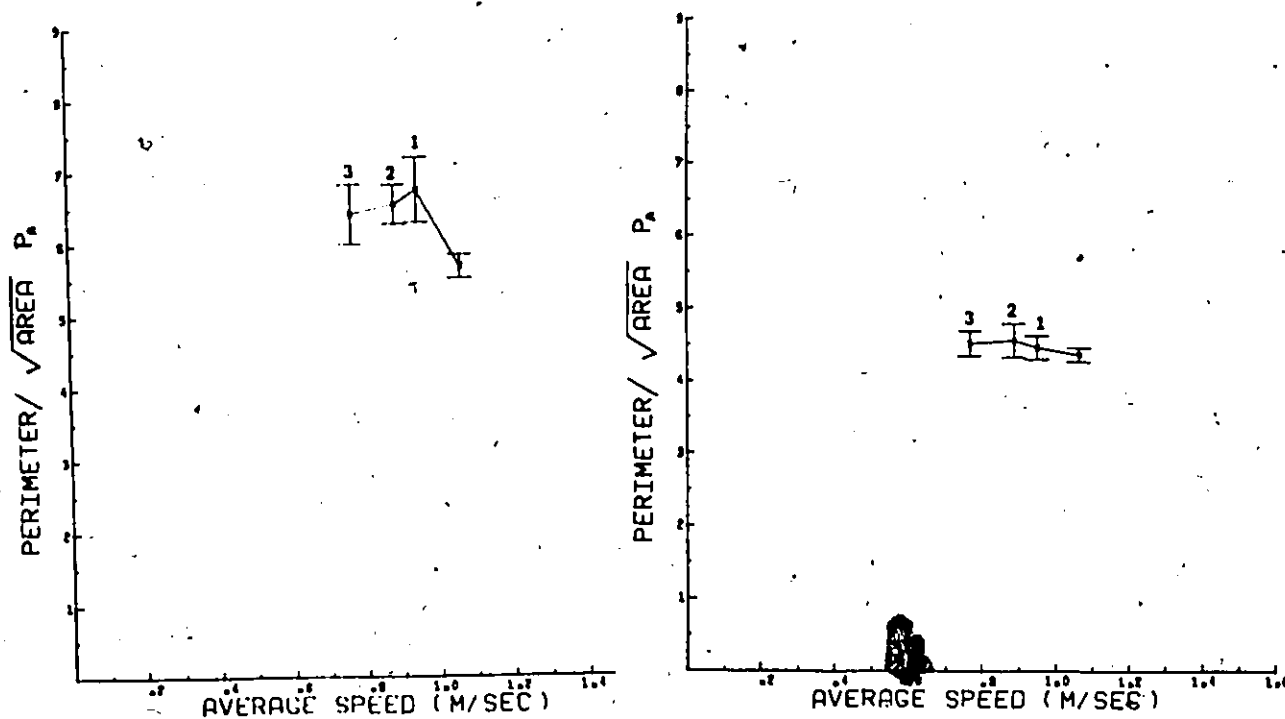
A: Right (intact) leg

B: Left (prosthetic) leg

Setting (1) is a medial whip 2° unpractised gait

Setting (2) is a medial whip 2° practised gait

Setting (3) is a medial whip 15° practised gait



A

B

amputee during stance is evident from the shape of segment (ST - SW - ST) of Figure 5.6. (ST-SW) along the perimeter of the angle-angle diagram is for the most part a straight line parallel to the X-axis.

(4) Smooth and symmetric flexion and extension of the knee and flexion of the hip through swing (SW) until stance (ST) with the thigh and prosthesis acting as a double pendulum.

(5) There is repeatability in both shape and area.

The shape of segment (SW - ST - SW) shows the smooth control exercised by the prosthetic leg during the swing phase. The symmetry of the step is indicative of the double pendulum action exercised by the prosthetic side. Examination of Table 5.4 shows that for the prosthetic leg of the A/K amputee the area A and perimeter P vary linearly with walking speed while P_A is essentially constant with walking speed.

Again, with the aid of a planimeter and calibrated wheel the area A and perimeter P respectively were measured for the stance (ST - SW - ST) and swing (SW - ST - SW) segments of 3 angle-angle diagrams representing 3 footsteps of the prosthetic leg of the A.K. amputee. For each of these angle-angle diagrams ratios of (stance area)/(swing

TABLE 5.4
BEST LINEAR FITS FOR AMPUTEE GAIT

<u>Subject</u>	<u>Leg</u>	<u>Area Versus Walking Speed</u>		
		<u>Y-intercept</u> (degrees) ²	<u>slope</u> (degrees) ² m/sec	<u>Coefficient</u> of <u>Determination</u>
F	Right	69.38	1129.79	.94
	Left (Prosthetic)	317.31	1694.8	.97

<u>Subject</u>	<u>Leg</u>	<u>Perimeter Versus Walking Speed</u>		
		<u>Y-intercept</u> (degrees)	<u>slope</u> (degrees) m/sec	<u>Coefficient</u> of <u>Determination</u>
F	Right	241.12	-21.87	.25
	Left (Prosthetic)	121.96	74.21	.94

<u>Subject</u>	<u>Leg</u>	<u>P_a Versus Walking Speed</u>		
		<u>Y-intercept</u>	<u>slope</u>	<u>Coefficient</u> of <u>Determination</u>
F	Right	11.07	-4.6	.88
	Left (Prosthetic)	5.21	-2.0	.06

area), (stance perimeter)/(swing perimeter), P_A (stance) and P_A (swing) were computed. These are shown in Table 5.5.

TABLE 5.5

Stance/swing ratios for area and perimeter of angle-angle diagrams taken from the prosthetic leg of the A/K amputee

<u>Footstep</u>	P_A (stance)	P_A (swing)	<u>Stance Area</u> Swing Area	<u>Stance Perimeter</u> Swing Perimeter
1	7.11	3.83	.08	.53
2	7.88	3.78	.07	.56
3	7.69	3.75	.08	.57

It is clear from these data that over 90% of the conjoint angular motion occurred during swing.

The value of the stance/swing perimeter ratio together with that for the stance/swing area ratio indicates that a substantially greater amount of perimeter is associated with the stance segmental area. This is not unlike the robot-like gait alluded to earlier in this chapter. Here a mechanical constraint is imposed maintaining a fixed knee angle while the hip angle varies during stance. These data reflect a tight imposed control during stance. The

values of P_A (stance) are substantially higher than the corresponding normal values shown in Table 5.3 while those for P_A (swing) are low (cf. Figure 5.3 P_A (circle) = 3.54). These values for P_A (stance) and P_A (swing) reflect the tight control during stance as well as the economical control occurring during swing. This latter type of control is typical of the double pendulum action mentioned before.

In Figure 5.7 one is able to observe pertinent features allied with the contralateral and intact limb rotations:

- (1) A complex loop shape compared with the prosthetic side and with normals.
- (2) Large amount of hip extension.
- (3) This leg seems to be compensating in a fairly repeatable yet highly abnormal manner for the prosthetic leg action.

The convoluted appearance of the portion of the angle-angle diagram following onset of stance (ST) "reading" the loops in a clockwise direction indicates the type of control exercised.

Following this convolution or "folding over" of the perimeter the next portion of the angle-angle diagram is

somewhat parallel to the X-axis indicating that the knee-angle hardly varied while the hip was extended substantially. Conjoint angular motion then takes place at both the hip and knee joints with the knee flexing, extending and then flexing again just before onset of stance (ST). Simultaneously the hip is flexing until just before stance when hip flexion is sharply diminished. Again the shapes of the angle-angle diagrams are indicative of the type of control mechanism in operation. The "rounded" portions indicating a smooth gradual control while sharp edges which change direction show up a form of "bang-bang" control. Examination of Table 5.4 for the right, intact leg of the A/K amputee elicits the following observations. The area varies linearly with walking speed but the linearity is less pronounced than that of the prosthetic side. Concerning the relationship of perimeter versus walking speed, the best fit is a quadratic with the parabola reaching a minimum at the subject's most comfortable speed and then increasing with speed. The relationship of P_A versus walking speed for the intact limb is radically different from that of the prosthetic side. P_A for the intact side decreases with speed until a minimum is reached whereupon it stays constant. The range of values covered is 6.0 - 9.0.

Using a planimeter and calibrated wheel a segmental analysis similar to that described before was completed on 3 angle-angle diagrams yielding results as in Table 5.6.

TABLE 5.6

Stance/swing ratios for area and perimeter of angle-angle diagrams taken from the right (intact) leg of the A/K amputee

<u>Footstep</u>	P_A (stance)	P_A (swing)	<u>Stance Area</u> Swing Area	<u>Stance Perimeter</u> Swing Perimeter
1	6.99	4.98	5.1	1.1
2	7.42	11.1	2.3	1.0
3	6.83	9.55	1.9	0.9

The stance/swing ratios for area and perimeter indicate that more conjoint angular motion occurs during the stance phase than during swing on the right leg. This is dramatically different from the conjoint angular activity on the prosthetic side. The values of P_A (stance) and P_A (swing) in Table 5.6 illustrate that compensatory control mechanisms are present both during the stance and swing segments of the non-prosthetic side.

Effect of alteration in prosthetic setting for the A/K
amputee

A second study was carried out on the A/K amputee which examined the effects of changing the setting of the prosthesis and allowing the patient to walk at his most comfortable speed. The three new settings (in addition to his normal setting) were:

- (1) Medial whip 20° , unpractised gait
- (2) Medial whip 20° , practised gait
- (3) Medial whip 15° , practised gait

An examination of the various quantified parameters elicited the following information. For the left (prosthetic) leg changing the setting of the prosthesis hardly affected the gait at all. The variations that did occur in area and perimeter could be accounted for by natural variations in the subject's walking speed and interestingly the ratio P_A remained constant in all cases at the same value of 4.5. This was the same value that had been obtained previously during the "whole range" study. For the contralateral side, however, there were significant changes in the gait patterns. The variations in area and perimeter could not be accounted for by variations in walking speed which had been established earlier by the "whole range" study.

There also was a significant increase in the value of

the P_A from 5.5 (normal) to 6.5 (new prosthetic settings). The control mechanism effecting the gait of the A/K patient seems to predominate on his non-prosthetic side. The A/K patient is limited in what he can accomplish with his prosthetic leg. It is not unlikely that postural control as manifested by trunk and upper extremity movements has a role to play. These aspects have not been examined.

C.P. patient

The angle-angle diagrams in Figures 5.11, 5.13 and 5.15 reflect loops for each walk cycle in experiments I, II and III respectively. Figures 5.12, 5.14 and 5.16 are graphic representations of P_A as a function of stimulator-on (off) time. In section 5.2 an in-depth study of the results of these experiments performed on the C.P. patient is presented. A similar segmental analysis using a planimeter and calibrated wheel was completed on 3 angle-angle diagrams of the C.P. patient. The results are shown in Table 5.7. The values of the stance/swing ratios for A and P taken together from Table 5.7 show that significant variability exists from footstep to footstep in the case of the C.P. patient. In general it appears though that more conjoint angular activity occurs during stance than during swing.

TABLE 5.7

Stance/swing ratios for the area and perimeter of angle-angle diagrams taken from the C.P. patient

<u>Footstep</u>	<u>P_A(stance)</u>	<u>P_A(swing)</u>	<u>Stance Area</u> <u>Swing Area</u>	<u>Stance Perimeter</u> <u>Swing Perimeter</u>
1	4.00	5.30	7.8	2.1
2	3.78	4.00	1.5	1.1
3	4.51	4.74	2.0	1.3

TABLE 5.8

Summary of Results for Normals, A/K and C.P. Subjects

<u>Relationship</u>	<u>Subject</u>	<u>Leg</u>	<u>Form of Relationship</u>
Area vs. Walking Speed	Normal A/K	Left and Right	Linear
		Prosthetic(Left)	Linear
		Non-prosthetic (right)	Linear
Perimeter vs. Walking Speed	Normal A/K	Left and Right	Linear
		Prosthetic(Left)	Linear
		Non-prosthetic (Right)	Quadratic
P _A vs. Walking Speed	Normal A/K	Left and Right	Constant
		Prosthetic(Left) Non-prosthetic (Right)	Constant Two linear segments
A, P, P _A vs. Stimulator-on		Left	Undulating
A, P vs. Stimulator-off	CP	Left	Undulating
P _A vs. Stimulator-off		Left	Undulating with distinct cyclic periodicities

5.1.10 Conclusions

The results of both the global and segmental analyses of angle-angle diagrams suggest that together with temporal information one has a quantitative indicator of gait pathology. A summary of the results presented is shown in Table 5.8.

The three parameters area A , perimeter P and the dimensionless ratio P_A as related to knee-angle/hip-angle diagrams emerge as useful quantitative descriptors of gait.

The physical meanings of these parameters have been examined in some detail. The total area A of an angle-angle diagram is shown to be expressive of the total conjoint range of angular motion experienced at the hip and knee joints. Areas of segments of the angle-angle diagram show how much conjoint angular motion occurred during the associated phase of the gait cycle.

The total perimeter P of the angle-angle diagram reflects the amount of coordination that occurred between the hip and knee joints during the entire gait cycle. The same interpretation applies to segmental P in the case where the stance and swing phases are studied.

The ratio P_A emerges as a useful relative quantifier of the shape of the angle-angle diagram. As the results of

section 5.1 show, the shapes of the angle-angle diagrams appear to reflect control mechanisms inherent in the observed gaits and P_A is thus potentially a quantifier of the neuromusculo-skeletal control of the lower limb. The same interpretation applies to segmental P_A in the case where the stance and swing phases are studied.

5.1.11 Potential Use

It is evident that this type of quantitative analysis coupled with a visual display of the angle-angle diagram assists in providing a more complete assessment of locomotor function. An obvious extension⁸ of this work would be to perform similar quantitative analyses on a number of quite distinct gait pathologies in both the sagittal and frontal planes to see whether corresponding characteristic patterns emerge. Brugger and Milner (1977) describe an optoelectronic system which would be especially amenable to this type of study.

In this study we have examined each leg of 5 normal subjects at 4 different walking speeds. Extension of the study to include more subjects walking at a greater number of speeds would enhance the reliability of using normal gait as a "baseline" for the quantitative assessment of locomotor function. It is conceivable that this type of loop analysis

might be valuable in other fields where cyclic loops are found e.g. vector-cardiogram loops and P-V loops in respirology.

Pattern Recognition

An examination of the pattern recognition literature (e.g. Underwood, 1975) after this work was well underway revealed that the descriptor P^2/A (i.e. P_A squared) had been used in expressing the shapes of planar sections of particles of single-phase materials. Furthermore it is evident that there are numerous other ways of attempting to quantify shape (Underwood, 1975). Freeman (1961) makes the comment that one of the difficulties in any shape processing task is the lack of a definitive way of describing shape.

It seems then that the use of pattern recognition techniques in the assessment of locomotor function holds promise as being both a challenging and rewarding endeavour.

5.2 PRELIMINARY INVESTIGATION OF INFLUENCE OF CEREBELLAR STIMULATION ON GAIT BY ANALYSING ANGLE-ANGLE DIAGRAMS

5.2.1 Introduction

Evaluation of the alterations in gait after cerebellar stimulation have until now been mainly

observational (Cooper et al 1973; Cooper et al, 1976). Video tapes of posture and gait are made before and at regular periods after placement of a stimulator. Changes in gait are often evident when viewing serial video tapes spanning several months. Up to now the characterisations of such long-term changes have neither been quantified nor objectively described. Also, no suitable technique has been applied to the study of immediate on or off effects on gait of cerebellar stimulation.

Standard means of assessment and evaluation now commonly in use for any therapeutic intervention in spastic patients include: (i) static evaluation of joint mobility, muscle tone, strength and range of movement; (ii) clinical impression of changes in gait (including raw video tapes) looking for such recognizable abnormalities as scissoring, toe walking, dragging through in swing phase, and jerkiness of movement; (iii) clinical assessment of abnormal deep tendon and postural reflexes.

Deficiencies in these procedures are readily discerned. It is sometimes impossible to correctly interpret the effect of static deformities on a dynamic process such as walking. Often, even the most careful observer cannot describe the mechanisms producing an

abnormality in gait because there are too many observations that must be made concurrently if all the variables are to be considered. Subtle changes in gait may not be readily apparent to the observer and may be important in producing a more efficient pattern of movement.

In recent years techniques and instrumentation have been developed which are capable of yielding detailed kinesiological information about gait with acceptable accuracy (Grieve, 1968; Lamoreux, 1971; Milner et al, 1973, 1974; Radcliffe, 1974; Smith et al, 1976). The computerized electrogoniometric analysis used in our Laboratory (de Bruin and Milner, 1977) permits rapid and accurate quantification of gait parameters in the sagittal plane and yields an immediate hard-copy display available for further analysis. This section of the chapter gives an introduction to the use of quantitative gait analysis in the study of immediate and short term alterations in walking seen in a patient with the stimulator on and off. The description of the experimental procedure followed in the three experiments performed on the C.P. patient has been previously described in section 5.1.8 (see C.P. patient). The results and interpretation of the above three experiments now follows.

5.2.2 Results and Interpretation

Multiple angle-angle diagrams from each experiment involving cerebellar stimulation characteristics have been acquired together with plots of P_A versus time following on transitional states of the stimulator. In what follows these data are depicted for each experiment.

Before proceeding with details pertinent to each experiment it is of value to examine some of the more general characteristics of the patient's gait. By observation and the examination of left footswitch patterns, the patient generally commenced the stance phase by making initial surface contact with his toes. The contact sequences were as follows: toe, heel and toe, toe, swing, etc.

The angle-angle diagrams in Figures 5.11, 5.13 and 5.15 reflect loops for each walk cycle in all experiments. These loops invariably differ from each other more markedly than those exhibited by normal subjects (see for example Figure 5.4). There are segments of each angle-angle diagram that can be reasonably well fitted by straight lines. In a number of instances these straight-line segments are fairly parallel to the axes of the diagrams. This signifies that angular movements are controlled separately for each joint,

i.e. the members about one joint remain fixed while those about the other joint move, thereby giving a more mechanical appearance relating to limb movements.

Movement ranges for the hip appear to be normal to excessive, whilst those for the knee are generally less than normal. The approximate position of the centroid of the diagrams remains roughly constant throughout the experimental runs and does not differ markedly from normals. At heel-strike the knee flexion angle is in the range 30-40 degrees. This is unlike the situation for normals where at heel-strike the knee flexion angle approaches 10 degrees.

Comparative analyses of diagrams generated may be done taking cognizance of variations in the parameters listed as follows:

- (i) ranges of angular motion
- (ii) shape of each closed loop
- (iii) area of each closed loop or defined segments
- (iv) perimeter of each closed loop or defined segments
- (v) position of the centroid for each loop
- (vi) P_A for the closed loop (see sections 5.1.6 and 5.1.7)

It should be stressed at this point that since this was a pilot experiment, only a limited number of footsteps were analysed. Hence the various conclusions and interpretations outlined later in this section should be considered with this in mind.

5.2.3 Experiment I

Angle-Angle Patterns

After five hours with the stimulator turned off, the patient produced angle-angle patterns after the manner shown in Figure 5.11. The following observations are pertinent. In "reading" the loops of Figures 5.11, 5.13 and 5.15 one proceeds in general from ST (stance) in a clockwise fashion around the loop to follow the sequence of the gait cycle

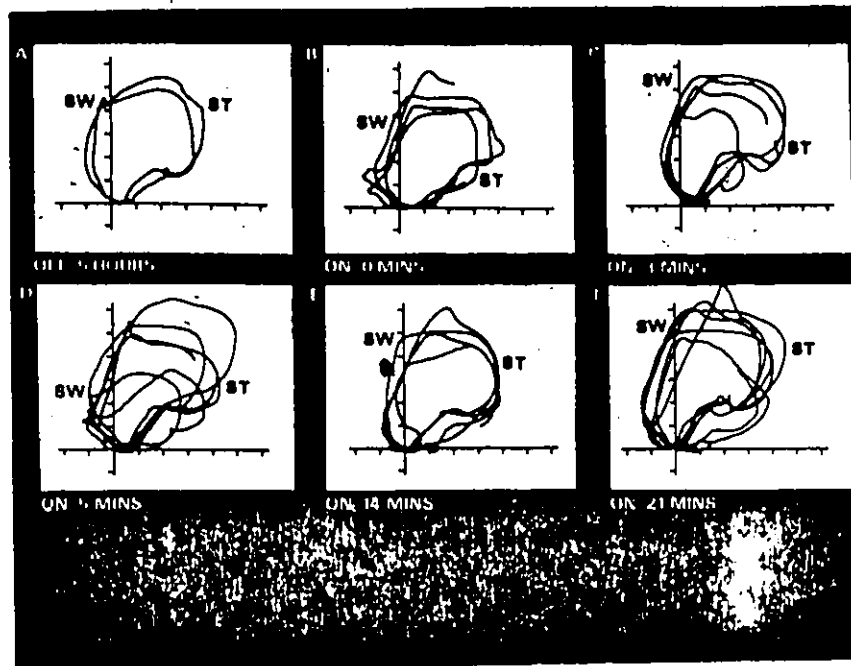


Figure 5.11

Angle-angle diagrams obtained in Expt. I when performance is measured at successive times with the stimulator on. ST and SW respectively reflect the start and termination of the stance phase. Hip angles are on the abscissa and knee angles are on the ordinate with graduations indicating 10 degree increments.

Figure 5.11A shows two loops prior to turning the stimulator on. Substantial motions occur at both the hip and knee joints during execution of the stance phase. From the footswitch characteristics it is noted that stance is commenced with toe-contact followed by rapid knee extension to heel-contact whilst the foot is subject to passive dorsiflexion. It is by the latter action that some kinetic energy of the swinging limb is taken up. During this period of stance, hip flexion remains substantially constant. With the subsequent diminution of hip flexion there occurs a momentary small knee flexion followed by conjoint extensions. The heel soon comes off the ground and push-off occurs with the hip in extension while the knee flexes substantially. It can be noted that the swing phase is executed with the knee flexed at about 50 degrees. Note the difference between the two loops.

Figure 5.11B shows the immediate effects of the stimulator having been turned on. The most dramatic observations to be made are the distinct changes in shape (from that in 5.11A) that occur in both the swing and stance phases. In addition substantial variability in the shapes of the loops can be noted. The commencement of stance occurs with the knee flexed at approximately 10 degrees. During the first part of the stance phase, until the knee is

fully extended, the angular histories are similar to those for the gait described in 5.11A. As the knee flexes, until onset of the swing phase, there are two distinct shapes present one of which is similar to that described in 5.11A. The swing phase is generally divided into two distinct facets in which firstly the knee angle remains fixed whilst the hip flexes and then with fixed hip flexion, knee flexion diminishes markedly. Although the knee range is approximately the same for 5.11B as in 5.11A, the hip range has been extended by about 15 degrees.

In Figure 5.11C stance commences at about 25 degrees of knee flexion. There is then a rapid knee flexion and extension pattern which together with diminution of the hip flexion produces a "kink" in that loop segment. This indicates some form of shock-absorber activity at the knee. The loop segment from maximum knee extension during stance until onset of swing has a very repeatable shape and resembles that of the corresponding segment in 5.11A. There is considerable variation in the swing phase segment of the loops. In addition the two distinct facets of the swing phase observed in 5.11B are still evident. The hip range is approximately the same as that in 5.11B but the knee range has extended by about 10 degrees.

In Figure 5.11D the early part of the stance segment in some of the loops resembles that of the corresponding segment in 5.11C. However, the latter part of stance and early swing resemble that of Figure 5.11B. In general there is considerable variability in the shapes and bound areas of the loops.

In Figure 5.11E the starts of swing and stance phases occur at about the same angles as in 5.11A. The early part of the stance phase resembles that of 5.11A up to and including values about the origin of the diagram. In the subsequent part of stance two distinct slopes emerge one of which resembles the normal pattern, and proceeding through the swing phase two distinct shapes are apparent. For the first shape the swing presents as a relatively constant knee flexion during hip flexion, while in the second case initially there is conjoint knee and hip flexion followed by a reduction in knee flexion with continuing hip flexion. This is not unlike a normal pattern.

Figure 5.11F shows that the commencement of the stance and swing phases occur at about the same relative positions as in 5.11A and 5.11E. The patterns for early stance are not unlike those for 5.11E. Significantly the subsequent phases of stance through the early part of swing

are very similar to the characteristics displayed by normal subjects - see for example Figure 5.4. In addition maximum knee extension occurs with the hip neutral or extended unlike the patterns shown in 5.11A to 5.11D. As for 5.11E, two distinct shapes are obtained for the swing phase with a shape not unlike normal patterns predominating. The ranges for both joints are larger than those reflected in 5.11A.

It is apparent that with continual stimulation over the 21 minutes of experimental observation that there has been an evolution in the angle-angle diagrams from robot-like movement characteristics to diagrams which include essential facets of more normal gait patterns. A major difference, however, lies in the fact that the stance phase commences with toes rather than heel contact. This accounts for the distinctly different pattern for the early part of the stance phase.

Area, perimeter and P_A for each set of patterns generated at each observed time interval are presented in Table 5.9. Figure 5.12 is a graphic representation of P_A as a function of stimulator-on time and follows directly from Table 5.9. The plotted values with increasing time correspond sequentially with the diagrams depicted in Figures 5.11B through 5.11F.

TABLE 5.9

Loop Parameters Derived from Data in Experiment I

Figure 3	Stim. Time minutes	Area $\pm \sigma_1$ degrees ²	Perimeter $\pm \sigma_2$ degrees	P_A $\pm \sigma_3$
A	300 OFF	1282 \pm 17	173 \pm 5	4.83 \pm .18
B	0 ON	1659 \pm 471	198 \pm 53	4.82 \pm .61
C	3 ON	1410 \pm 341	172 \pm 13	4.67 \pm .46
D	5 ON	1620 \pm 801	182 \pm 36	4.82 \pm .74
E	14 ON	1405 \pm 186	189 \pm 24	5.08 \pm .80
F	21 ON	1676 \pm 211	186 \pm 20	4.56 \pm .37

The loop parameters are given as means \pm one standard deviation.

Quantitative analysis is an adjunct to the visual examination of the angle-angle diagrams presented above. The mean value for P_A over the range of experimental values acquired was between 4.5 and 5.0. Interestingly the nominal value for the normal subject (see Fig. 5.4) is about 5.2. This suggests that the two processes are similar. It is noteworthy that after producing an undulating trend, the least value and standard deviation occur at 21 minutes (Fig. 5.11F). The next lowest value and standard deviation occur at 3 minutes (Fig. 5.11C). In general the larger values of P_A are also accompanied by larger standard deviations. The

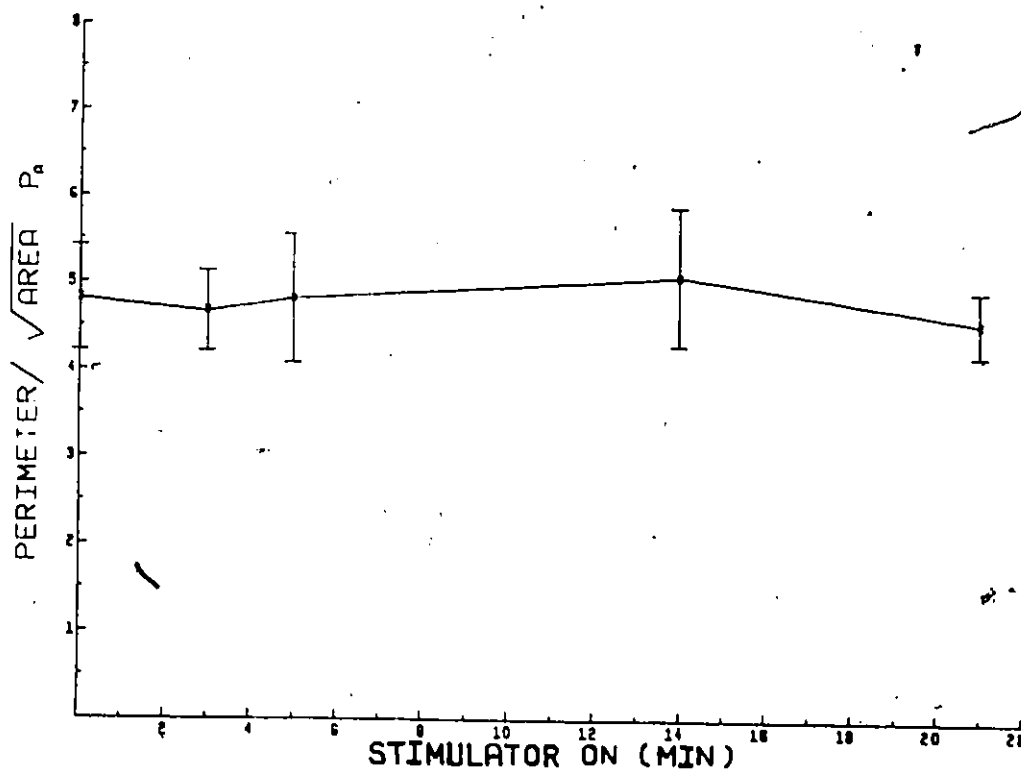


Figure 5.12
 P_A versus stimulator-on time for Expt. I.
 The error bars indicate ± 1 standard deviation.

increase in the standard deviations is more marked than would be expected by the increase in the means alone.

Commencing with the value of P_A allied with Figure 5.11B as reference, the influence of perimeter (P) and area (A) respectively on subsequent mean values of P_A can be described. At 3 minutes (Fig. 5.11C), the decrease in P_A can be attributed to a larger decrease in P than in A. At 5 minutes (Fig. 5.11D), relatively little change in both P and

A relative to the reference has occurred. At 14 minutes (Fig. 5.11E), the increase in P_A can be attributed to a larger decrease in A than in P. Similarly at 21 minutes (Fig. 5.11F), a larger increase in A accounts for the decrease in P_A .

It is suggested that the reduction in perimeter in proceeding from Figure 5.11B to 5.11C implies an improvement in coordination. Next, moving from 5.11C to 5.11F, the area increase is more substantial than the corresponding increase in perimeter. This again reinforces the notion of improved coordination.

Relative values of P_A within an experimental set of data such as those presented above appear to have potential as quantitative indicators of overall co-ordination and control.

Stance and Swing Timing Characteristics

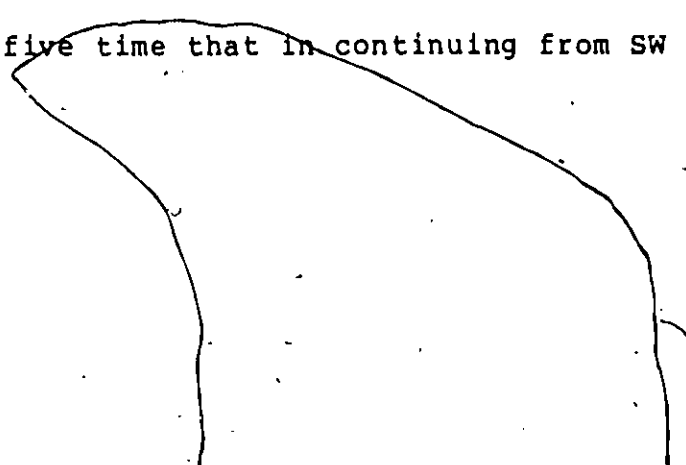
An examination of the bilateral footswitch timing characteristics originally acquired showed that the left side sequence, starting from onset of stance consisted of toe only, heel and toe, toe only and swing. The right side footswitch sequence, however, consisted of toe only and swing with no heel contact whatever. Table 5.10 gives the

TABLE 5.10
Footswitch Parameters for Experiment I

Figure 3	Stim. Time minutes	Velocity m/s.	L. Period $\pm \sigma_1$ sec.	L ST/SW $\pm \sigma_2$	R. Period $\pm \sigma_3$ sec.	R ST/SW $\pm \sigma_4$
A	300 OFF	.68	1.04 \pm .07 (2)	5.02 \pm 1.17	1.04 \pm .04 (5)	2.79 \pm .67
B	0 ON	.63	1.11 \pm .07 (2)	3.73 \pm 1.0	1.12 \pm .17 (6)	4.76 \pm 3.16
C	3 ON	.83	.97 \pm .13 (4)	3.65 \pm 1.06	1.01 \pm .13 (5)	1.47 \pm .27
D	5 ON	.67	1.12 \pm .21 (6)	4.06 \pm 1.51	1.07 \pm .08 (3)	1.57 \pm .16
E	14 ON	.69	1.04 \pm .07 (5)	2.32 \pm .71	.99 \pm .01 (2)	2.58 \pm 1.13
F	21 ON	.68	1.01 \pm .08 (5)	2.76 \pm .36	1.01 \pm .04 (5)	1.47 \pm .37

Footswitch parameters are given as means \pm one standard deviation. In the footstep period column are given the number of footsteps analyzed for each leg.

velocity of walking, the left footstep period, left stance-swing ratio (ST/SW) and the corresponding right footswitch parameters. For the entire set of data acquired in Experiment I, the velocity was substantially constant with a mean value of approximately 0.7 metres per second. The only major deviation occurs for stimulator-on 3 minutes and this does not appear to have a marked influence on the gait patterns and derived data. Left and right footstep periods are substantially identical. It is significant to note that the stance-swing ratio for the right side is generally lower than the corresponding ratio for the left side. This suggests that the time spent in stance on the left side is usually greater than on the right side. Interestingly, after initial divergence the stance-swing ratios for both legs come together, again indicating an evolutionary trend. Note that the stance-swing ratios for the right side are often close to the nominal value of 1.5 for normal subjects. It is useful to realize that the stance-swing ratios provide an indication of time scaling in Figure 5.11. For example, in Figure 5.11A the time spent in going in a clockwise direction from ST to SW is approximately five times that in continuing from SW to ST.



5.2.4 Experiment II

Angle-Angle Diagrams

After 25 minutes of stimulation, that is 4 minutes after the completion of Experiment I, the stimulator was turned off and the patient produced angle-angle patterns as shown in Figure 5.13. The loop parameters: area, perimeter and P_A for each set of patterns generated at each observed time interval are presented in Table 5.11. Figure 5.14 is a graphic representation of P_A as a function of stimulator-off time and follows directly from Table 5.11. The plotted values with increasing time in Figure 5.14 correspond sequentially with the diagrams depicted in Figures 5.13A through 5.13G.

For the sake of brevity a detailed discussion of these results similar to those for Experiment I will not be presented. However, certain general observations are pertinent.

A visual examination of the angle-angle diagrams depicted in Figure 5.13 shows that some of the patterns are similar to those in figure 5.11. For example Figures 5.13E and 5.13G correspond favourably with Figures 5.11E and 5.11F. Whereas in Figure 5.11 an evolutionary trend in the

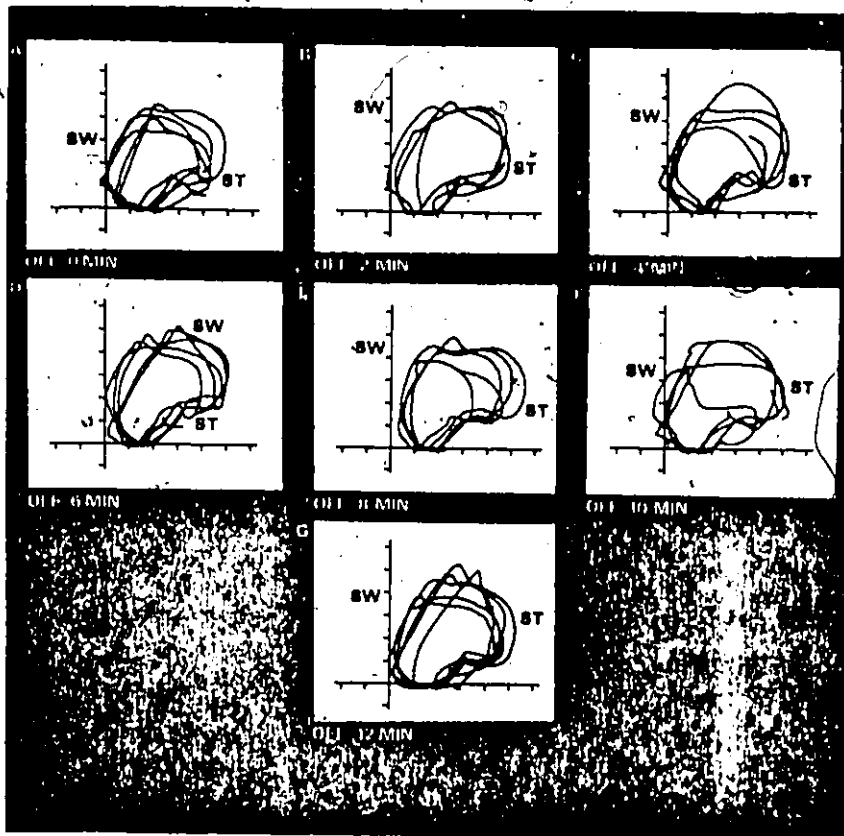


Figure 5.13

Angle-angle diagrams obtained in Expt. II when performance is measured at successive times with the stimulator off. ST and SW respectively reflect the start and termination of the stance phase. Hip angles are on the abscissa and knee angles are on the ordinate with graduations indicating 10 degree increments.

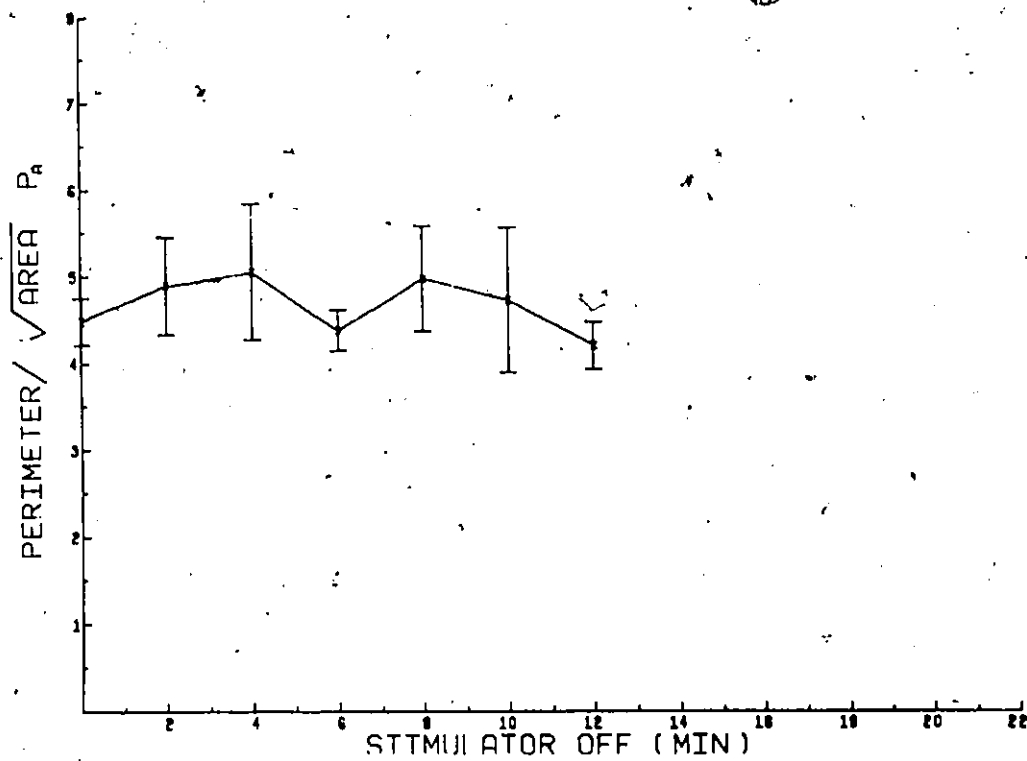


Figure 5.14
P_A versus stimulator-off time for Expt. II.
The error bars indicate ± 1 standard deviation.

TABLE 5.11
Loop Parameters Derived from Data in Experiment II

Figure 3	Stim. Time minutes	Area $\pm \sigma_1$ degrees ²	Perimeter $\pm \sigma_2$ degrees	P_A $\pm \sigma_3$
A	0 OFF	1067 \pm 238	145 \pm 10	4.48 \pm .27
B	2 OFF	1344 \pm 127	179 \pm 16	4.89 \pm .56
C	4 OFF	1313 \pm 321	179 \pm 12	5.06 \pm .79
D	6 OFF	1269 \pm 184	155 \pm 8	4.38 \pm .24
E	8 OFF	1167 \pm 224	169 \pm 27	4.98 \pm .61
F	10 OFF	1318 \pm 420	164 \pm 9	4.74 \pm .84
G	12 OFF	1374 \pm 200	156 \pm 20	4.21 \pm .27

The loop parameters are given as means \pm one standard deviation.

patterns is evident as one progresses with time, a similar progression through the patterns of Figure 5.13 shows different characteristics.

It is interesting to note that Figures 5.13A, 5.13D and 5.13G contain similar patterns. In addition these patterns show some characteristics of normal gait. In contrast the patterns shown in Figures 5.13B, 5.13C, 5.13E and 5.13F are more abnormal. An impression is gained that following both periods of markedly abnormal gait (Figures 5.13B, 5.13C and 5.13E, 5.13F) a return occurs to more

normal patterns (Figures 5.13D and 5.13G).

Examination of Figure 5.14 shows that the P_A associated with Figures 5.13A, 5.13D and 5.13G are the lowest with again the smallest standard deviations (see also Table 5.11). Generally the trend of P_A with increasing stimulator-off time is markedly undulating. This confirms the visual impression gained from Figure 5.13. Figure 5.14 shows that there is a greater variation in P_A than for Experiment I. Reference to Table 5.11 indicates that the predominant influence on P_A is variations in the perimeter since the area remains substantially constant. Essentially coordination and control appear to fluctuate and are best at successive 6 minute intervals. It would certainly have been of interest to explore further 6 minute epochs. However, data storage and time limitations when this experiment was conducted precluded further data acquisition.

Stance and Swing Timing Characteristics

Bilateral footswitch sequences were the same as those observed for Experiment I. Table 5.12 presents data after the manner of Table 5.10. The velocity for the entire set of data acquired in Experiment II was essentially constant with a mean value of .77 metres per second. This was somewhat higher than the average velocity in Experiment I.

TABLE 5.12
Footswitch Parameters for Experiment II

Figure 5	Stim. Time minutes	Velocity m/s.	L. Period $\pm \sigma_1$ sec.	L ST/SW $\pm \sigma_2$	R. Period $\pm \sigma_3$ sec.	R. ST/SW $\pm \sigma_4$
A	0 OFF	.75	1.12 \pm .05 (4)	1.99 \pm .15	1.16 \pm .07 (7)	2.42 \pm .86
B	2 OFF	.74	1.01 \pm .06 (6)	2.49 \pm .28	1.01 \pm .03 (5)	1.52 \pm .29
C	4 OFF	.87	1.09 \pm .05 (4)	2.11 \pm .42	1.05 \pm .08 (4)	1.53 \pm .18
D	6 OFF	.70	1.13 \pm .13 (5)	3.84 \pm 2.16	1.11 \pm .07 (6)	1.36 \pm .14
E	8 OFF	.80	.99 \pm .12 (5)	3.51 \pm 1.55	1.02 \pm .11 (5)	1.41 \pm .22
F	10 OFF	.78	1.06 \pm .07 (5)	2.49 \pm .41	1.09 \pm .09 (3)	1.08 \pm .02
G	12 OFF	.68	1.02 \pm .13 (4)	4.02 \pm 2.14	1.11 \pm .07 (5)	1.54 \pm .30

Footswitch parameters are given as means \pm one standard deviation. In the footstep period column are given the number of footsteps analyzed for each leg.

Left and right footstep periods are substantially identical to each other and to the corresponding footstep periods observed for the previous experiment. With the increase in walking velocity, this indicates that the average stride lengths during Experiment II were essentially constant but about 10 per cent greater than those for Experiment I. It is interesting to note that generally the footstep periods are longest and the velocities least at 0,6 and 12 minutes stimulator-off. These six minute epochs correspond to the epochs noticed for P_A depicted in Figure 5.13. It appears that at these times the patient was able to walk more slowly with a greater degree of control and coordination. It should be noted that he generally walked with a rapid lurching gait.

The stance-swing ratios do not show these six minute epochs. As for Experiment I, the stance-swing ratios for the right side are significantly less than those for the left side and in addition, are much more repeatable. Furthermore, whereas the stance-swing ratios for the left side varied considerably with time, those for the right remained essentially constant. This indicates not only that less time is usually spent in stance on the right side but also that the periods of stance and swing are more repeatable. It is also interesting to note that after

initial divergence the bilateral stance-swing ratios do not come together again. Since the bilateral temporal footswitch patterns are substantially different, one is led to believe that the angular patterns will also be markedly different. Future investigations should therefore include bilateral angular patterns.

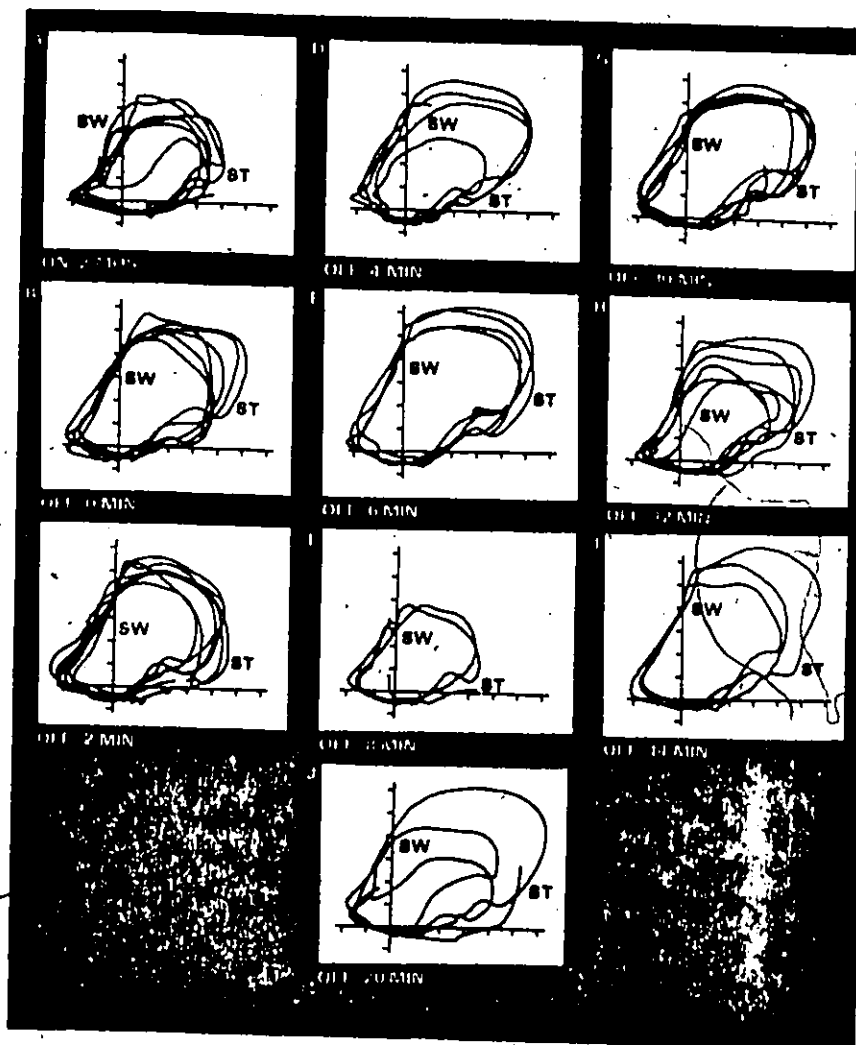
5.2.5 Experiment III

Angle-Angle Diagrams

After 2 months of uninterrupted stimulation, a series of angle-angle diagrams was collected, firstly with the stimulator on and then at essentially 2 minutes intervals after the stimulator was turned off as shown in Figure 5.15. The loop parameters: area, perimeter and P_A for each set of patterns generated at each observed time interval are presented in Table 5.13. Figure 5.16 is a graphic representation of P_A as a function of stimulator-off time and follows directly from Table 5.13. The plotted values with increasing time in Figure 5.16 correspond sequentially with the diagrams depicted in Figures 5.15B through 5.15J.

An examination of Figures 5.15A through 5.15J shows that the angle-angle patterns are not dramatically different in shape. There are variations in area that occur

Figure 5.15
 Angle-angle diagrams obtained in Expt. III when performance is measured at successive times with the stimulator off. ST and SW respectively reflect the start and termination of the stance phase. Hip angles are on the abscissa and knee angles are on the ordinate with graduations indicating 10 degree increments.



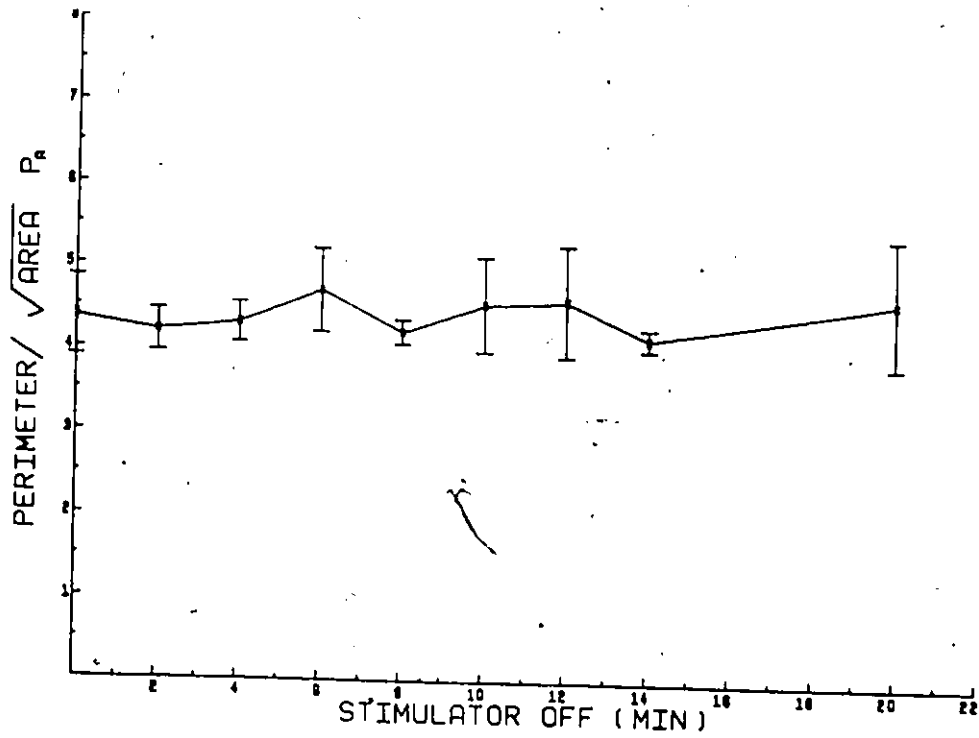


Figure 5.16
 P_A versus stimulator-off time for Expt. III.
The error bars indicate ± 1 standard deviation.

TABLE 5.13

Loop Parameters Derived from Data in Experiment III

Figure 7	Stim. Time minutes	Area $+ \sigma_1$ degrees ²	Perimeter $+ \sigma_2$ degrees	P_A $+ \sigma_3$
A	2 mths. ON	2225 \pm 878	-262 \pm 97	5.47 \pm .97
B	0 OFF	2146 \pm 225	210 \pm 16	4.37 \pm .48
C	2 OFF	2154 \pm 313	194 \pm 16	4.20 \pm .26
D	4 OFF	1905 \pm 644	196 \pm 39	4.30 \pm .24
E	6 OFF	3152 \pm 475	265 \pm 48	4.70 \pm .50
F	8 OFF	1186 \pm 208	143 \pm 8	4.20 \pm .15
G	10 OFF	2306 \pm 784	220 \pm 67	4.54 \pm .58
H	12 OFF	1804 \pm 556	190 \pm 29	4.58 \pm .67
I	14 OFF	2626 \pm 324	211 \pm 18	4.13 \pm .13
J	20 OFF	2030 \pm 791	197 \pm 20	4.61 \pm .78

The loop parameters are given as means \pm one standard deviation.

particularly in Figures D, F and H. In mid- and late-stance phase there is substantial consistency between the diagrams, and the major variability occurs in the swing and early stance phases. The patterns are markedly different from those reflected in Figures 5.11 and 5.13. Primarily, there are more substantial hip extension excursions, with a pronounced "nose".

Turning to Figure 5.16, P_A fluctuates about a mean value of approximately 4.4. This constitutes a dramatic drop from the mean value of P_A for the stimulator-on as reflected in Figure 5.15A and Table 5.11. This latter value corresponds closely with those presented in Tables 5.9 and 5.11. By using similar arguments to those presented in Experiment I in regard to co-ordination and control as expressed through P_A , it appears that switching off the stimulator after 2 months leads to an improvement of these factors in the period of observation. This result coupled with those results from Experiment I suggest that there are short-term and long-term influences associated with cerebellar stimulation and future experiments should be conducted with time scales appropriately adjusted to attempt to elucidate these effects.

It is interesting to note that at 6 minute epochs commencing at 2 minutes stimulator-off, there are distinct minima in P_A . It should be recalled that the same phenomenon has manifested itself in Experiment II.

Stance and Swing Timing Characteristics

Examination of the footswitch characteristics acquired for Experiment III showed that there were marked improvements from the patterns observed for the previous

experiments. The left side sequence starting from onset of stance consisted of heel only, heel and toe, toe only and swing. The only difference from the pattern generated by a normal subject is a somewhat shorter "heel only" phase. In addition, the right footswitch pattern showed frequent incidence of heel-strike just before onset of stance and even infrequent "heel only" phases at the onset of stance. Two months of stimulation has therefore resulted in more normal footswitch patterns. The presence of the "heel only" phase in early stance is also manifested in Figure 5.15 which shows on the average less and more normal knee flexion at onset of stance (ST) than in Figure 5.13.

Table 5.14 presents data after the manner of Tables 5.10 and 5.12. With the exception of 4 and 14 minutes stimulator-off times, the velocity for the set of data acquired in Experiment III was essentially constant with a mean value of .82 metres per second. There does not seem to be a marked difference in the other gait parameters for these two times other than shorter average footstep periods for the former. As for the previous experiments, left and right footstep periods are substantially identical and somewhat less for the early stimulator-off times than the corresponding periods for Experiment II. The average stride lengths were again essentially constant and identical to

TABLE 5.14
Footswitch Parameters for Experiment III

Figure 7	Stim. Time minutes	Velocity m/s.	L. Period $\pm \sigma_1$ sec.	L. ST/SW $\pm \sigma_2$	R. Period $\pm \sigma_3$ sec.	R. ST/SW $\pm \sigma_4$
A	2 mths. ON	.77	.94 (5)	1.66 \pm .29	.95 \pm .05 (8)	1.14 \pm .16
B	0 OFF	.91	.97 \pm .08 (6)	1.78 \pm .25	.98 \pm .13 (6)	1.07 \pm .17
C	2 OFF	.85	.98 \pm .03 (7)	1.75 \pm .26	.98 \pm .04 (6)	1.08 \pm .17
D	4 OFF	1.0	.82 \pm .05 (4)	1.80 \pm .58	.80 \pm .11 (6)	1.24 \pm .18
E	6 OFF	.87	1.06 \pm .14 (5)	1.88 \pm .50	1.02 \pm .11 (6)	1.00 \pm .13
F	8 OFF	.78	1.07 \pm .05 (3)	1.60 \pm .35	1.07 \pm .09 (6)	1.12 \pm .18
G	10 OFF	.83	.95 \pm .09 (4)	2.39 \pm .79	.99 \pm .15 (6)	1.11 \pm .14
H	12 OFF	.77	1.07 \pm .08 (6)	1.79 \pm .24	1.02 \pm .06 (6)	1.29 \pm .25
I	14 OFF	.59	1.00 \pm .09 (4)	1.72 \pm .28	1.05 \pm .16 (6)	1.12 \pm .17
J	20 OFF	.83	1.16 (1)	2.33	1.01 \pm .08 (7)	1.14 \pm .28

Footswitch parameters are given as means \pm one standard deviation. In the footstep period column are given the number of footsteps analyzed for each leg.

those for Experiment II. Generally, the footstep periods are longest and the velocities least at 2, 8 and 14 minutes stimulator-off. These six minute epochs correspond to the epochs noticed for P_A depicted in figure 5.17. It appears that at these times the patient was able to walk more slowly with a greater degree of control and coordination. It is important to note that while Experiments II and III were conducted two months apart their protocols were identical. Significantly, in both sets of experiments, the phenomenon of the simultaneous occurrence of minimum P_A , minimum velocity and maximum footstep period is exhibited at six minute epochs.

The bilateral stance-swing ratios behave similarly with time to those measured for Experiment II. However, the left ratios demonstrate less variability and in addition are more repeatable for each time than in the previous experiment. Also, both ratios are lower with the right ratio substantially less than normal and the left ratio somewhat higher than normal.

Several parameters of the patient's gait in Experiment III showed improvement over those for the previous experiments. The footswitch patterns are more normal with the addition of a "heel only" phase at the onset

of stance. Although the angle-angle patterns depicted in Figure 5.15 are still abnormal, they have a more repeatable shape at each time interval. This is supported by the fact that the standard deviations for P_A depicted in Figure 5.16 are generally smaller. Finally, the stance-swing ratios are closer to normal values especially for the left side and in addition are more repeatable at each time during the experiment. These observations with the stimulator turned off after two months of continual stimulation suggest that there is a tendency for the gait of the patient to begin to incorporate features that attach to the gait characteristics of normal subjects.

5.2.6 Summary and Conclusions

The patient automatically selects an average walking speed which for each set of experiments remains essentially constant. The angle-angle patterns show evidence of a general lack of smooth coordination in the control of the conjoint motions about the hip and knee. It is observed that in all experiments marked variations (as compared with normals) occurred in both the average values and the standard deviations of virtually all parameters. Turning to P_A in particular, it is noted that throughout the entire set of experiments P_A lies between 4.2 and 5.5. This range of

values is embraced in the studies of normal subjects that have been conducted thus far, but for normals the variability in P_A is significantly less. Minimum variability in P_A accompanies minimum average values of this parameter. Hence, the relative values of P_A within an experimental set of data such as those presented for each experiment appear to have potential as quantitative indicators of overall coordination and control. For P_A to fully convey its meaning from one condition to another within a set of experimental data, it is necessary also to note the corresponding values of P and A.

A significant finding is that left and right footstep periods remained essentially identical to each other. Although there is symmetry in respect to the footstep periods, the footswitch patterns and stance-swing ratios are markedly different with the right side ratio significantly less.

Strikingly, a number of parameters in both Experiments II and III appear to undergo significant consistent phasic variations at cyclic intervals of six minutes. At the pertinent times P_A and its standard deviation, as well as velocity attain minima while bilateral footstep periods attain maxima. Experiment I on the other

hand does not show these six minute phasic variations. The implication of these findings is that irrespective of two months of continual stimulation, the control mechanism associated with the patient's gait appear to be making continual cyclic adjustments. It would have been interesting to have acquired data from the patient prior to the implantation of the stimulator to determine whether the cyclic phenomenon is inherent in the gait or is a function of any previous stimulation. A question also arises regarding the persistence time of this cyclic phenomenon.

The short-term effects of turning the stimulator on can be described as follows. In general, the gait parameters for Experiment I exhibit an evolutionary trend with the angle-angle patterns evolving from diagrams which exhibit robot-like movement characteristics to diagrams which include some essential facets of more normal gait patterns. This is markedly different from the phasic trends for Experiments II and III. Considering the variations with time of the gait parameters in all three experiments, it can be concluded that turning the stimulator off results in short-term effects on the control mechanisms different from those elicited by turning the stimulator on.

Certain angle-angle diagrams from each set for

Experiments I and II exhibited some characteristics in common. The long-term effects of two months of continual stimulation resulted in angle-angle patterns which were markedly different from those obtained for the previous experiments. In addition the variability of P_A and the stance-swing ratios were significantly reduced. Finally the footswitch patterns demonstrated more normal stance sequences. Therefore turning the stimulator off after long-term stimulation has resulted in several improved gait characteristics. However, it should be noted that the improvement in the parameters mentioned above was marked only after the stimulator was turned off. This leads one to suggest that possibly the stimulation parameters were not optimum for long-term stimulation.

The pilot experiments reported here demonstrate that objective data are able to be acquired which records the functional performance specifically relating to gait of a cerebral palsy patient implanted with a cerebellar stimulation. The processing, display and subsequent interpretations of the data acquired have been done in what is believed to be a unique fashion with considerable future potential for these kinds of patients. The measures adopted are sensitive to changes in functional performance and provide quantitative and statistical information. Where

possible physical interpretations of acquired information have been indicated and in particular stress has been laid on the issues of coordination and control. While these studies have been confined to measures associated with the consequences of stimulation effects, it is evident that the tools described could be used to evaluate the consequences of other therapeutic and surgical strategies. Recent technological advances in the optoelectronic tracking of body motions (Brugger and Milner, 1977) have the potential for expediting the acquisition of kinematic data which will lead to angle-angle displays.

Much has been learnt from these experiments to the extent that future work should recognize the need for acquiring bilateral angular and temporal information; that the protocol for studies should include recordings prior to implantation and that time scales should be selected to more fully elucidate long and short-term effects during and after stimulation. The character of this work is such that a multifactorial analysis involving statistical techniques is necessitated and one is led to suggest that electromyographic analyses of major muscle groups would serve as a valuable adjunct. Furthermore correlations with other neurological findings would be of value. It should be noted at this point that the amplitudes of the H-reflexes for the

same C.P. patient follow an undulating trend with stimulator off time. Even more striking is the evidence of cyclic periodicities in this trend similar to those observed in the plot of P_A versus stimulator off (Milner, et al, 1977).

CHAPTER 6

TRANSFER FUNCTION TIME SERIES MODELLING

6.1 Introduction

In this chapter an initial attempt has been made to model the neuromusculo-skeletal (NMS) system, which is represented by a black box, with the averaged and rectified electromyographic (EMG) activities of selected leg muscles as inputs and the angular rotations in the sagittal plane of the limbs about the hip and knee joints as outputs. There are a number of reasons which justify this type of work. These are listed as follows:

(1) By attempting to obtain physical interpretations for the various parameters in the model and by noting the sensitivity of these parameters to various changes one might answer some of the queries put forward by physiotherapists and other concerned medical personnel. For example, questions might relate to the best therapy to be used in gait rehabilitation or to the optimal surgical procedure to be employed in a certain circumstance.

(2) If one were then able to model on a digital computer the transfer functions relating the inputs and

outputs of the system, one would be able to incorporate the computer in utilizing the model for adaptive control of gait.

(3) At this stage one could consider the possibilities of programmed electrostimulation of paralysed musculature. By placing electrodes over the appropriate muscle groups of the lower limbs, percutaneous electrostimulation of the musculature could be invoked and contraction of the muscle groups could be accomplished.

In order to recreate the gait pattern, however, it is imperative to know which are the dominant muscle groups involved, in what sequence they contract and then lengthen and what the relative magnitudes of muscular activity are (i.e. the electromyographic activity is taken to be representative of muscular activity). Knowing this information one could pass appropriate amounts of current through localized regions of the chosen muscle groups in a certain phasic cycle so as to artificially recreate as far as is possible, gait pattern. A study which provides an insight into some of the problems inherent in programmed electrostimulation is available in the literature (Milner and Quanbury, 1971b). Such a digital model would be an invaluable aid towards the successful realization of programmed electrostimulation.

A careful perusal of the literature (see Chapter 2) has indicated that there has been no study made of the causal relationship between patterns of muscular activity and consequent gait patterns in the lower extremities during walking. It must be concluded, therefore, that such a relationship is very much an open question. It would be interesting to determine whether such a model, if found to be reliable under repeated laboratory testing, could provide a one-to-one correspondence between model form and class of subject with the latter being defined by both the gait pathology and the physical dimensions of the subject. Varying each of the stride length, pace frequency and gait speed, independently or constraining two of these factors at once, could then move the model to different portions of the parameter space without necessarily changing the form of the model. The successful realization of the proposed model could then bring to the study of locomotion in both normal and pathological subjects a unity and a generalization which is lacking in the present literature.

The rationale for using the black-box approach will now be presented followed by a brief review of those authors who have used transfer-function models in biological research.

6.2 Justification of the Black-Box Modelling Approach

In trying to understand the workings of physical systems, attempts have generally been made to analyse such systems by breaking them into smaller and smaller sub-systems which are physically realizable. An understanding of the function and role of each sub-system could then lead to an explanation for the whole. One major disadvantage of this approach, particularly for biophysical systems, is that it is usually almost impossible to do such an analysis without causing some sort of permanent damage to the organism. This is especially true in the analysis of normal and pathological gait in human subjects. To analyse the locomotor system by the method described in the first paragraph would imply the removal of muscles from limbs which would be highly impractical. It was for this reason that animal models have been introduced as an indirect means of studying the system. There is thus justification for regarding the whole locomotor system as a black box (or grey depending on the amount known about the system). From a careful examination of the inputs and outputs of the system, which can be obtained with the use of experimental techniques which hardly affect the physical system at all, conclusions might be reached about the inner workings of the system.

One disadvantage of the black-box approach, used with the input-output data collected in the manner described in this chapter, is that because of interactions between the inputs (both known and unknown), cause-effect relationships might be mis-interpreted. In fact, using this method, one is able only to postulate hypotheses concerning cause and effect and make predictions which have to be verified experimentally. In order to understand cause and effect in a system as well as investigate cross-correlations between hidden inputs and the inputs being recorded one needs to interfere with the system so as to perturb the biological loops.

An experimental technique that holds promise in this regard is selective nerve blocking of various muscle groups in the leg. With the aid of a local dilute anaesthetic injected into the appropriate nerve(s), the selected muscle group could be effectively blocked of its neural inputs. This technique has been used already in other areas e.g. Edeland and Stefansson (1973) blocked the suprascapular nerve in reduction of acute anterior shoulder dislocation and Angle et al (1973) examined the mechanism of the unloading reflex by blocking the antagonist muscle nerves.

It is hoped that the utilization of this experimental

technique in conjunction with the collection of pertinent input-output data will yield useful information on cause and effect relationships in the NMS system.

It is pertinent to examine the literature for those papers concerning transfer-function modelling of biological systems.

6.3 The Use of Transfer-Function Models in Biological Research

Those papers in the area of muscle physiology which have attempted to model the transfer functions of load-moving systems have resorted to essentially statistical approaches. Williams et al (1972) used the Fourier transform of the input auto-correlation function and the input-output cross-correlation to obtain a transfer function. Transfer functions of load-moving muscle systems, the human oculomotor system and several types of mechanoreceptors have been obtained using this technique.

Coggshall and Bekey (1970) by using steepest descent methods have related muscle force to the average rectified value of the electromyogram. Inbar and Baskin (1970) determined certain parameters of striated muscle by using a least squares method for nonlinear discrete system identifi-

cation. Groupe and Cline (1975) achieved the functional separation of EMG (electromyographic) signals from noise and other interacting EMG signals via an autoregressive - moving average (ARMA) model and used this model for prosthesis control purposes. Conscious of the need for a rigorous statistical analysis of EMG signals and noting the application of rigorous time-series analysis techniques to the EMG of the upper extremity muscles by Groupe and Cline (1975), to the ECG by Zetterberg (1969) and to the EEG by Fenwick et al' (1971) the initial approach chosen for identification of the neuromusculo-skeletal system during normal locomotion has been the methods of time series analysis. The excellent text of Box and Jenkins (1970) contains the essential mathematics as well as many of the programs associated with time series analysis. Appendix 2 contains a summary of the theoretical background to the transfer function modelling procedure taken from Box and Jenkins' text.

For the reader who is interested in additional uses of time-series analysis the IEEE Transactions on Automatic Control has published a special issue on System Identification and Time Series Analysis (Vol AC-19, No. 6, December 1974). This issue contains a good cross-section of papers applying similar techniques of time series analysis to those

described in this chapter but in a number of different areas. The system that is being studied in the work presented here is multi-input and single output. Although some work has been done in the identification of multivariable systems using time series analysis (Priestley et al, 1974) the theory and application of these methods have not yet sufficiently advanced to be of immediate use.

The method invoked in this thesis is to initially guess the form of the transfer function model incorporating as much knowledge of the physical system as is possible. The transfer function model is then fitted by first assuming white noise and the residual auto and partial auto-correlations (see Appendix 2) are then used to identify a better model for the noise.

6.4 Proposed Form of Model

The general form of the model proposed for the neuromusculo-skeletal system is

(system dynamics) $y_{t}^{knee} =$

$$C_8 + (C_1 X_{1,t-b} + C_2 X_{2,t-b} + C_3 X_{3,t-b} + C_4 X_{4,t-b}) + N_t$$

and (system dynamics) $y_{t}^{hip} =$

$$C_7' (C_1' X_{1,t-b} + C_2' X_{2,t-b} + C_3' X_{3,t-b}) + N_t'$$

where (system dynamics) = $f(B)$.

where $(C_1, \dots, i = 1, 4)$ = knee input coefficients
 $(C_1', \dots, i = 1, 3)$ = hip input coefficients
 C_7, C_8 = level parameters
 b = delay (msec)
 X_1 = m. rectus femoris EMG
 X_2 = m. biceps femoris EMG
 X_3 = m. semitendinosus EMG
 X_4 = m. gastrocnemius EMG
 y_{knee} = knee angle
 y_{hip} = hip angle
 N_t = noise model

The noise model N_t models the contributions to the output of all the other muscle groups not being used as inputs. N_t also includes all experimental and measurement errors.

6.5 Design of Experiment

A description now follows of some of the methods employed by this author in an effort to minimize the experimental errors associated with the collection of pertinent input-output data off an ambulating subject walking on a level surface.

(1) As described in Chapter 3, the choice of a

motion-measuring system is crucial if one wishes to measure the angular rotations at the hip and knee joints in the sagittal plane with minimal error. In this work the angular rotations were acquired using self-aligning electrogoniometers after the design of Lamoreux (1971). The advantages and disadvantages of such a system over the stroboscopic flash-photography system have been carefully outlined in Chapter 3. Preliminary work utilizing an optoelectronic system (Brugger and Milner, 1977), however, show that this system would be an even better system for future studies. The advantages and disadvantages of the optoelectronic system have also been included in Chapter 3. Essentially by careful placement of the electrogoniometer system about the hip and knee joints (see Figure 3.11) errors due to motion in other planes and movement of muscle bulk during gait have been minimized.

(2) The rectified and averaged EMG activities of selected skeletal muscles in the leg were considered as inputs. The choice of this form of processed signal is justified since it has been shown by de Bruin (1976) that the rectified and averaged EMG signal is as sensitive to changes in muscular contraction (isometric) as any other commonly considered amplitude processor. Also simplicity in both hardware and software applications is an added reason

for choosing the rectified and averaged EMG signal as the form of processed signal. Chapter 4, deals at length with a method in which the optimal averaging window for the rectifier and averager can be computed as well as the optimal position for placement of the surface electrodes on the muscle. This method enables the researcher to enhance the reliability of his results by averaging out randomities in the signals as well as providing a consistent means of comparing results with those in other laboratories.

(3) The use of surface electrodes "floating" on an electrode-skin tissue interface consisting essentially of electrode paste and other chemicals on the skin allows one to minimize errors due to relative motion of the skin under the electrodes.

(4) Motion artifacts are further reduced by using short leads between the electrodes and the differential amplifier. The characteristics of this differential amplifier is summarized in Table 3.1, Chapter 3 and with a high common mode rejection ratio, high input impedance, low output impedance and shielded cable, a clean acquisition of the EMG signal (less 60 Hz interference) is attained. Finally the use of high pass filters (Chapter 3, Figure 3.17) eliminates the low frequency component due to any

remaining motion artifact.

(5) Amplification of the signals prior to computer acquisition reduces quantization noise due to the A/D converter. These amplifiers are described in Chapter 3 (Figure 3.17).

6.6 Experimental Acquisition of Input-Output Data

With the subject walking comfortably along a level walkway, the EMG signals were acquired simultaneously from four different muscle groups (m. rectus femoris, m. biceps femoris, m. semitendinosus and m. gastrocnemius) of the left leg. The optimal positions for placement of the surface electrodes on each muscle group had been determined from an earlier experiment using the method described in Chapter 3. The optimal averaging window for obtaining the rectified and averaged EMG signal to be used in this analysis was derived again using the method described in Chapter 3. For the subject studied in this chapter and for each muscle group examined the optimal averaging window length was found to be 74 msec.

The reasons for the choice of the four muscle groups mentioned above as inputs were:

- (1) Examination of the relevant section in Chapter 2

showed that these muscles were considered to play active roles in rotation about the knee during normal locomotion. Excluding the m. gastrocnemius the remaining muscle groups mentioned were considered to be active during the hip rotation while walking.

(2) The muscle groups were superficial and easily able to be palpated. With the aid of an experienced physiotherapist each muscle group was carefully delineated and surface electrodes were applied to the skin.

Figure 6.1 depicts the four rectified and average EMG signals for the aforementioned muscle groups as well as the hip and knee angles for the period of one footstep of the subject.

6.6.1 Order of the System Dynamics

In order to determine the order of the system dynamics the modelling procedure was repeated using the data for a given footstep with linear and quadratic system dynamics for the case of:

$$N_t = (1 - \theta B)a_t$$

where B is the backward shift operator defined by $BN_t = N_{t-1}$.

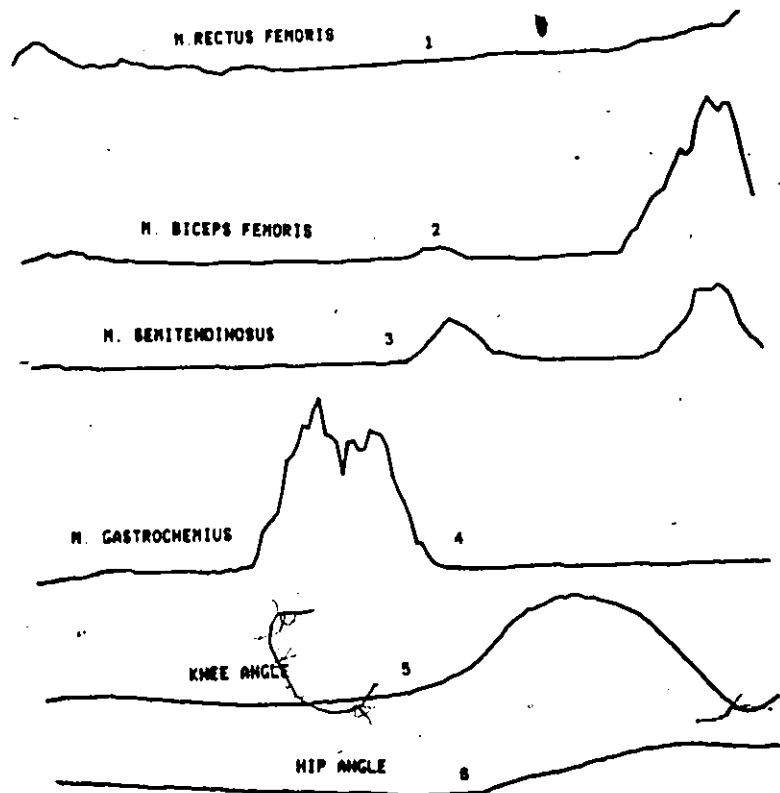


Figure 6.1
 Input-output data for footstep #4
 1,2,3,4 = inputs
 5,6 = outputs

The variances of the residuals obtained in each case are shown in Table 6.1. Clearly the model incorporating a 2nd order dynamics in the denominator converges with better statistical significance. This result seems to confirm the work of Crochetiere et al (1967) and Coggshall and Bekey (1970) among others who suggested that muscle behaves as a 2nd order dynamic system. The results obtained with 3rd order hip and knee dynamics showed no improvement over those

Table 6.1
Determination of Order of System Dynamics

<u>System Dynamics (b=4)</u>	<u>Noise Model</u>	<u>Variance of Residuals</u>
1st Order Hip Dynamics	$N_t = (1-\delta B)a_t$	0.34
2nd Order Hip Dynamics	$N_t = (1-\delta B)a_t$	0.24
1st Order Knee Dynamics	$N_t = (1-\delta B)a_t$	1.89 /
2nd Order Knee Dynamics	$N_t = (1-\delta B)a_t$	0.40

obtained with the corresponding 2nd order dynamics.

6.6.2 Delay b

Ralston et al (1976) simultaneously recorded electrical activity in the m. rectus femoris, acceleration of the shank and force at the ankle during reflex and voluntary extension of the knee. They found that time lags of the order of 30-40 msec occurred between onset of electrical activity and onset of extension and between cessation of electrical activity and onset of flexion. Since the sampling frequency used for the rectified and average EMG's and knee, hip rotations was 100Hz their work suggested a value for 'b' of either 3 or 4 (i.e. a delay of 30

or 40 msec). If a different sampling frequency were to be utilized, other delays between 3 and 4 could be investigated. This was not done for this study. In order to establish the value of b the modelling procedure was repeated for $b=3$ and $b=4$ using the model form with a 2nd order denominator and $N_t = (1-\theta B)a_t$. The statistics displayed in Table 6.2 for four different footsteps make it clear that in general a delay of $b=3$ provides a statistically more significant model.

Table 6.2

Statistics for Determination of Delay b

Footstep	Model	Delay (msec)	Variance of Residuals	Variance Explained by T.F. Model Only (%)
1	Knee	30	0.38	59.08
		40	0.40	63.97
	Hip	30	2.38	50.04
		40	2.41	59.54
2	Knee	30	0.413	81.06
		40	0.415	75.86
	Hip	30	0.26	86.42
		40	0.23	85.58
3	Knee	30	0.37	96.6
		40	0.39	93.8
	Hip	30	0.19	95.9
		40	0.18	84.6
4	Knee	30	0.49	91.9
		40	0.50	69.9
	Hip	30	0.24	92.8
		40	0.26	50.2

6.7 Results

The final forms of the knee and hip models which incorporated the least number of parameters and which also reduced the residuals to white noise in the most statistically significant manner were

$$(1 - C_5B - C_6B^2) \cdot y_t^{\text{knee}} = C_8 + (C_1X1_{t-3} + C_2X2_{t-3} + C_3X3_{t-3} + C_4X4_{t-3}) + (1 - C_7B)a_t$$

$$Ba_t = a_{t-1} \text{ backward shift operator}$$

and

$$(1 - C_4B - C_5B^2) \cdot y_t^{\text{hip}} = C_7 + (C_1X1_{t-3} + C_2X2_{t-3} + C_3X3_{t-3}) + (1 - C_6B) a_t$$

Model adequacy in each case was checked (see Appendix 2) by examining the autocorrelation function of the residuals and cross-correlation functions involving the inputs and residuals. The chi-square statistics associated with the autocorrelations of the residuals and cross-correlations of the residuals and inputs are compared with the corresponding numbers in the chi-square distribution table (for a given significance and number of degrees of freedom).

Table 6.3 contains the final parameter values and confidence limits for the parameters in the knee and hip models for footstep #4 of the same subject.

Table 6.3

Final Parameter Values for Knee and Hip ModelsKnee Model Final Parameter Values Footstep #4

1	2	3	4
-0.2562E-02	0.1304B-03	0.1275F-01	0.2356B-03
5	6	7	8
0.1999E 01	-0.1005E 01	0.8442B 00	0.2159E-01

Individual Confidence Limits for Each Parameter
(on Linear Hypothesis)

1	2	3	4
0.2750E-02	-0.4181E-02	0.2029E-01	0.1409E-02
-0.7873E-02	-0.3920E-02	0.5203E-02	-0.9381E-03
5	6	7	8
0.2023E 01	-0.9813E 00	0.9480E 00	0.4445E-01
0.1976E 01	-0.1028E 01	0.7405E 00	-0.1275E-02

Hip Model Final Parameter Values Footstep #4

1	2	3	4
-0.1280E-03	-0.2628E-02	0.6216E-02	0.1960E 01
5	6	7	
-0.9604E 00	0.1022E 01	-0.5282E-02	

Individual*Confidence Limits for Each Parameter
(on Linear Hypothesis)

1	2	3	4
0.8686E-03	0.5489E-03	0.1080E-01	0.2020E 01
-0.3435E-02	-0.5806E-02	0.1627E-02	0.1899E 01
5	6	7	
-0.08976E 00	0.1120E 01	0.3387E-01	
-0.1023E 01	0.9239E 00	-0.4443E-01	

Figure 6.2 contains the actual knee and hip outputs (output data for the footstep shown in Figure 6.1), modelled (transfer function and noise) knee and hip outputs, modelled (transfer function only) knee and hip outputs for the input-output data shown in Figure 6.1.

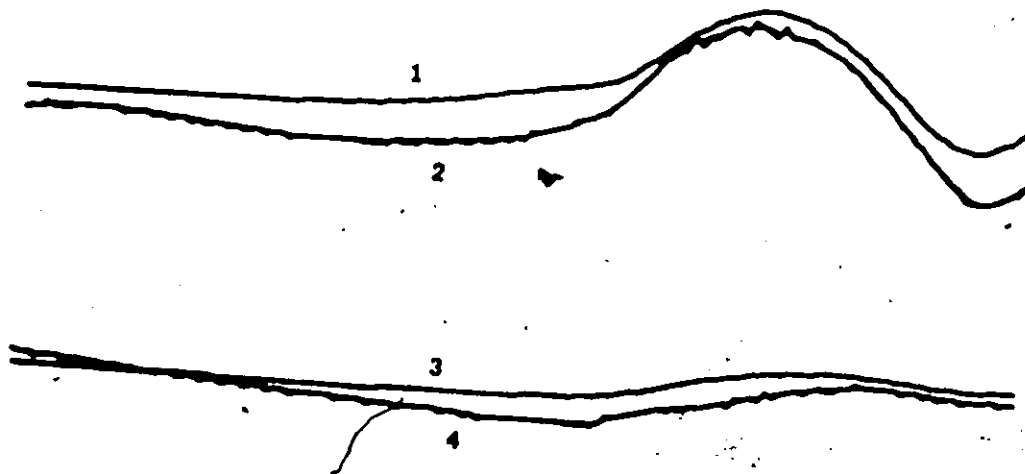


Figure 6.2

Model predictions for footstep #4

- 1: Modelled knee output (Transfer Function Only)
- 2: Modelled knee output (Transfer Function + Noise Model) lying on top of actual knee output
- 3: Modelled hip output (Transfer Function Only)
- 4: Modelled hip output (Transfer Function + Noise Model) lying on top of actual hip output

Table 6.4 contains the chi-square statistics associated with the autocorrelations of the residuals and cross-correlations of the residuals and the various inputs for the footstep described in Figure 6.1.

Table 6.4

Chi-square Statistics for Footstep #4 (b=3)

Model	Variance of Residuals	χ^2 AUTO-CORR. RES	χ^2 CROSS 1,R	χ^2 CROSS 2,R	χ^2 CROSS 3,R	χ^2 CROSS 4,R	Variance explained by T.F. Model %
Knee	0.49	40.0	0.44	1.95	8.95	21.05	91.9
		cf 40.1	cf36.4	cf36.4	cf36.4	cf36.4	
Hip	0.24	34.92	29.01	16.88	23.25	-	92.8
		cf 40.1	cf37.7	cf37.7	cf37.7		

6.8 Discussion of Results

The results of the modelling procedures outlined in the preceding sections elicit some interesting observations.

1. The cross-correlations between inputs show up inputs which are highly correlated. One of these inputs could then be possibly removed from modelling consideration... It was found that consistently for the subject studied that the m. biceps femoris and m. semitendinosus were highly correlated. This seems to indicate that one could characterize the m. hamstrings by a single muscle group and that anyone of the muscle groups within the hamstrings group would be equally good for prediction purposes.

2. The variance explained by the transfer function model alone shows whether the inputs used were adequate for predicting the output. For the results analyzed in this chapter, it was found that the four inputs chosen accounted on the average for > 80% of the variance. The three inputs used for predicting the hip angle accounted also on the average for > 80%. If it should turn out, however, that there is a large difference between the output predicted by the transfer function alone and the actual output, this difference could suggest the phasic activity of an additional muscle group that is needed for better prediction of the output.
3. The product of an input coefficient and its standard deviation ($C_i \sigma_{x_i}$) reflects the weighting of the contribution of each input in predicting the output. It should be stressed again that this prediction is obtained from passively observed data in which no perturbation of the system has taken place. Table 6.5 shows the inputs sequenced in order of decreasing weighting (i.e. the first input has the highest weighting). These results indicate that as far as predictions of the knee and hip angles are concerned the hamstring muscle group represented by m.

Table 6.5

Weighting of Inputs

<u>Footstep</u>	<u>Model</u>	<u>Sequence of Inputs in order of Decreasing Weight</u>			
1	Knee	S	BF	RF	G
	Hip	BF	S	RF	
2	Knee	S	BF	RF	G
	Hip	S	RF	BF	
3	Knee	S	RF	BF	G
	Hip	S	BF	RF	
4	Knee	S	BF	RF	G
	Hip	S	BF	RF	

S - m. semitendinosus
 RF - m. rectus femoris
 BF - m. biceps femoris
 G - m. gastrocnemius

semitendinosus and m. biceps femoris seem to be more important than the m. rectus femoris (in case of hip) and m. rectus femoris and m. gastrocnemius (in case of knee).

4. As can be seen from Figure 6.2 the modelled outputs (transfer function only) seem to follow certain segments of the actual outputs better than other segments. As far as the knee angle is concerned flexion-extension during stance was not modelled as well as flexion-extension during swing. For the hip angle, extension during stance was not followed as

well as flexion during swing. These observations generally held for all the footsteps studied.

5. It is interesting to note that when the input-output data of three footsteps were modelled as one set of input-output data there was less success in modelling the output than when each footstep was modelled separately. This reflects the inability of this modelling procedure to model the transitions between footsteps and illustrates a limitation of the modelling procedure.

6.2 Conclusions

It is noteworthy that Transfer Function Time Series Modelling has produced a number of interesting physiologically-based hypotheses viz.

1. The model is able to suggest which muscles, forming part of a larger muscle group, are synergistic.
2. Model adequacy can show whether the muscles chosen as inputs are good predictors of the output. Differences between predicted output and actual output allow one to possibly determine the phasic activity of an unrecorded muscle input.

3. The results of the modelling can allow the user to associate with each muscle input a weighting thus giving the relative contribution of each input in predicting the output.

It is apparent, however, that for further understanding to be gained of the nature of the neuromusculo-skeletal system, the modelling procedure should be extended primarily in the following two ways:

1. A mechanistic model describing the possible nonlinearities of the system should be included in the time series modelling procedure.
2. The system should be perturbed in such a way that input-output data could be more causally related. Nerve-blocking as described previously presents exciting possibilities in this direction.

APPENDIX 1

TWO PROGRAMS USED FOR QUANTITATIVE ANALYSIS OF EMG SIGNALS AND ANGLE-ANGLE DIAGRAMS.

Program 1

Name: 10E2 . FOR

Subroutines: None

Aim of Program: The EMG signals associated with a specified number of footsteps can be read in and processed (rectified and averaged). Before processing, the individual signals are "massaged" to equal length by either deleting or adding data points uniformly throughout the signal length. A variance ratio is then computed (see Chapter 4).

<u>Variable</u>	<u>Meaning of Variable</u>	<u>Format</u>
NUM	Number of data points in the signal record	I4
NSTEP	Initial number of footsteps to be read in	I4
INUM	Total number of channels (inputs)	I3
IREC	First channel number to be read	I3
IDIC1	Do you want Full-Wave Rectification? Yes or No	A2
IDIC2	Do you want an EMG envelope? Yes or NO	A2
NUMP	Window length for averaging (Even no. of increments)	I4
NSTEP	Maximum number of footsteps to be read in	I3
IRECL	Maximum channel number	I3

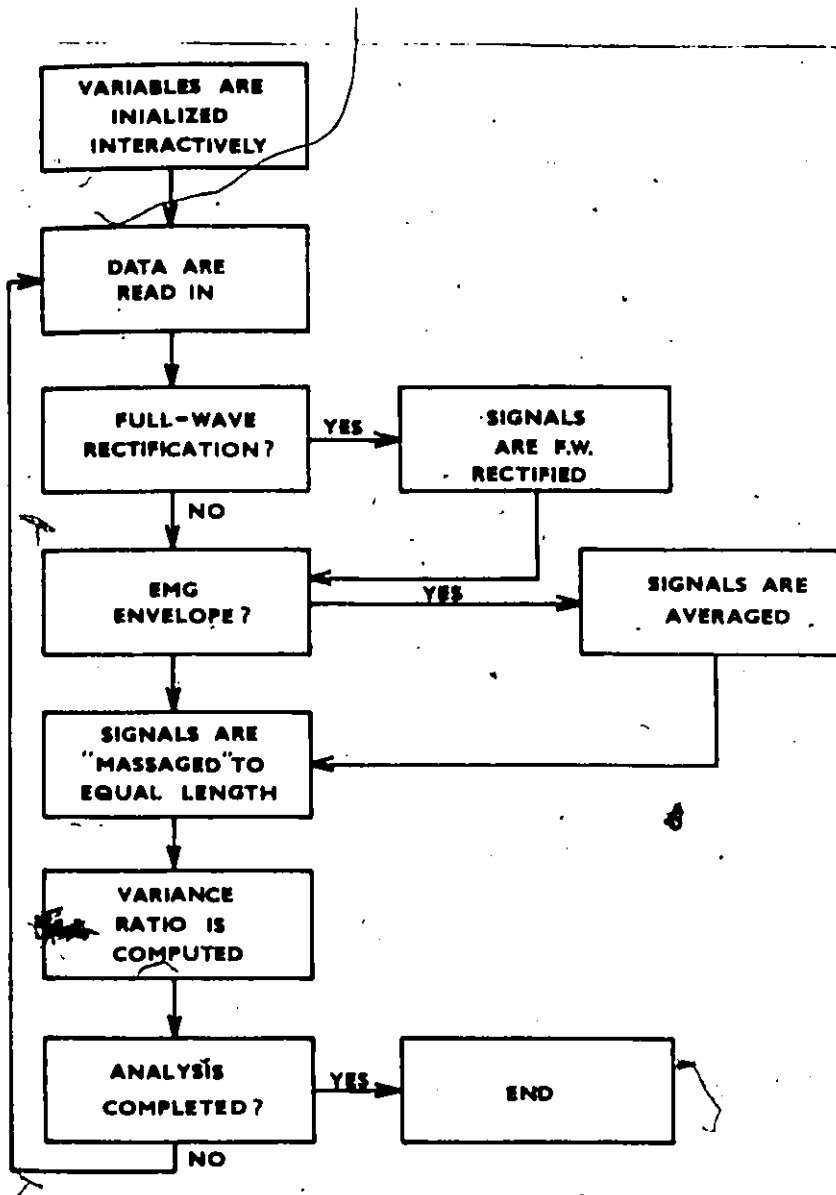


Figure A1.1
Flow-chart for Program 10E2.FOR

Program 2Name: 10XYX . FORSubroutines: OUTXY, LABEL, MOMENT, LOOPS, CENTRO, CRPTS

Aim of Program: This program accomplishes quantitative analyses of the angle-angle diagrams. Three data records are read in containing successively footswitch, hip angle and knee angle data. Depending on the user's need the x, y coordinates of loop intersection points, area and perimeter and even higher order moments can be computed. The program displays the angle-angle diagram including coordinate axes on an oscilloscope. Using the footswitch data, temporal information can be obtained and time labels affixed to the angle-angle diagram.

<u>Variables</u>	<u>Meaning of Variable</u>	<u>Format</u>
NUM	Number of data points in signal record	I4
NSTEP	Number of footsteps in file	I3
INUM	Number of channels	I3
IBU	Visual scale factor for oscilloscope display	I3
IREQF	Footswitch record number	I3
IRECX	X-data (hip angle) record number	I3
IRECY	Y-data (knee angle) record number	I3
IN	Noise level for pattern recognition of footswitch data	I3

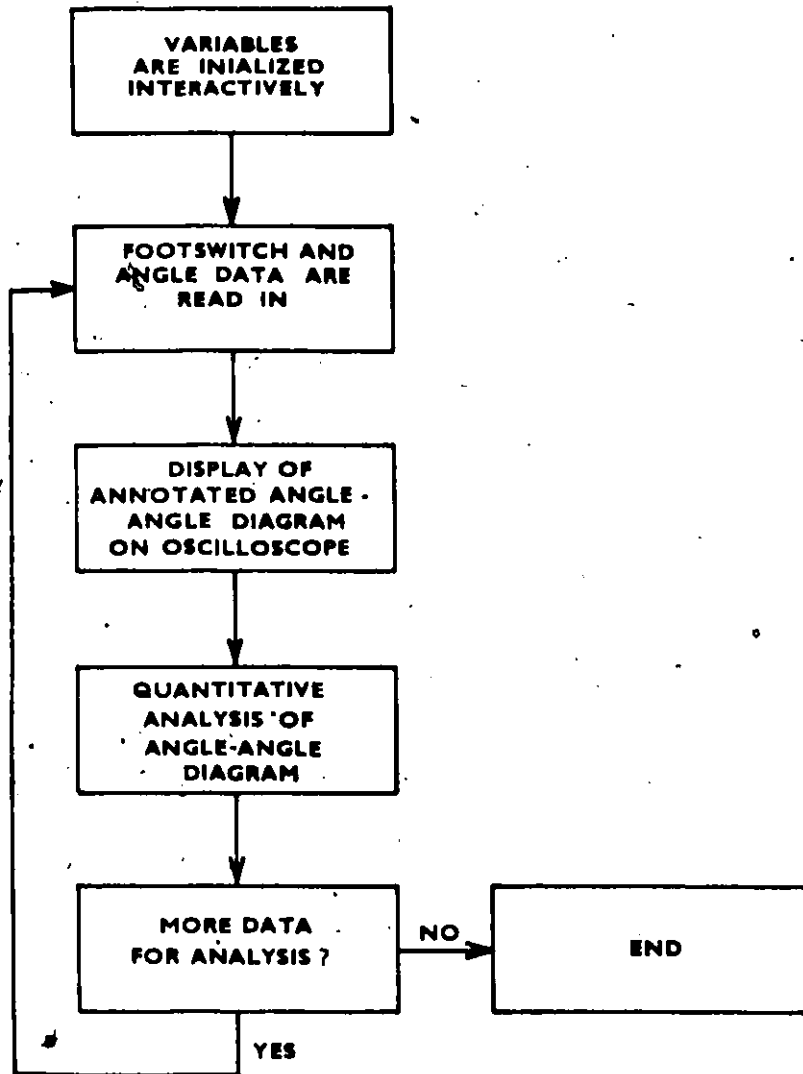


Figure A1.2
Flow-chart for program 10XYX.FOR

APPENDIX 2

THEORETICAL BACKGROUND TO THE MODELLING PROCEDURE

A2.1 Transfer Function Models



Since the model describes a dynamic response, it is called a transfer function model, and since the observations of input and output are made at equispaced intervals of time, the associated transfer function model will then be called a discrete transfer function model.

Even under carefully controlled conditions, influences other than X will affect Y. The combined effect on Y of such influences is referred to as disturbance or noise. A model such as can be related to real data must take account not only of the dynamic relationship associating X and Y but also of the noise disturbing the system. Such joint models are obtained by combining a deterministic transfer function model with a stochastic noise model.

For simplicity it is proposed initially to make use only of linear transfer function models and to extend this to the non-linear case only if the results deem it necessary.

The relating of the model to data is accomplished by the following processes:

- (i) Identification of the model
- (ii) Estimation of the parameters
- (iii) Diagnostic checking of the model

A2.2 Discrete Dynamic Models Represented by Difference Equations

Discrete dynamic systems are often represented by the general linear difference equation.

$$(1 - \delta_1 B - \dots - \delta_r B^r) Y_t = (\omega_0 - \omega_1 B - \dots - \omega_s B^s) X_{t-b}$$

$$\text{or as } \delta(B) Y_t = \omega(B) X_{t-b}$$

where B is the backward shift operator defined by

$$B Y_t = Y_{t-1}$$

and (X_t, Y_t) are observations of the input and output data at time t ,

$$\text{Thus if } \Omega(B) = \omega(B)B^b$$

$$\delta(B)Y_t = \Omega(B)X_t$$

$$\text{or } Y_t = \delta^{-1}(B)\Omega(B)X_t$$

$$(Y_0 = 0)$$

initial conditions
specified

Thus knowing r , s , b and the values of the corresponding parameters $\delta_1, \dots, \delta_r$ and $\omega_0, \dots, \omega_s$; we can employ the difference model recursively to compute the output for any input whatsoever.

A2.3 Transfer Function Models with Added Noise

If we assume the disturbance or noise N_t to be independent of the level of X and additive with respect to the influence of X , then we can write

$$Y_t = \delta^{-1}(B)\Omega(B)X_t + N_t$$

If the noise model can be represented by an Autoregressive Integrated Moving Average process (ARIMA(p, d, q))

$$N_t = \phi^{-1}(B) \theta(B) a_t$$

where a_t is white noise (random normally distributed with mean 0 and variance σ^2) then finally

$$Y_t = \phi^{-1}(B) \alpha(B) X_t + \phi^{-1}(B) \theta(B) a_t$$

A2.4 Identification, Fitting and Checking of Transfer Function Models

In this section methods are described for identifying, fitting and checking transfer function-noise models when simultaneous pairs of observations (X_1, Y_1) , (X_2, Y_2) , ..., (X_N, Y_N) of the input and output are available at discrete equispaced times 1, 2, ..., N.

The approach is to estimate parameters in parsimonious difference equation models. Throughout both Y_t and X_t are assumed to be stochastic processes.

In the same way that the autocorrelation function was used to identify stochastic models of time varying quantities, the data analysis tool employed for the identification of transfer function models is the cross correlation function between the input and output.

We regard the pair of time series (sampled-data) as realizations of a hypothetical population of pairs of time series, called a bivariate stochastic process.

The dimensionless quantity

$$\rho_{xy}(k) = \frac{r_{xy}(k)}{\sigma_x \sigma_y} \quad k = 0, \pm 1, \pm 2, \dots$$

is called the cross correlation coefficient at lag k and the function $\rho_{xy}(k)$ defined for $k = 0, \pm 1, \pm 2, \dots$ the cross

correlation function of the bivariate stochastic process $r_{xy}(k)$ is the cross covariance coefficient σ_x^2, σ_y^2 , are the variances of the time series. Since $\rho_{xy}(k)$ is not in general equal to $\rho_{xy}(-k)$, the cross correlation function in contrast to the autocorrelation function is not symmetric about $k = 0$.

Estimation of the Cross Covariance, Cross Correlation Functions

It can be shown that an estimate of the cross covariance coefficient at lag k is provided by

$$C_{xy}(k) = \begin{cases} \frac{1}{n} \sum_{t=1}^{n-k} (x_t - \bar{x})(y_{t+k} - \bar{y}) & k = 0, 1, 2, \dots \\ \frac{1}{n} \sum_{t=1}^{n+k} (y_t - \bar{y})(x_{t+k} - \bar{x}) & k = 0, -1, -2, \dots \end{cases}$$

where $n = \#$ of pairs of values (x_t, y_t) available

\bar{x}, \bar{y} are the means of the x series, y series

Thus the estimate $r_{xy}(k)$ of the cross correlation coefficient $\rho_{xy}(k)$ at lag k may be obtained by substituting estimates $C_{xy}(k)$ for $\gamma_{xy}(k)$, $s_x = \sqrt{C_{xx}(0)}$, $s_y = \sqrt{C_{yy}(0)}$ for σ_x and σ_y respectively

$$r_{xy}(k) = \frac{C_{xy}(k)}{s_x s_y} \quad k = 0, \pm 1, \pm 2, \dots$$

A2.5 Identification of Transfer Function Models

We now show how to identify a combined transfer function-noise model

$$Y_t = \delta^{-1}(B) \omega(B) X_t + N_t$$

or

$$Y_t = \delta^{-1}(B) \omega(B) X_{t-b} + N_t$$

for a linear system corrupted by noise N_t and assumed to be generated by an ARIMA process which is statistically independent of the input X_t .

Specifically, the objective at this stage is to obtain some idea of the orders r and s of the left-hand and right-hand operators in the transfer function model and to derive initial guesses for the parameters δ , ω and the delay parameter b . In addition, we aim to make rough guesses of the parameters p , d , q of the ARIMA process describing the noise at the output and to obtain initial estimates of the parameters θ , ϕ in that model. The tentative transfer function and noise models so obtained can then be used as a starting point for more efficient estimation methods to be described later.

An Outline of the Identification Procedure

$$\begin{aligned} \text{Model: } Y_t &= \delta^{-1}(B)\omega(B)X_{t-b} + N_t \\ &= V(B)X_t + N_t \end{aligned}$$

The basic tool which is employed here in the identification process is the cross correlation function between input and output. When the processes are nonstationary it is assumed that stationarity can be induced by suitable differencing. Nonstationary behaviour is suspected if the estimated auto- and cross-correlation functions of the (X_t, Y_t) series fail to damp out quickly. We assume that a degree of differencing d necessary to induce stationarity has been achieved when the estimated auto- and cross-correlations $r_{xx}(k)$, $r_{yy}(k)$ and $r_{xy}(k)$ of $x_t = \nabla^d X_t$ and $y_t = \nabla^d Y_t$ damp out quickly ($\nabla_t = Y_t - Y_{t-1}$).

Identifying the Noise Model

$$\text{Model: } Y_t = V(B)X_t + N_t$$

Given that a preliminary estimate $\hat{V}(B)$ of the transfer function has been obtained as described in the previous section then an estimate of the noise series is provided by

$$\hat{N}_t = Y_t - \hat{V}(B)X_t$$

Then a study of the estimated autocorrelation function of \hat{N}_t

can lead to identification of the noise model in the normal manner.

A2.6 Fitting the Transfer Function Model

We now consider the problem of efficiently and simultaneously estimating the parameters $b, \delta, \omega, \beta, \theta$ in the tentatively identified model

$$Y_t = \delta^{-1}(B) \omega(B) X_{t-b} + n_t.$$

where $Y_t = \omega Y_t, X_t = \omega X_t, n_t = \omega N_t$ are all stationary processes and

$$n_t = \beta^{-1}(B) \theta(B) a_t$$

If starting values x_0, y_0, a_0 prior to the commencement of the series were available then given the data for any choice of the parameters $(b, \delta, \omega, \beta, \theta)$ and of the starting values (x_0, y_0, a_0) we could calculate successively values of

$$a_t = a_t(b, \delta, \omega, \beta, \theta | x_0, y_0, a_0) \quad t = 1, 2, \dots, n$$

Under the normal assumption for the a 's a close approximation to the maximum likelihood estimates of these parameters can be obtained by minimizing the conditional sum

of squares function

$$S_0(b, \delta, \omega, \theta, \theta) = \sum_{t=1}^n a_t^2 (b, \delta, \omega, \theta, \theta | n_0, y_0, a_0)$$

Three Stage Procedure for Calculating the a's

First the output \hat{Y}_t from the transfer function model may be computed from

$$\hat{Y}_t = \delta^{-1}(B) \omega(B) X_{t-b}$$

i.e. from $\delta(B)\hat{Y}_t = \omega(B) X_{t-b}$

or from $Y_t - \delta_1 Y_{t-1} - \dots - \delta_r Y_{t-r} = \omega_0 X_{t-b} - \omega_1 X_{t-b-1} - \dots - \omega_s X_{t-b-s}$

Having calculated the \hat{Y}_t series then the noise series can be generated from

$$n_t = y_t - \hat{Y}_t$$

Finally the a's can be obtained from

$$a_t = \theta^{-1}(B) \theta(B) n_t$$

i.e. $a_t = \theta_1 a_{t-1} + \dots + \theta_q a_{t-q} + n_t - \theta_1 n_{t-1} \dots - \theta_p n_{t-p}$

Note: For stochastic model estimation, the effect of transients can be minimized if the difference equations are started off from a value t for which all previous x 's and y 's are known. Thus y_t is calculated from $t = u + 1$ onwards where $u = \max(r, (s+b))$. This means that n_t will be available from n_{u+1} onwards; hence, if unknown a 's are set equal to their unconditional expected values of zero, the a 's may be calculated from a_{u+p+1} onwards. Thus the conditional sum of squares function becomes

$$S_0(b, \delta, \omega, \beta, \theta) = \sum_{t=u+p+1}^n a_t^2(b, \delta, \omega, \beta | x_0, y_0, a_0)$$

Clearly we can slightly alter the parameters until the S_0 function is minimized and we should then have the optimal set of parameters.

Nonlinear Estimation

A nonlinear least squares algorithm may be derived as follows: At any stage of the iteration, and for some fixed value of the delay parameter b , let the best guesses available for the remaining parameters be denoted by $\beta_0 = (\delta_1, 0, \dots, \delta_r, 0, \omega_1, 0, \omega_s, 0, \beta_1, 0, \beta_p, 0)$.

Now let $a_{t,0}$ be that value computed from the model as

described in the previous section and denote the negative of the derivatives of a_t w.r.t. the parameters as follows:

$$d_{i,t}^{(\delta)} = \frac{-\partial a_t}{\partial \delta_i} \Big|_{\beta_0} = \{a_t(\delta_{1,0}, \dots, \delta_{r,0}, \omega_{0,0}, \dots, \omega_{s,0}, \dots; \beta_{1,0}, \dots, \beta_{p,0}, \theta_{1,0}, \dots, \theta_{q,0})\} / \Delta_i$$

$$-a_t(\delta_{1,0}, \dots, \delta_{i,0} + \Delta_i, \dots, \delta_{r,0}, \omega_{0,0}, \dots, \omega_{s,0}, \beta_{1,0}, \dots, \beta_{p,0}, \theta_{1,0}, \dots, \theta_{q,0}) / \Delta_i$$

$$d_{j,t}^{(\omega)} = - \frac{\partial a_t}{\partial \omega_j} \Big|_{\beta_0}$$

$$d_{g,t}^{(\beta)} = - \frac{\partial a_t}{\partial \beta_g} \Big|_{\beta_0}$$

$$d_{h,t}^{(\theta)} = - \frac{\partial a_t}{\partial \theta_h} \Big|_{\beta_0}$$

Then expanding a_t in a Taylor Series about $a_{t,0}$ and neglecting higher orders we get

$$a_t = a_{t,0} - \sum_{i=1}^r (\delta_i - \delta_{i,0}) d_{i,t}^{(\delta)} + \sum_{j=1}^s (\omega_j - \omega_{j,0}) d_{j,t}^{(\omega)}$$

$$+ \sum_{g=1}^p (\beta_g - \beta_{g,0}) d_{g,t}^{(\beta)} + \sum_{h=1}^q (\theta_h - \theta_{h,0}) d_{h,t}^{(\theta)}$$

$$\text{or } a_{t,0} = \sum_{i=1}^r (\delta_i - \delta_{i,0}) d_{i,t}^{(\delta)} + \sum_{j=1}^s (\omega_j - \omega_{j,0}) d_{j,t}^{(\omega)}$$

$$+ \sum_{g=1}^p (\beta_g - \beta_{g,0}) d_{g,t}^{(0)} + \sum_{h=1}^q (\theta_h - \theta_{h,0}) d_{h,t}^{(0)} + a_t$$

We can now obtain the adjustments $\delta_i - \delta_{i,0}$, $\omega_j - \omega_{j,0}$ by fitting this linearized equation by standard least squares (i.e. by multiple regression). By adding the computed adjustments (viz. the coefficients found by the regression) to the first-guesses β_0 a second set of guesses can be formed and the process repeated until convergence is reached.

The derivatives can be computed recursively. If b , which is an integer, needs to be estimated then the iteration may be run to convergence for a series of values of b and that value of b giving the minimum sum of squares will be selected.

Use of Residuals for Diagnostic Checking

Serious model inadequacy can usually be detected by examining

- (a) the autocorrelation function $r_{aa}(k)$ of the residuals $\hat{a}_t = a_t$ (\hat{b} , $\hat{\delta}$, $\hat{\omega}$, $\hat{\beta}$, $\hat{\theta}$) from the fitted model.
- (b) certain cross correlation functions involving input and residuals in particular the cross correlation

function $r_{aa}(k)$ between the prewhitened input a_t and the residuals \hat{a}_t .

If a wrong model is selected in general the a 's will be autocorrelated and also cross correlated with the x_t 's and hence with the a_t 's which generate the x_t 's. (This would occur if the transfer function model only is incorrect). If, however, the transfer function model were incorrect and the noise model correct then the a_t 's would only be autocorrelated.

Reference

The report above is a summary of the Transfer Function Model outlined in Part III of Time Series Analysis: Forecasting and Control by G.E.P. Box and G.M. Jenkins (Holden - Day).

REFERENCES

- [1] Angel, R.W.; Garland, H. and Moore, W. (1973):
"Clinical Note. Unloading reflex during blockade of antagonist muscle nerves"
Electroencephalography and Clinical Neurophysiology, Vol. 34, pp. 303-307.
- [2] Babb, M.E. and Dymond, A.M. (1975):
"Electrode Implantation In The Human Body"
Bulletin of Pros. Res., Spring 1975, pp. 51-150.
- [3] Bajd, T.; Kljajic, M.; Trnkoczy, A. and Stanic, V. (1974):
"Electrogoniometric measurement of step length"
Scand. J. Rehab. Med., Vol. 6, pp. 78-80.
- [4] Basmajian, J.V. and Greenlaw, R.K. (1968):
"Electromyography of iliacus and psoas with inserted fine-wire electrodes" (abstract)
Anat. Rec., Vol. 160, pp. 310.
- [5] Basmajian, J.V. (1970):
Primary Anatomy
6th Edition (Williams & Wilkins Co.)
- [6] Basmajian, J.V. (1974):
Muscles Alive Their functions revealed by electromyography.
3rd Edition (Williams & Wilkins Co.)
- [7] Battye, C.K. and Joseph, J. (1966):
"An investigation by telemetering of the activity of some muscles in walking"
Med. & Biol. Engg., Vol. 4, pp. 125-135.
- [8] Bernstein, N.A. et al (1935):
"Biodynamics of Locomotion"
VIEM, Moscow, U.S.S.R., Vol. 1.
- [9] Borelli, J.A. (1682):
De Motu Animalium, Dissertationibus physiomechanicis de motu musculorum, et de effervescentia et fermentatione.
Hagae Comitum. P. Gosse.
- [10] Box, G.E.P. and Jenkins, G.M. (1970):
Time Series Analysis. Forecasting and Control

(Holden Day)

- [11] Braune, W. and Fischer, O. (1895):
Der Gang des Menschen
I. Theil Abh. K. Sachs. Ges. Wiss. Math. - Phys. Classe
Vol. 21, pp. 153.
- [12] Brugger, W. and Milner, M. (1977):
"Computer-aided tracking of body motions using a
CCD-image sensor"
Accepted for publication in Medical and Biological
Engineering and Computers.
- [13] Brugger, W. (1977):
Ph.D. Thesis
McMaster University (In preparation)
- [14] Close, J.R. and Todd, F.N. (1959):
"The phasic activity of the muscles of the lower
extremity and the effect of tendon transfer"
The J. of Bone and Joint Surgery, Vol. 41-A, No. 2, pp.
189-208.
- [15] Coggshall, J.C. and Bekey, G.A. (1970):
"EMG - force dynamics in human skeletal muscle"
Med. & Biol. Engineering, Vol. 8, pp. 265-270.
- [16] Cooper, I.S., Crighel, E. and Amin, I. (1973):
"Clinical and physiological effects of stimulation of
the paleocerebellum in humans"
Journal of the American Geriatric Society, Vol. 21, pp.
40-43.
- [17] Cooper, I.S., Riklan, M., Amin, I., Waltz, J.M. and
Cullinan, T. (1976):
"Chronic cerebellar stimulation in Cerebral Palsy"
Neurology, Vol. 26, pp. 744-753.
- [18] Crochetiere, W.T., Vodovnik, L. and Reswick, J.B.
(1967):
"Electrical stimulation of skeletal muscle, a study of
muscle as an activator"
Med. Biol. Engng., Vol. 5, pp. 111-125.
- [19] deBruin, H. (1976):
"Aspects of analysis and processing of electromyo-
graphic signals"
Ph.D. Thesis, McMaster University.
- [20] deBruin, H. and Milner, M. (1977):

"A software system for acquisition, processing and display of gait data"
Progress Report. Human Locomotor Engineering Programme.
 Department of Biomedical Engineering, Chedoke
 Rehabilitation Centre, Hamilton.

- [21] Eberhart, H.D., Inman, V.T. and Bresler, B. (1968):
 "The principal elements in human locomotion"
 Chapter 15 in Human Limbs and Their Substitutes
 edited by Klopsteg, P.E. and Wilson, P.D., pp. 437-471.
 (Hafner Publishing Company)
- [22] Edeland, H.G. and Stefansson, T. (1973):
 "Block of the suprascapular nerve in reduction of acute
 anterior shoulder dislocation. Case Reports"
Acta. Anaesth. Scand., Vol. 17, pp. 46-49.
- [23] Edelstein, J.E. (1965):
 "Biomechanics of normal ambulation"
Physioth. Can., Vol. 17, No. 3, pp. 173-184.
- [24] Edgett, G.L.; Burford, F.J.; Kippen, J.W.; Mitchell,
 R.G. and Newnham, W.T. (1960):
A Modern Analytic Geometry
 The Ryerson Press, Toronto.
- [25] Elftman, H. (1934):
 "Cinematic study of the distribution of pressure in the
 human foot"
Anat. Record, Vol. 59, pp. 481-491.
- [26] Elftman, H. (1938):
 "The measurement of the external force in walking"
Science, Vol. 88, pp. 152-153.
- [27] Elftman, H. (1939a):
 "Forces and energy changes in the leg during walking"
Am. J. Physiol., Vol. 25, No. 2, pp. 339-356.
- [28] Elftman, H. (1939b):
 "The function of the muscles in locomotion"
Am. J. Physiol., Vol. 125, No. 2, pp. 357-366.
- [29] Elftman, H. (1939c):
 "The rotation of the body in walking."
Arbeitsphysiol., Vol. 10, pp. 477-484.
- [30] Elftman, H. (1939d):
 "The force exerted by the ground in walking"
Arbeitsphysiol., Vol. 10, pp. 485-491.

- [31] Elftman, H. (1939e):
"The function of the arms in walking"
Human Biology, Vol. 11, No. 4, pp. 529-535.
- [32] Elftman, H. (1940):
"The work done by muscles in running"
Am. J. Physiol., Vol. 129, No. 3, pp. 672-684.
- [33] Elftman, H. (1941):
"The action of muscles in the body"
Biol. Symp., Vol. 3, pp. 191-209.
- [34] Elftman, H. (1945):
"Torsion of the lower extremity"
Am. J. Phys. Anthrop., Vol. 3, pp. 255-265.
- [35] Elftman, H. (1951):
"The basic pattern of human locomotion"
Ann. N.Y. Acad. Sci., Vol. 51, pp. 1207-1212.
- [36] Elftman, H. (1955a):
"Body dynamics and dynamic anthropometry"
Ann. N.Y. Acad. Sci., Vol. 63, No. 4, pp. 553-558.
- [37] Elftman, H. (1955b):
"Knee action and locomotion"
Bull. Hosp. for Joint Diseases, Vol. 16, No. 2, pp. 103-110.
- [38] Elftman, H. (1966):
"Biomechanics of muscle, with particular application to studies of gait"
J. Bone Joint Surg., Vol. 48-A, No. 2, pp. 363-377.
- [39] Elftman, H. (1967):
"Basic function of the lower limb"
Biomedical Engineering, Vol. 2, pp. 342-345.
- [40] Elftman, H. (1969):
"Dynamic structure of the foot"
Artificial Limbs, Vol. 13, No. 1, pp. 49-58.
- [41] Elliot, B.C. and Blanksby, B.A. (1976):
"Reliability of averaged integrated electromyograms during running"
Journal of Human Movement Studies, Vol. 2, pp. 28-35.
- [42] Fenwick, P., Mitchie, P., Dollmire, J. and Fenton, G. (1971):
"Mathematical simulation of the EEG using an autoregressive series"

International Jour. Biomed. Comput., Vol. 2, pp. 281-307.

- [43] Freeman, H. (1961):
"On the encoding of arbitrary geometric configurations"
IRE Trans. EC-10, No. 2, June, pp. 260-268.
- [44] Gray, E.G. and Basmajian, J.V. (1968):
"Electromyography and cinematography of leg and foot
("normal" and flat) during walking"
Anat. Rec., Vol. 161, pp. 1-16.
- [45] Graupe, D. and Cline, W.K. (1975):
"Functional separation of EMG signals via ARMA
identification methods for prosthesis control purposes"
IEEE Transactions on Systems, Man and Cybernetics, Vol.
S.M.C.-5, No. 2, pp. 252-259.
- [46] Grieve, D.W. and Gear, R.J. (1966):
"The relationships between length of stride, step
frequency, time of swing and speed of walking for
children and adults"
Ergonomics, Vol. 5, No. 9, pp. 379-399.
- [47] Grieve, D.W. (1968):
"Gait patterns and the speed of walking"
Biomedical Engineering, Vol. 3, March, pp. 119-122.
- [48] Grieve, D.W. and Cavanagh, P.R. (1974):
"The validity of quantitative statements about surface
electromyograms recorded during locomotion"
Scand. J. Rehab. Med. Suppl., Vol. 3, pp. 19-25.
- [49] Grundy, M., Tosh, P.A., McLeish, R.D. and Smidt, L.
(1975):
"An investigation of the centres of pressure under the
foot while walking"
Journal of Bone & Joint Surg., Vol. 57-B, No. 1, pp.
98-103.
- [50] Hagy, J.L. (1973):
"Normal angular and force measurement data"
Prepared by the Gait Analysis laboratory, Shriners
Hospital for Crippled Children. San Francisco,
California.
- [51] Hershler, C. and Milner, M. (1976):
"A suggested optimality criterion for an
electromyographic (EMG) processor,"
Digest of the 11th International Conference on Medical
and Biological Engineering, Ottawa, Canada.

- [52] Hershler, C. (1976):
"Kinematic analysis of gait by stroboscopic flash photography and computer"
Progress Report No. 1 Human Locomotor Engineering Programme. Biomedical Engineering Department, Chedoke Rehabilitation Centre, Hamilton.
- [53] Hershler, C. (1977a):
"A background review of human locomotion"
Educational Monograph No. 1, Human Locomotor Engineering Programme. Biomedical Engineering Department, Chedoke Rehabilitation Centre, Hamilton.
- [54] Hershler, C. (1977b):
"Current experimental techniques and equipment used in locomotion studies"
Progress Report No. 3, Human Locomotor Engineering Programme. Biomedical Engineering Department. Chedoke Rehabilitation Centre, Hamilton.
- [55] Hershler, C. and Milner, M. (1977a):
"An optimality criterion for processing electromyographic (EMG) signals relating to human locomotion"
Progress Report No. 2, Human Locomotor Engineering Programme, Biomedical Engineering Department, Chedoke Rehabilitation Centre, Hamilton. Also accepted for publication in IEEE Transactions on Biomedical Engineering.
- [56] Hershler, C. and Milner, M. (1977b):
"Quantitative analyses of angle-angle diagrams in the assessment of locomotor function"
Progress Report No. 4, Human Locomotor Engineering Programme. Biomedical Engineering Department, Chedoke Rehabilitation Centre, Hamilton.
- [57] Horning, M.R., Kraft, G.H. and Guy, A. (1972):
"Latencies recorded by intramuscular needle electrodes in different portions of a muscle. Variation and comparison with surface electrodes"
Arch. Phys. Med. Rehab., Vol. 53, pp. 206-211.
- [58] Inbar, G.F. and Baskin R.J. (1970):
"Parameter identification analysis of muscle dynamics"
Math. Biosciences, Vol. 7, pp. 61-79.
- [59] Johnston, R.C. and Smidt, G.L. (1969):
"Measurement of hip-joint motion during walking. Evaluation of an electrogoniometric method"
J. Bone and Joint Surg., Vol. 51-A, pp. 1083-1094,

September.

- [60] Jonsson, B. and Bagge, U.E. (1968a):
 "Displacement, deformation and fracture of wire electrodes in electromyography"
Electromyography, Vol. 8, pp. 329-347.
- [61] Jonsson, B., Omfeldt, M. and Rundgren, A. (1968b):
 "Discomfort from the use of wire electrodes in electromyography"
Electromyography, Vol. 8, pp. 5-17.
- [62] Jonsson, B. and Reichmann, S. (1968c):
 "Reproducibility in kinesiological EMG - investigations with intramuscular electrodes"
Acta Morph. Neerl. - Scand., Vol. 7, pp. 73-90.
- [63] Joseph, J. (1964):
 "The activity of some muscles in locomotion"
Physioth., Vol. 50, No. 6, pp. 180-183.
- [64] Karlsson, E. and Jonsson, B. (1965):
 "Function of the gluteus maximus muscle. An electromyographic study"
Acta Morph. Neerl. Scand., Vol. 6, pp. 161-169.
- [65] Kettelkamp, D.B., Johnson, R.J., Smidt, G.L., Chao, E.Y.S. and Walker, M. (1970):
 "An electrogoniometric study of knee motion in normal gait"
J. of Bone and Joint Surgery, Vol. 52-A, No. 4, pp. 775-790, June.
- [66] Komi, P.V. and Buskirk, E.R. (1970):
 "Reproducibility of electromyographic measurement with inserted wire electrodes and surface electrodes"
Electromyography, No. 4, pp. 357-367.
- [67] Kramer, H., Klichler, G. and Brauer, D. (1972):
 "Investigations of the potential distribution of activated skeletal muscles in man by means of surface electrodes"
Electromyography, Vol. 12, No. 1, pp. 19-27.
- [68] Lamoreux, L.W. (1971):
 "Kinematic measurements in the study of human walking"
Bull. Prosthetics Res., BPR 10-15, pp. 3-84 (Spring)
- [69] Leavitt, L.A., Zuniga, E.N., Calvert, J.C., Canzoneri J.C. and Peterson, C.R. (1971):
 "Gait analysis of normal subjects"

- Southern Medical Journal, Vol. 64, No. 9, pp. 1131-1138.
- [70] Levens, A.S., Inman, V.T. and Blosser, J.A. (1948):
"Transverse rotation of the segments of the lower extremity in locomotion"
The Journal of Bone and Joint Surgery, Vol. 30-A, No. 4, pp. 859-872.
- [71] Liberson, W.T. (1936):
"Une Nouvelle Application du Quartz Piezoelectrique: Piezoelectrographic de la Marche et des Mouvements Volontaires", Paris
Le Travail Humain, Vol. 4, pp. 1-7.
- [72] Liberson, W.T. (1965):
"Biomechanics of gait: A method of study"
Arch. Phys. Med., Vol. 46, pp. 37-48.
- [73] Marey, E.J. (1885):
"Locomotion de l'homme; Images stereoscopiques des trajectoires que decrit dans l'espace un point du tranc pendant la marche, la course et lest autres allures"
Compt. Rend. Acad. Sc., Paris: 100.
- [74] Merit Students Encyclopaedia (1976):
Leonardo da Vinci
Vol. 77, pp. 75-76.
Macmillan Educational Corporation
- [75] Milner, M., Basmajian, J.V. and Quanbury, A.O. (1971a):
"Multifactorial analysis of walking by electromyography and computer"
American Journal of Physical Medicine, Vol. 50, No. 5, pp. 235-258.
- [76] Milner, M. and Quanbury, A.O. (1971b):
"Programmed stimulation of skeletal muscle - some problems"
Medicine and Sport, Vol. 6, Biomechanics II, pp. 277-284.
- [77] Milner, M., Dall, D., McConnell, V.A., Brennan, P.K. and Hershler, C. (1973):
"Angle diagrams in the assessment of locomotor function. Studies on normal subjects for various speeds and some preliminary work on patients requiring total hip reconstruction (Charnley low-friction arthroplasty)"
S.A. Med. Journal, Vol. 47, pp. 951-957.

- [78] Milner, M., Dail, D., Ruff, A.L. and Brennan, P.K. (1974):
 "Pre- and post-operative angle diagrams in cases of total hip reconstruction"
Digest 5th Canadian Medical and Biological Engineering Conf., pp. 17.3 a,b, September, Montreal.
- [79] Milner, M., Hershler, C., deBruin, H., Baker, R., Upton, A.R.M. and Cooper, I.S. (1977):
 "Preliminary investigation of influence of cerebellar stimulation on gait by analyzing angle-angle diagrams"
 Accepted for publication in a book edited by I.S. Cooper (New York).
- [80] Murray, M.P., Kory, R.C., Clarkson, B.H. and Sepic, S.B. (1966):
 "comparison of free and fast speed walking patterns of normal men"
Amer. Jour. of Phys. Med., Vol. 45, No. 1, pp. 8-24.
- [81] New Encyclopedia Britannica (1976):
 (Macropaedia Volume 1 - Knowledge in Depth)
 Vol. 1, page 1168, (15th Edition)
- [82] Norman, R.W., Nelson, R.C. and Cavanagh, P.R. (1977):
 "Minimum sampling time required to extract stable information from digitized EMG's"
 Paper presented at Vith International Congress of Biomechanics, Copenhagen, Denmark, July 11-14.
- [83] Paul, J.P. (1969):
 "The action of some two-joint muscles in the thigh during walking"
J. Anat., Vol. 5, No. 1, pp. 208-210.
- [84] Paul, J.P. (1971):
 "Comparison of EMG signals from leg muscles with corresponding force actions calculated from walkpath measurements"
 Human Locomotor Engineering. Proceedings of a Symposium held at Sussex, pp. 13-28.
- [85] Paul, J.P. (1976):
 "Loading on normal hip and knee joints and on joint replacements"
Engineering Advances in Medicine, Vol. 2.
Advances in Artificial Hip and Knee Joint Technology
 Springer Verlag (Berlin)
- [86] Radcliffe, C.W. (1962):
 "The biomechanics of below-knee prostheses in normal,

level, bipedal walking"
Artif. Limbs., Vol. 6, pp. 16-24.

- [87] Radcliffe, C.W. (1974):
 "Locomotion and lower limb prosthetics"
Bull. Prosth. Res., Vol. 10-22 Fall, pp. 167-187.
- [88] Ralston, H.J., Todd, F.N. and Inman, V.T. (1976):
 "Comparison of electrical activity and duration of
 tension in the human rectus femoris muscle"
Electromyography Clin. Neurophysiol., Vol. 16, pp.
 277-286.
- [89] Rozin, R., Robin, G.C., Magora, A., Simkin, A. and
 Gonen, B. (1971):
 "Investigation of gait. 2. Gait analysis in normal
 individuals"
Electromyography, Number 2, pp. 183-190.
- [90] Saunders, J.R.M., Inman, V.T. and Eberhart, H.D.
 (1953):
 "The major determinants in normal and pathological
 gait"
J. of Bone & Joint Surgery, Vol. 35-A, pp. 543-558.
- [91] Scherb, R. (1927):
 "Mitteilungen zur Myo Kinesiographie"
Ztschr f Orthop. Chir., Vol. 49.
- [92] Schwartz, R.P. and Heath, A.L. (1947):
 "The definition of human locomotion on the basis of
 measurement"
J. of Bone and & Joint Surg., Vol. 29, pp. 203-314.
- [93] Scott, R.N. and Thompson, G.B. (1969):
 "An improved bipolar wire electrode for
 electromyography"
Med. Biol. Eng., Vol. 7, pp. 677-678.
- [94] Smidt, G.L., Arora, J.S. and Johnston, R.C. (1971):
 "Accelerographic analysis of several types of walking"
Amer. Jour. of Phys. Med., Vol. 50, No. 6; pp. 285-300.
- [95] Smith, F., Blackstone, I., Hershler, C., Milner, M. and
 Wallace, T. (1976):
 "The use of angle-angle diagrams in the assessment of
 total knee-joint replacement"
Digest of 11th Conf. on Med. & Biol. Eng., pp. 578-579.
- [96] Smith, K.U., McDermid, C.D. and Shideman, F.E. (1960):
 "Analysis of the temporal components of motion in human

- gait"
Amer. Jour. of Phys. Med., Vol. 39, pp. 142-151.
- [97] Steindler, A. (1953):
 "A historical review of the studies and investigations made in relation to human gait"
Journal of Bone and Joint Surgery, Vol. 35-A, pp. 540-542 and page 728.
- [98] Sutherland, D.H. (1966):
 "An electromyographic study of the plantar flexors of the ankle in normal walking on the level"
Jour. of Bone & Joint Surgery, Vol. 48-A, pp. 66-71.
- [99] Sutherland, D.H., Hagy, J.L. (1972):
 "Measurement of gait movements from motion picture film"
Jour. of Bone & Joint Surg., Vol. 54-A, No. 4, pp. 787-797, June.
- [100] Underwood, E.E. (1975):
 "Three-dimensional shape parameters from planar sections"
Proceedings of the 4th International Congress for Stereology held at the National Bureau of Standards, Gaithersburg, Md., Sept. 4-9, pp. 91-92.
- [101] University of California (1953):
 "The pattern of muscular activity in the lower extremity during walking"
Prosthetic Devices Research Report, Series M, Issue 25.
- [102] Upton, A.R.M., and Cooper, I.S. (1976):
 "Some neurophysiological effects of cerebellar stimulation in man"
The Canadian Journal of Neurological Sciences, Vol. 3, pp. 237-254.
- [103] Upton, A.R.M. and Cooper, I.S. (1977):
 "Some neurophysiological mechanisms in control of spasticity"
Cerebellar Stimulation in Man, Raven Press, Ed. I.S. Cooper, 1977.
- [104] Viitasalo, J.H.T. and Komi, P.V. (1975):
 "Signal characteristics of EMG with special reference to reproducibility of measurements"
Acta Physiol. Scand., Vol. 93, pp. 531-539.
- [105] Weber, W., Weber, E. (1836):

"Mechanik der menschlichen Gehwerkzeuge" ("Mechanics of Human Locomotion") Gottingen, Germany.
Scand. J. Rehab. Med., Vol. 6, pp. 78-80.

- [106] Williams, W.J. Gesink, J.W. and Stern, M.M. (1972):
"Biological system transfer function extraction using swept-frequency and correlation techniques"
Med. & Biological Engineering, Vol. 10, pp. 609-620.
- [107] Winter, D.A., Greenlaw, R.K. and Hobson, D.A. (1972):
"Television-computer analysis of kinematics of human gait"
Comp. Biomed. Res., Vol. 5, pp. 498-504.
- [108] Winter, D.A., Sidwall, H.G. and Hobson, D.A. (1974):
"Measurement and reduction of noise in the kinematics of locomotion"
J. Biomechanics, Vol. 1, pp. 157-159.
- [109] Wonnacott, T. and Wonnacott, R. (1969):
Introductory Statistics, New York (Wiley)
- [110] Zetterberg, L.A. (1969):
"Estimation of parameters for a linear difference equation with application to ECG analysis"
Math. Biosc., Vol. 5, pp. 227-275.